The legacy of polders: Diagnosing complex flooding processes and adaptation options in the coastal region of Bangladesh

Mohammed Sarfaraz Gani Adnan
Oriel College

A Thesis submitted for the degree of
Doctor of Philosophy

School of Geography and the Environment
University of Oxford
Hilary Term 2020

Abstract

Polders (enclosed coastal embankments) are often constructed to protect river and coastal floodplains in deltas. In Bangladesh, a total of 139 polders have been constructed between the 1960s and 1980s to safeguard agricultural lands from potential damage due to tidal floods, storm surge floods, and salinity intrusion. Whilst such flood control measures reduce the probability of flooding, they have had complex impacts on geomorphological and hydrological processes with consequence for human wellbeing. This legacy of interventions in the coastal system and subsequent human adaptations, now makes decision making even more challenging at a time of increasing environmental pressures.

This thesis analyses historical floods in the coastal zone in Bangladesh, diagnosing whether the floods were attributable to monsoonal precipitation (pluvial flooding), high upstream river discharge into the tidal delta (fluvio-tidal flooding), or cyclone-induced storm surges. It quantifies polders' effectiveness by modelling different forms of inundation to estimate what flooding might have been had the polders not been constructed.

Considering the societal impacts of flooding, the effects of changing land-use and flood risk on poverty are quantified. The results answer the questions of (i) how the pattern of land use/land cover (LULC) change influences flood risk at present and continue to do so in the future; (ii) how LULC change and flood risk impact poverty spatially.

The last section of the thesis focuses on estimating the impacts of potential Tidal River Management (TRM) on elevating the floodplains and reducing the annual probability of flooding. It identifies suitable TRM sites to model sediment deposition in those areas. The potential impact of TRM on flooding is investigated by comparing flood susceptibility 'before and after' the implementation of TRM.

By analysing complex coastal flood processes and adaptation options spatially and quantitatively, this thesis provides new evidence to the effectiveness of the past (polders), and potential future (TRM) adaptation options. It also presents a new approach to flood risk estimation, considering the societal impacts of flooding. The results of this thesis could be of importance both in research and practice for making scientifically informed decisions on coastal flood risk management, particularly in Bangladesh.

Acknowledgements

This research has been supported by the Commonwealth PhD Scholarships, funded by the UK Department for International Development (DFID).

Firstly, I am grateful to my supervisor Professor Jim Hall for his constant guidance, inspiration, and support throughout my DPhil studies. To Jim, thank you for your wise advice, incisive questions, and thorough feedback. I would also like to thank the assessors who reviewed my progress during the confirmation of status and transfer of status examinations: Professor Rob Hope, Professor Edmund Penning-Rowsell, and Dr Katrina Charles. I owe much to the REACH project team, particularly Bangladesh Coastal Risk Observatory Research group, for sharing a wide range of data to support my DPhil research. I feel very privileged to have been a part of the REACH programme to which my DPhil is affiliated. I also thank my research collaborators who contributed in journal articles prepared for this thesis: Dr Ashraf Dewan, Professor Anisul Haque, Abu Yousuf Md Abdullah, Dr Rocky Talchabhadel, and Professor Hajime Nakagawa.

I thank my wife Khatun E Zannat for giving me the motivation to move beyond my comfort zone and providing constructive criticisms on my approach towards research and academia. I am particularly thankful to all my fellow DPhil colleagues from Professor Hall's research group for their constant support throughout my DPhil studies. Last but not the least, I am grateful to my parents and sister for their constant support and encouragement, which eventually helped me to finish my DPhil thesis.

Publications

1. **Adnan, M. S. G.**, Haque, A., & Hall, J. W. (2019). Have coastal embankments reduced flooding in Bangladesh?. *Science of the Total Environment*, *682*, 405-416. doi:10.1016/j.scitotenv.2019.05.048 (Chapter 3)
2. **Adnan, M. S. G.**, Abdullah, A.Y.M., Dewan, A., & Hall, J. W. (2020). The effects of changing land use and flood hazard on poverty in coastal Bangladesh. *Land Use Policy, 99,* 104868. doi:10.1016/j.landusepol.2020.104868 (Chapter 4)
3. **Adnan, M. S. G.**, Talchabhadel, R., Nakagawa, H., & Hall, J. W. (2020). The potential of Tidal River Management for flood alleviation in South Western Bangladesh. *Science of the Total Environment, 731*. doi: 10.1016/j.scitotenv.2020 (Chapter 5)

Contents

List of figures

Supplementary figures

List of tables

Supplementary tables

Chapter 1 Introduction

1.1. Background and motivation

A polder is defined as "a level area which was originally subject to a high water-level, either permanently or seasonally and due to either groundwater or surface water. It becomes a polder when it is separated from the surrounding hydrological regime so that its water-level can be controlled independently of the surrounding regime" (Segeren 1983). Dykes or embankments have been constructed in many places around the world to create polders, in order to protect low-lying deltas particularly from coastal flooding (Bouwer et al. 2009, Day et al. 2016).

Generally, deltaic coasts are the regions of diversified ecosystems, with arable soils for agriculture and convenient for navigation and trade fisheries, forestry, fossil energy production, and manufacturing (Syvitski et al. 2009, Day et al. 2016). Therefore, many important cities are located in deltaic coasts (Hanson et al. 2011, Nicholls et al. 2008). Contrarily, these regions are among the most stressed and degraded natural systems (Day et al. 2016, Syvitski et al. 2009). Coastal flooding has become an increasing problem in deltas due to growing populations and assets along coastlines, climate change-induced sea level rise (SLR), subsidence, and anthropogenic activities leading to land-use change (Karamouz et al. 2019, Bilskie et al. 2014, Nicholls et al. 2008, Syvitski 2008). Although historically, many deltaic coasts focused solely on structural flood control measures such as polders, for the last three decades, researchers and policymakers have been seeking alternative measures to minimise flood consequences, in order to achieve comprehensive flood risk management (Klijn et al. 2010).

The Dutch are well known for their polders, which is a measure for wresting land from the sea, and reduce the flood probability (Warner et al. 2018). Following the Dutch model, polders have been constructed in some other countries such as Bangladesh, to protect lands from increasing the risk of coastal flooding (Amir and Khan 2019). Bangladesh, located in the floodplains of the Ganges, Brahmaputra, and Meghna rivers, has a unique geographic, physiographic, and hydraulic setting, making the country prone to multiple types of flooding (Brammer 1990, Rahman and Salehin 2013). On average, 20–25% of the area is susceptible to flooding in a normal year, while extreme flood events such as those that occurred in 1987, 1988, and 1998 inundated more than 60% of the total land area (Dewan 2013). Cyclone strikes the country almost every year with a severe cyclone striking every three years on average (surge heights range between 2 m and 10.6 m) (Karim and Mimura 2008). This type of hazard causes a significant loss of life and property (Bhuiyan and Dutta 2012). For instance, from 1953 to 2007, most of the fatalities of the world caused by major tropical cyclone events occurred in Bangladesh (Jonkman and Vrijling 2008). The country is also considered to be one of the most vulnerable countries in the world for climate change impacts, due to high population density, climate-sensitive subsistence economy (e.g., rice monoculture), and lack of technological support to deal with climate change impacts (Paul and Rashid 2017).

Coastal flood processes in Bangladesh are more complex than most of the deltaic coasts of the world. Coastal floods are generally caused by either astronomical tides or surges particularly during windstorms such as hurricanes, cyclones, and typhoons (Jonkman and Vrijling 2008). For instance, in the Mekong River Delta in Vietnam, astronomical tides induce coastal flooding (Hoa et al. 2008). The Mahanandi Delta in India has a geographical context similar to the Bangladesh coastal zone. This delta is prone to waterlogging, tidal, and surge induced floods (Hazra et al. 2020). In coastal Bangladesh, five types of floods

affect the coastal region: (i) pluvial, (ii) fluvial, (iii) tidal, (iv) fluvio-tidal, and (v) storm surge floods (Haque and Nicholls 2018). In response to surge induced floods, the then government invested in the Coastal Embankment Project (CEP) to construct a total of 139 polders in between the 1960s and 1980s to safeguard agricultural lands from potential damage due to tidal floods, storm surge floods, and salinity intrusion (Warner et al. 2018). Although polders yielded good results, in the form of increased agricultural production until the 1980s, the separation of floodplains from adjacent rivers caused geomorphological changes in the embanked regions (Auerbach et al. 2015). The embanked region has experienced land subsidence, which increased the number of surface depressions. Lack of sedimentation in adjacent floodplains promoted siltation in riverbeds, reducing water retention capacity of the rivers (Gain et al. 2017, Auerbach et al. 2015). All these processes have led to an increased inundation and associated unplanned changes in land use, damage to property, and loss of livelihoods of affected people (Khan et al. 2015).

Flood depths and extents are the consequential effects of various combinations of process drivers such as land-use change, nearshore geomorphology, meteorological conditions, tidal conditions, flood control measures and their associated likelihood of failure (Hall et al. 2003c, Karamouz et al. 2019, Bates et al. 2005, Bilskie et al. 2014, Hall et al. 2003b). The devastating impacts of storm surges in the coastal region are well recognised and measures are usually implemented to minimise their impacts. But, phenomena such as fluvial and pluvial flooding are often overlooked, which could exacerbate the impacts of surge events (Wright et al. 2019a). Results of several studies indicated that the occurrence of compound flood events (various combinations of the surge, fluvial, and pluvial floods) pose a greater damage potential in the coastal region (Wahl et al. 2015, Ikeuchi et al. 2017). However, few studies focused on analysing coastal inundations caused by multiple types of floods (Chen and Liu 2014).

Towards the end of the 20th century, ecologists and environmentalists started showing a lack of confidence in the thought process behind the decision to create polders (Zegwaard et al. 2019). The implementation of such flood control measures, which generally aim to reduce the probability of flooding (Merz et al. 2010a), could increase the complexities of coastal flood processes and associated risks. The dynamic interplay between societies and hydrological extremes could alter the frequency, magnitude, and spatial distribution of flood events (Di Baldassarre et al. 2017). The implementation of flood control measures such as embankments, dykes, and levees (Bamberg et al. 2017) tend to change the hydrological (Montz and Tobin 2008), ecological, geomorphological, and anthropogenic environment of floodplain areas (Hupp et al. 2009, Gergel et al. 2002, Morrison et al. 2018, Steinfeld and Kingsford 2013). For instance, the construction of embankments in deltas forces sediment-laden floodwater to enter and exit the protected areas, promoting sediments being deposit in the adjacent drainage channels. This reduces the drainage capacity of the protected areas (Day et al. 2016). Besides, the water-surface height of the flood tends to change in the vicinity of the flood control structure (Heine and Pinter 2012). Maintenance of floodplains is a complex process, as many factors related to the natural environment and anthropogenic activities alter the dynamics of floodplains (Tockner and Stanford 2002). Alteration of floodplains through the construction of structural flood control systems might impact the connectivity of the floodplain to sediment-laden flood flow, which may lead to a change in floodplain geomorphology (Hupp et al. 2009, Gergel et al. 2002, Morrison et al. 2018).

The construction of structural flood control measures, such as polders, shapes the pattern of human settlements and other land uses, which in turn impacts the extent of flood risk. Such flood control measures create the so-called “levee effect” (White 1945). Whilst people tend to settle in less flood-prone areas, the presence of a structural flood defence system encourages floodplain development by improving the perceptions of safety (Di

Baldassarre et al. 2013, Montz and Tobin 2008). Therefore, the failure of structural flood defence systems in the form of overtopping or breaching may exacerbate flood damages (Hui et al. 2016). In Bangladesh, millions of people inhabit the polders, where the majority of rural householders live under the national poverty line (Tuong et al. 2014). The pattern of land use in the coastal region has gone through major changes over the last half-century following the construction of polders (Parvin et al. 2017). Such changes largely occurred due to frequent and diverse natural disasters (e.g., floods) and associated increases in inundation, soil salinity, and land erosion (Khan et al. 2015). Land use has a strong influence on flood risk, as it determines the amount of peak discharge and the number of population and assets exposed to flooding (Szwagrzyk et al. 2018). Floods are inextricably linked with poverty (Dasgupta 2007), as increasing flood risk and unplanned land-use change could create a social-ecological poverty trap (Ahmed 2018). Marginalised people tend to settle in low-lying floodplains because of, for example, the availability of cheaper land (Dasgupta 2007). Whilst the transformation of agricultural lands into aquaculture use was perceived as an adaptation measure to increasing flood risk in coastal Bangladesh (Khan et al. 2015), marginalised farmers with small land parcels were unable to transform their lands due to the high costs associated with such a change (Islam et al. 2015).

Globally, a paradigm shift of flood control measures is happening, from a flood prevention towards a risk-based flood management approach. This is due to recent experiences of several catastrophic flood events in many regions around the world (Poussin et al. 2015), as well as projected increases in the frequency and severity of flooding in the future (Koks 2018). Empirical analyses of flood risk support decision-makers to appraise and sequence investments for flood management (Dawson et al. 2011, Hall et al. 2003a, Sayers et al. 2002). Concerning polders, the notion has been changing from ‘flood control to controlled flooding’ (Warner et al. 2018). In Bangladesh, the introduction of Tidal River

Management (TRM) is one example of the nature-based approach, which can potentially alleviate pluvial flooding by increasing land elevation through promoting sedimentation in low-lying areas (Seijger et al. 2019). TRM involves the temporary breaching of embankments to enable sediment-laden river water flow into low-lying depressions twice a day, increasing land elevation by promoting sedimentation, removing channel siltation and reducing salinity intrusion (Masud et al. 2018, Gain et al. 2017). However, the implementation of TRM is a complex process, which needs strong participation and consensus of stakeholders who need to sacrifice their land for 3-5 years, depending on the tidal volume and area of TRM projects (Amir and Khan 2019). Whilst the benefits of TRM are widely reported (Amir and Khan 2019, Gain et al. 2017, Masud et al. 2020), in several cases TRM failed to achieve its full potential in terms of the extent of flood risk reduction.

The problems associated with polder construction in Bangladesh (Gain et al. 2017, Amir and Khan 2019, Warner et al. 2018) and its impacts on land-use change and peoples' livelihoods (Ahmed 2018, Akber et al. 2018, Khan et al. 2015) are reported in the existing literature. In other regions, few studies focus on analysing polders' impact on peak river discharge and river water level (Huang et al. 2007, Heine and Pinter 2012). But overall, there is a lack of quantified evidence on the impacts of (i) polders on the frequency and extent of multiple types of flooding; and (ii) land-use change (a consequential effect of polder construction) on flood risk and associated poverty. In response to diversified problems resulting from flooding in polders in Bangladesh, few studies have conceptualised the benefits of TRM (Gain et al. 2017, Masud et al. 2018) and modelled sediment deposition during TRM implementation (Amir and Khan 2019, Talchabhadel et al. 2018a). Until now, there has not been a scientific study that quantifies the impact of TRM on flooding. This DPhil research, therefore, addresses these limitations by establishing an array of models to provide insights into (i) the polders' effectiveness, to the frequency and extent of flooding;

(ii) flood risk to different land-use scenarios and its impact on poverty; and (iii) the effectiveness of TRM in reducing flooding potential in the embanked region of coastal Bangladesh.

1.2. Aim and objectives of the research

This DPhil research aims to diagnose complex flooding processes and adaptation options, to assess the effectiveness of different flood interventions in the coastal region of Bangladesh. The following research questions are addressed by achieving corresponding objectives:

a) Have coastal embankments reduced flooding in Bangladesh?
   - Analysing past events to diagnose different types flooding.
   - Estimating the extent of flooding that might have occurred had the polders not been constructed.

b) What is the association between land use/land cover (LULC) change and risk of flooding, and how they impact poverty spatially?
   - Estimating flood risk in relation to current and future LULC scenarios.
   - Estimating the change in poverty in relation to a change in LULC and flood risk.

c) How much of the south western delta of Bangladesh can be restored with Tidal River Management (TRM)?
   - Analysing flood mechanisms in the south western embanked region, estimating the influence of various flood causative factors on flood susceptibility.
   - Modelling sediment transportation and deposition in suitable TRM sites and comparing flood susceptibility before and after TRM implementation.

1.3. The case study choice: South western coast of Bangladesh

The coastal region of Bangladesh includes heavily engineered river basins (Day et al. 2016). Following three major cyclone induced surge events in the 1950s, a flood commission was developed by the then Government to investigate the problems and to advise on remedial measures. The government received the assistance of a group of experts on water resources management, working under the UN Technical Assistance Mission in 1956, known as the Krug Mission. This Mission submitted the 'Krug Mission report' in 1957 after analysing the complex problems associated with the flooding. The Krug Mission Report's recommendations primarily emphasized on structural flood control through a system of dykes and polders as higher flood control through major water control schemes was perceived to be the key to increase agricultural production. Based on the recommendations of the Krug Mission, the East Pakistan Water and Power Development Authority (EPWAPDA) (now the Bangladesh Water Development Board (BWDB)) was created in 1959, who started the construction of polders in the 1960s as part of a major Coastal Embankment Project (CEP) (Ali 2002, Mirza and Ericksen 1996). Subsequently, from the 1960s to 1980s, a total of 139 polders have been constructed (Figure 1.1 (b)) throughout the coastal region of Bangladesh (Warner et al. 2018, Islam et al. 2016b).

This research focuses on the polders in the south western coastal region of Bangladesh (Figure 1.1 (c)), as (1) the area is prone to flooding from multiple sources (Haque et al. 2018, Haque and Nicholls 2018); (2) it has been experiencing significant changes in land use which potentially impact flood risk and subsequently, the livelihoods of the inhabitants (Rahman et al. 2017, Khan et al. 2015, Parvin et al. 2017); and (3) Tidal River Management (TRM) has been tested in the area in response to increasing land subsidence and pluvial flooding (Gain et al. 2017, Masud et al. 2020, Amir and Khan 2019). The study area covering 5187 km^2 of land includes 44 (out of 139) polders, located in five

coastal districts: Bagerhat, Jessore, Khulna, Pirojpur, and Satkhira (WARPO 2018). Approximately, a total of 5.3 million people inhabited in 2015 in the study area (WorldPop 2018). The area is characterised by a unique brackish water ecosystem, low-lying alluvial landscape, heavily intersected by tidal rivers, and water-filled depressions (locally termed 'beel'). The river system is highly active, carrying a large concentration of sediments (Nishat et al. 2010).

The rate of population growth in the coastal districts of Bangladesh is low (Szabo et al. 2018). In the case of south western polder area, the average annual population growth rate of 0.15% between 2000 and 2010 has decreased to 0.042% within the period 2011-2019 (WorldPop 2018). Such change in population growth rates can be relatable to a low fertility rate due to sociodemographic change and increase in out-migration rates due to environmental stresses, economic vulnerability and prospects of remittance income in coastal Bangladesh (Szabo et al. 2018).

The south western coast has been experiencing major changes in land use over the past two to three decades, with a significant proportion of agricultural lands being transformed into aquaculture use, especially brackish water shrimp farming (Mukhopadhyay et al. 2018, Abdullah et al. 2019, Rahman et al. 2020). Approximately 80% of the total shrimp ponds of Bangladesh are located in south western coast (Ahmed 2018). Agriculture, shrimp farming, and the natural resources of the Sundarban mangrove forest (located in the south of the study area) are the major sources of livelihoods and economy of the inhabitants (Khan et al. 2015).

Generally, most climate adaptations in deltas are related to agriculture and fisheries (Arto et al. 2019). The contribution of agriculture and fisheries to the GDP in deltas of developing countries, such as the GBM delta, is higher than that of developed countries (Arto et al. 2020). In 2011, the GDP per capita in the Bangladesh side of the GBM delta was

higher than the rest of the country (Cazcarro et al. 2018). In Bangladesh, the International Monetary Fund (IMF) predicted an annual average GDP per capita growth of 7.3% between the years 2020 and 2030. The study area has an increasing trend of GDP per capita growth, with an annual growth rate of 1.14% between 1990 and 2015. However, the extent of increase in annual GDP per capita growth rate is low compared to the national average of 4.04%, for the same years (estimated using data from Kummu et al. (2018)). A lower rate of GDP per capita growth may be associated with the increasing soil salinity which impairs agricultural production (Johnson et al. 2016). The situation potentially affects the livelihoods of the poorest segments of society (Szabo et al. 2016, Borgomeo et al. 2017). Transformation of lands to aquaculture use (e.g. brackish water shrimp farming) is one of the main causes of biodiversity degradation, increasing soil salinity (Lázár et al. 2020, Borgomeo et al. 2017). Such a transformation of lands has been a common practice in the area since the 1980s as it can be more profitable (Khan et al. 2015). Although net profit from shrimp cultivation is twelve times higher than high yielding rice varieties, shrimp farming is reportedly less profitable for the poor and marginalised farmers. This is due to low employment rates in shrimp farming and a lack of access of poor farmers to the international market (Johnson et al. 2016).

In response to increasing land subsidence and pluvial flooding, TRM has been tested in a few selected locations in the south western embanked area (Gain et al. 2017). TRM involves temporary breaching in polders to allow sediment-laden tidal water in low-lying depressions (locally termed as ‘beel’) for enabling natural silt deposition during ebb tides (Masud et al. 2018). An explicit engagement of landowners is necessary to implement this approach, as lands become unsuitable for agricultural activities during the implementation period (Mutahara et al. 2018). Historically, this water management practice was a community-driven approach. Before the construction of polder in the 1960s, local

communities would build temporary earthen embankments for 8 months to prevent saline water intrusion. Water was permitted to enter during the monsoon season (when salinity level was low) through breaching in embankments (Nowreen et al. 2014, Nishat et al. 2010). Whilst the construction of polders increased agricultural productivity until the 1980s, drainage congestions and the subsequent waterlogging problem began to emerge afterwards, deteriorating socio-economic conditions of the local people and damaging ecosystem services (Gain et al. 2017). As a result, the local people initiated 'public cuts' of the polders to relieve drainage congestion in the early 1990s, a process which was later overtaken by the Bangladesh Water Development Board (BWDB) after strong public protests. Institutionally, the process was termed 'Tidal River Management' (TRM)' (Nowreen et al. 2014). In between 1991 and 2013, TRM has been tested (either by local people or the BWDB) in 12 out of 35 designated 'beels' in the south western coastal zone (Masud et al. 2018, Gain et al. 2017). TRM has resulted in mixed outcomes in terms of its impact on society and the environment. Evidence from an existing study suggest that although TRM makes 'beels' unsuitable for agricultural activities, a successful implementation of this approach results in a greater financial benefit from agricultural sector, compared to 'beel' where TRM was not implemented (Masud et al. 2020). However, this measure requires scientifically informed decision-making, along with strong community participation, particularly in selecting suitable TRM sites.

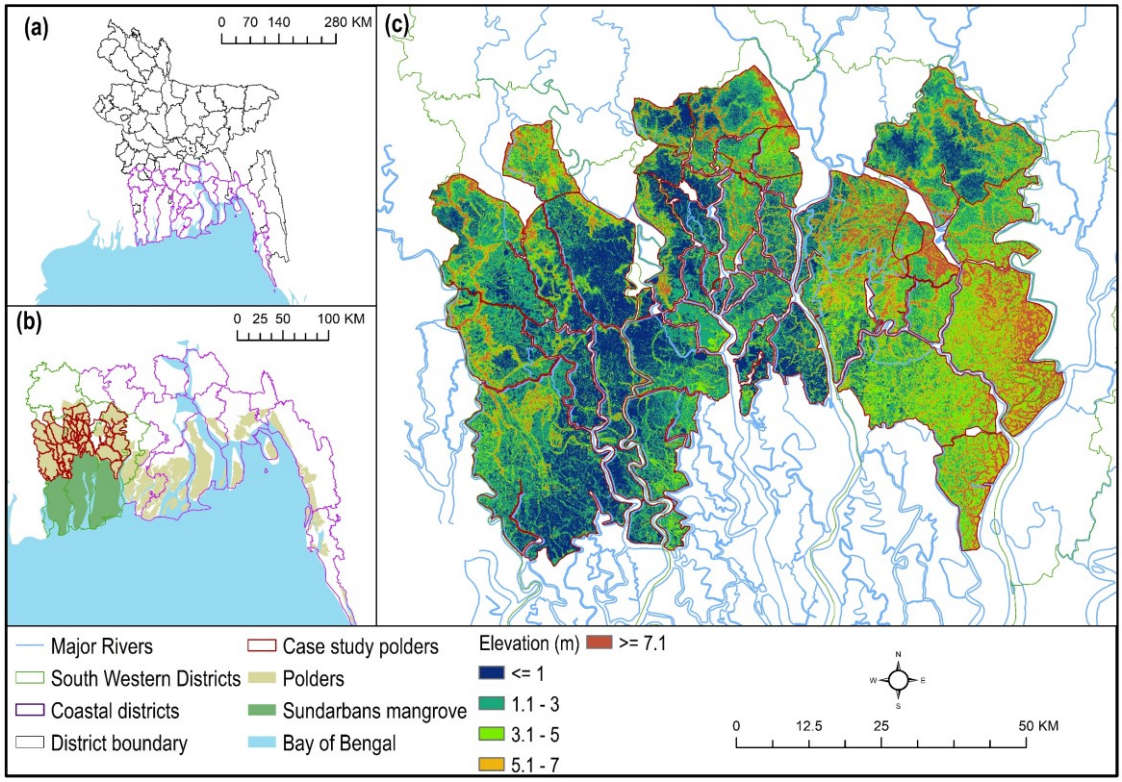

Figure 1.1 Case study area

1.4. Structure of thesis

This thesis follows the guidelines, of the School of Geography and the Environment of the University of Oxford, for an article-based thesis. The thesis is divided into six chapters. Following the introduction, Chapter 2 presents a critical discussion on challenges in diagnosing the impacts of different coastal flood adaptation options in a complex system, based on an extensive review of the existing literature. This chapter supports the theoretical and methodological development of the thesis. This includes a discussion on various challenges in understanding coastal flood dynamics, flood risks in changing environments, and the effectiveness of measures to mitigate future risks.

Chapter 3 addresses the first research question by investigating the effect of polders on different types of flooding through remote sensing-based flood observation, flood event classification, and flood modelling. This chapter develops a modelling framework that estimates the inundation extent from pluvial, fluvio-tidal, and storm-surge flooding within

embankment protected portions (i.e., polders) of the south western coastal region of Bangladesh. It also assesses the impact the polders and associated land subsidence have had on the extent of flood inundation throughout the study region.

Chapter 4 presents a spatio-temporal appraisal of poverty to land use/land cover (LULC) change and pluvial flood risk in the south western embanked region of Bangladesh. This chapter utilises a LULC change model to predict LULC of the near future (e.g. 2030) based on historical LULC data. It estimates flood risks at present and for future LULC scenarios, hypothesising that LULC changes influencing flood risks in the region. Finally, it also estimates poverty, in terms of the Wealth Index (WI), to flood risk and LULC change, along with other socio-economic and spatial parameters. The results indicate the extent to which the WI in the study region is likely to change in the future compared to the present-day scenario.

Chapter 5 responds to research question three by quantifying the potential effectiveness of Tidal River Management (TRM) in restoring land elevation and reducing flood susceptibility in the south western embanked region of Bangladesh. This chapter identifies suitable sites to implement TRM to model sediment deposition in those areas. The potential impact of TRM on flooding is investigated by comparing flood susceptibility 'before and after' the implementation of TRM.

Chapter 6 presents the conclusions of the thesis. The chapter first summarises the thesis. Then theoretical contributions and practical implications of this research are explained. Finally, I provide an outlook for future research.

1.5. Methodological overview

This research uses a combination of statistical, geospatial, and hydrodynamic approaches to diagnose complex flooding processes and adaptation options in the coastal region of Bangladesh. This section provides a brief overview of the methods used in this

research (Figure 1.2). However, detailed explanations and justifications of the research methods are given in chapters 3, 4, and 5.

1.5.1. Flood observation and classification

To perform an ex-post evaluation of coastal embankments, past flood events in the coastal zone in Bangladesh are analysed. A combination of remote sensing-based and statistical approaches is used. Remote sensing data are analysed to detect the extent of inundation in every year between 1988–2012 within the south western embanked region of Bangladesh. An emergence of high-resolution open-source satellite images in the last few decades has prompted the development of various remote sensing techniques for detecting flood inundation. Among various remote sensing-based methods (Wang et al. 2002, Sanyal and Lu 2004, Demirkesen et al. 2007, Jain et al. 2005), water-indexing techniques have proved to be very useful for quick flood detection (Sarp and Ozcelik 2017). A well-known water indexing technique called the Modified Normalized Difference Water Index (MNDWI) (Xu 2006) is applied to detect water surfaces from remote sensing imagery during pre (dry) and post (wet) monsoon period in a year. Then a change detection algorithm is used in Geographic Information System (GIS) to identify cells that changed from being normally dry to wet, which are classified as flood cells for that year. The observed flood inundation data has been utilised in this research to (i) identify and classify flood events (chapter 3); (ii) validate pluvial flood model (chapter 3 and 4); and (iii) generate training and test datasets for flood susceptibility model (chapter 5).

Whilst identification of flood inundations using remote sensing data provides spatial information of inundation extent, the process is unable to detect the sources of flooding. To attribute the observed floods to different types of flooding (i.e. pluvial, fluvio-tidal, and storm surge), the severity of monsoon rainfall and elevated water levels within the region are analysed. Flood frequency analysis has been carried out by fitting to a generalized

extreme-value (GEV) distribution using the L-moment method (Coles et al. 2001, Gilleland and Katz 2016). Several recent studies have conducted extreme value analyses to quantify the relationship between hydro-meteorological patterns and flood types (Nied et al. 2014, Singh 2017, Santos and Fragoso 2016). In this research, outputs from flood frequency analysis are integrated with the observed flood inundation data to optimise the thresholds of hydro-meteorological records triggering flood events (chapter 3). Flood frequency analysis has also been carried out to estimate recurrence intervals of the monsoon precipitation to estimate pluvial flood risk (chapter 4).

1.5.2. Simulating flood hazard

A pluvial flood rainfall-runoff and spreading model (Diaz-Nieto et al. 2011) is established to (i) simulate the effect of polders on pluvial flood severity (chapter 3), and (ii) quantify flood risk (chapter 4). A Thornthwaite and Mather (TM) water balance model (Thornthwaite and Mather 1957) is accompanied with the flood model, which estimates monthly excess precipitation at each grid cell, after subtracting evapotranspiration from monthly total precipitation. Monthly excess precipitation from May to October (monsoon) are aggregated to prepare excess precipitation layers during the monsoon. Whilst there exists many hydrodynamic flood hazards models (Apel et al. 2009), simulating flood inundation over a large area using those models is often computationally expensive (Diaz-Nieto et al. 2011). Besides, those models require high-resolution topographic data and detailed hydraulic information (Chen et al. 2009), which are unavailable in the studied region. Therefore, in this research, a GIS-based flood hazard model is established using open-source DEMs for hydrological applications. The similar modelling approach has been followed in several recent studies to simulate surface water flood inundation (Chen et al. 2009, Diaz-Nieto et al. 2011, Liu et al. 2003, Liu and Wang 2008, Jones et al. 2008).

To quantify polders' impact on multiple types of flooding, two scenarios are developed: 'with' and 'without' polders. To simulate pluvial inundation 'with' polders, the exiting DEM is used. The construction of polders eliminated the annual deposition of sediments on the embanked region, whilst compaction of sediment and anthropogenic activities exacerbated land subsidence. This research assumes that 'without' polders, there would not have been any land subsidence. Therefore, the observed DEM is reconstructed by adding total land elevation loss since the construction of polders in the 1960s, estimated using yearly land subsidence rates documented by (Brown and Nicholls 2015). The reconstructed DEM is used to simulate pluvial flood inundations in the 'without' polder scenario. To simulate the effect of polders on the severity of fluvio-tidal and storm surge induced floods, the Delft 3D hydrodynamic model (Haque et al. 2018) is used to estimate inundation extent from fluvio-tidal (1998) and storm surge flooding (2007) for 'with' and 'without' polder scenarios.

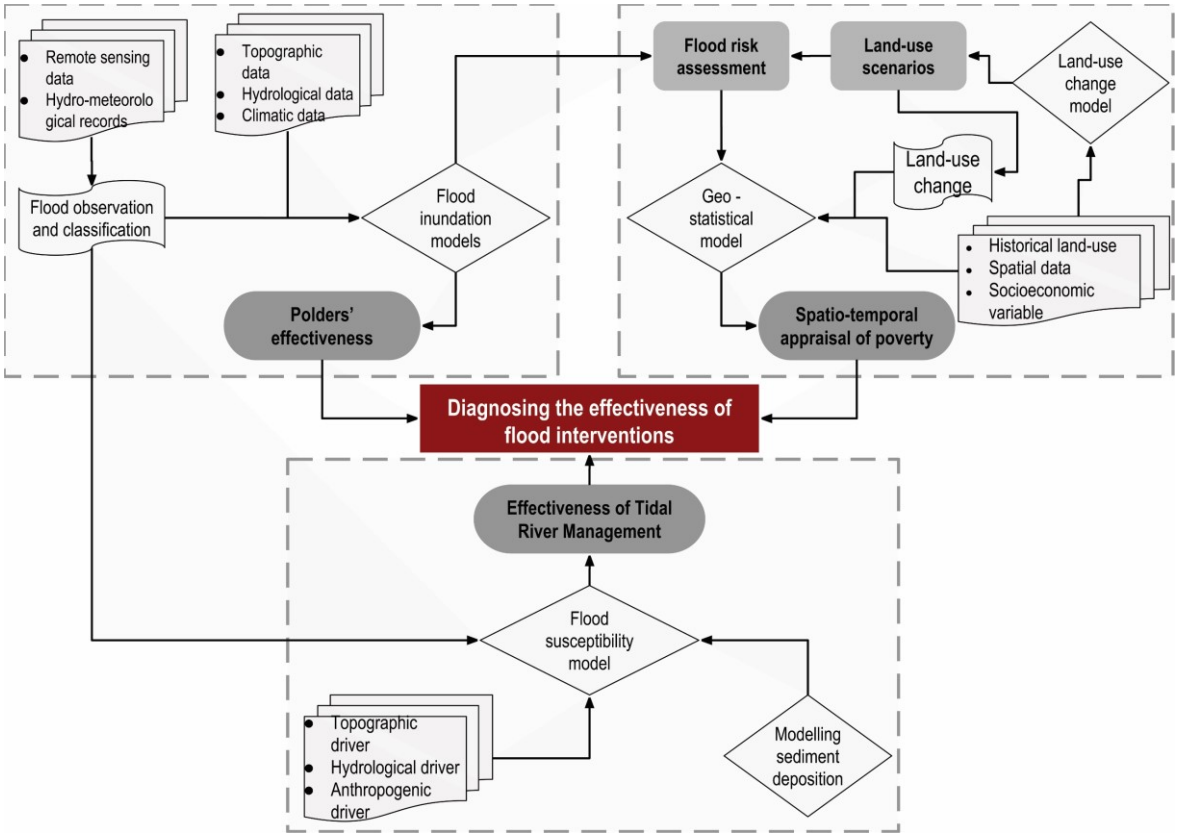

Figure 1.2 Methodological overview

1.5.3. Modelling land-use change and estimating flood risk

To understand the existing pattern of land-use change and predict future land-use, a spatial model is established (chapter 4). The land-use change model used in this research is a combination of logistic regression (LR), cellular automata (CA), and Markov Chain models (Arsanjani et al. 2013). This widely used modelling approach has been followed in several recent studies for detecting and simulating land-use change (Mitsova et al. 2011, Kityuttachai et al. 2013, Shahbazian et al. 2019, Wang et al. 2019). In this research, this approach has been applied for following reasons: (i) it can incorporate both environmental and socio-economic variables; (ii) the model can integrate a wide range of spatial factors; (iii) the LR model can use data at different scales; and (iv) the CA model can control spatial dynamics of land-use changes (Arsanjani et al. 2013, Shahbazian et al. 2019).

To understand the association between land-use change and flood risk, flood risk assessment is carried out for various land-use scenarios. A traditional approach of flood risk assessment is followed where risk is the product of flood hazard and vulnerability of exposed communities. In the absence of structural level land-use data and local-level flood damage functions, the scope of flood risk assessment in this research is limited to the estimation of direct flood damages for various categories of land-use. Pluvial flood inundation model developed in chapter 3 has been used to derive flood inundation maps of various recurrence intervals of monsoon precipitation. To analyse flood vulnerability, country scale depth-damage curves have been adopted from Huizinga et al. (2017) and Islam et al. (2019).

1.5.4. Developing geo-statistical model of poverty

This research hypothesises that unplanned land-use change and increasing flood risk influence the livelihoods of people inhabit in the south western embanked region. Thus, it seeks to quantify the impact of land-use change and flood risk on poverty. Poverty has been estimated in terms of the Wealth Index (WI). A GIS-based ordinary least square (OLS)

model is developed incorporating a gridded WI data developed by Steele et al. (2017) as a dependent variable and land-use change, flood risk, and various socioeconomic and spatial parameters as independent factors. The WI is estimated at present-day and future scenarios of land-use change and flood risk.

1.5.5. Modelling flood susceptibility

Chapter 5 of this thesis aims to assess the potential of Tidal River Management (TRM) for flood alleviation in the south western embanked region of Bangladesh. The influence of TRM has been quantified in relation to its ability in reducing flood susceptibility. The pluvial flood hazard model, developed in this research (chapter 3), shows that a change of geomorphological changes due to land subsidence impacts the extent of flood inundation. TRM aims to increase land elevation, a process which would potentially alter various geomorphological and hydrological processes (Tehrany et al. 2014a, Khosravi et al. 2016, Pradhan et al. 2010). The flood susceptibility model developed in this research aims to determine the changes in various flood causative factors resulting from a change in land elevation due to TRM. To develop the model, a combination of the bivariate frequency ratio (FR) and multivariate logistic regression (LR) models (Tehrany et al. 2019b, Tehrany et al. 2014a) has been applied. Remote sensing-based flood observation data, obtained in chapter 3, is used to develop and validate the model. Potential TRM sites have been delineated using the DEM-based flood routing model established in chapter 3. As there is no government regulation to select TRM sites, GIS-based suitability analysis is performed to identify suitable locations for TRM. River bathymetry and measured sediment concentration data are not available for the whole area under study. Therefore, simulated sediment deposition data is collected from Talchabhadel et al. (2018a) for a few sample TRM sites in a polder. Based on the simulated sediment deposition in sample TRM sites, sediment deposition in remaining suitable locations is parameterised, developing an ordinary

least square (OLS) regression in GIS. To quantify the impacts of TRM, the changes in land elevation and flood susceptibility for pre- and post-TRM implementation scenarios are compared.

Chapter 2 Challenges in understanding the impacts of different flood adaptation options in complex deltaic coastal systems and possible ways forward

2.1. Introduction

Deltaic coastal systems are complex, as numerous factors, particularly related to topographic, atmospheric, ecological, hydrological, and anthropogenic environments interact dynamically (Wright et al. 2019b, Day et al. 2016). Flood exposure in coastal cities has been increasing due to growing populations and associated assets, climate change-induced sea level rise, and anthropogenic land-use changes (Karamouz et al. 2019, Bilskie et al. 2014, Syvitski et al. 2009, Day et al. 2016). In 2005, the average global flood losses were estimated at US$6 billion per year, which is likely to increase to US$52 billion by 2050 as a result of projected socio-economic changes (Hallegatte et al. 2013). The number of people exposed to extreme coastal flooding (e.g. a 100-year storm surge event) is the highest in Asia, particularly in Bangladesh, China, India, Indonesia, and Vietnam. The trend of increasing flood exposure in those countries is also expected to continue (Neumann et al. 2015). In order to diagnose flood adaptation options in deltaic regions, especially those located in developing countries, it is essential to understand the complex connections between biophysical and socio-economic environments (Cazcarro et al. 2018).

While the paradigm of the 'flood control approach' has shifted towards 'flood risk management' (Merz et al. 2010b), the choice of risk-reducing measures requires a careful evaluation of their potential impacts. It is well recognised that the choice of flood risk management plans, strategies, and measures is subject to uncertainties (Hall 2014, Penning-Rowsell and Korndewal 2019); Hall (2014) explicitly argued that flood risk management is 'a process of decision making under uncertainty'.

The decision to adopt effective coastal flood risk-reducing measures could be hindered by several challenges associated with limited understanding of coastal flood processes and risks, as well as potential impacts of adaptation measures. Diagnosing the impacts of different coastal flood adaptation options is a complex process, due to various challenges in understanding coastal flood dynamics, flood risks in changing environments, and the effectiveness of measures to mitigate future risks. The following sections present a critical discussion on these challenges based on an extensive review of the existing literature, which support the theoretical and methodological development of the thesis. Section 2.2 provides an overview of sources of coastal flooding, influences of structural flood defences on the coastal floodplain, and challenges in evaluating the impacts of historical flood interventions. Section 2.3 outlines the challenges in quantifying flood risk. Section 2.4 summarises the challenges in evaluating potential flood risk reduction measures. Section 2.5 outlines different pathways to address the challenges discussed in the previous sections. Section 2.6 summarises the chapter.

2.2. Challenges in understanding complex coastal flood processes

2.2.1. Multiple sources of floods

Various types of floods could affect coastal regions, such as Tsunami, storm surges, tidal, fluvial, and pluvial floods (Wright et al. 2019a). These floods could either occur from a single source or multiple sources, creating compound events (Lian et al. 2013). Floods in the coastal region of Bangladesh are caused by several interrelated physical drivers. Five types of floods occur in the region: (i) pluvial, (ii) fluvial, (iii) tidal, (iv) fluvio-tidal, and (v) storm surges induced by tropical cyclones (Haque and Nicholls 2018, Rahman and Salehin 2013). The diversified physical characteristics of the region create a complex flood regime. Tidal flooding is largely dictated by daily regimes of astronomical tides. Tidal heights could range from 2-4 m in the western and central coasts (Paul and Rashid 2017). Fluvial and

fluvio-tidal floods depend on the flow in the upstream major rivers (the Ganges, Brahmaputra, and Meghna) of the delta, which are associated with the magnitude of precipitation in the upstream river catchments (Haque and Nicholls 2018). The region is also prone to storm surge-induced flooding, caused by tropical cyclones in the Bay of Bengal. This form of flooding primarily occurs either in the pre-monsoon or post-monsoon seasons (Rahman and Salehin 2013). Pluvial flooding is the most frequent form of flooding in the region, particularly in polders in the south western coast. Increasing land subsidence inside the polders, inadequate drainage, and unreliable operation of sluice gates are reportedly associated with prolonged inundation during the monsoon seasons (Auerbach et al. 2015, Van Staveren et al. 2017).

Tidal or storm surge induced floods have been well-researched in different coastal regions. For example, the existing studies related to storm surge modelling in Bangladesh have major focuses on (i) quantifying the magnitude and extent of inundations (Haque et al. 2018, Islam et al. 2019); (ii) understanding the impacts of coastal land use (e.g. Mangroves) on the extent of inundation (Deb and Ferreira 2017); (iii) simulating compound flood events (e.g. fluvial and storm surge) (Ikeuchi et al. 2017); and (iv) estimating risk to storm surge flooding in a polder (Islam et al. 2019). Few studies have been conducted on modelling the fluvio-tidal flooding system (Haque et al. 2018).

In recent years, pluvial flooding has received growing global attention, due to its potential to pose a threat to populations in areas that are typically not at risk from flooding (Bubeck et al. 2017). But, the consequences of pluvial flooding are uncertain, as they depend on the spatial distribution of inundations, rainfall variability, and spatial variation of population density, property, and activity centres. Therefore, managing future pluvial flood risk is difficult, as decision-makers are often uncertain about what strategy to adopt when managing this uncertain risk (Penning-Rowsell and Korndewal 2019). Pluvial flooding in

coastal Bangladesh has received relatively less attention compared to other forms of flooding. This type of flooding, particularly in polders, has largely been understood in terms of waterlogging, where drainage congestion is being attributed to being the main cause of flooding (Alam et al. 2017, Tareq et al. 2018). But the process by which geomorphological and hydrological changes affect pluvial flooding is largely unknown.

Notably, evidence from various studies suggests that compound events (e.g. various combinations of the surge, fluvial, and pluvial floods) pose greater damage potential in coastal regions (van den Hurk et al. 2015, Wahl et al. 2015, Ikeuchi et al. 2017). Compound events are usually driven by similar meteorological conditions. For instance, deep cyclones are the result of low-pressure conditions that could cause both storm surge inundations and pluvial flooding due to heavy precipitation (van den Hurk et al. 2015).

2.2.2. Flood defence and environmental change

Implementation of flood control measures, which generally aim to reduce the probability of flooding (Merz et al. 2010a), could increase complexities in coastal flood processes. It is widely accepted that the construction of flood defences affects the hydrological regime of a floodplain. But, it is difficult to quantify the effects of flood control measures (Morrison et al. 2018), as the dynamic interplay between societies and hydrological extremes could alter the frequency, magnitude, and spatial distribution of flood events (Di Baldassarre et al. 2017). For instance, embankments, dykes, and levees (Bamberg et al. 2017) tend to change hydrological (Montz and Tobin 2008), ecological, geomorphological, and anthropogenic environments of floodplains (Hupp et al. 2009, Gergel et al. 2002, Morrison et al. 2018, Steinfeld and Kingsford 2013). Such interventions generally disconnect a floodplain from a sediment-laden flow, which may lead to a change in floodplain geomorphology (Hupp et al. 2009, Gergel et al. 2002, Morrison et al. 2018). The dynamic and complex interactions between flood defences and biophysical

characteristics of a riverine floodplain, make the quantification of cumulative effects of flood defences a challenging task (Morrison et al. 2018). Studies aimed at assessing the impacts of flood defences primarily concentrate on estimating changes in the (i) extent of the wetland areas (Morrison et al. 2018); (ii) fluvial flow dynamics (Stone et al. 2017); (iii) floodplain geomorphology (Hupp et al. 2009); and (iv) flow velocity, frequency, and duration of inundations (Gergel et al. 2002). These studies have largely been concentrated on fluvial flooding.

The Coastal Embankment Project (CEP) in Bangladesh is a classic example of how a human intervention alters the geomorphological characteristics of an active delta. The construction of polders led to a change in geomorphological and hydrological conditions in the coastal region. The presence of polders has disrupted sediment supply in low-lying islands, particularly in the south western coastal zone, whilst accelerating sedimentation in adjacent riverbeds and increasing river water levels, preventing the gravity drainage system within the embanked region from functioning (Mutahara et al. 2018). Auerbach et al. (2015) estimated that due to a lack of sedimentation in the south western embanked region, associated subsidence has reduced land elevation inside a polder by approximately 100 cm, compared to the adjacent Sundarban Mangrove forest. A lower elevation was attributed to a greater extent of tidal inundation during Cyclone Sidr in 2007, which caused breaching in a few polders and extensive waterlogging. In addition, subsidence can also exacerbate the frequency of localised flooding (Brown and Nicholls 2015). Various studies have indicated that more frequent floods (e.g. pluvial), although less severe, contribute the most to overall damage (Ramirez et al. 1988). In polders, surface runoff, particularly during the monsoon season, frequently inundates the low-lying depressions (locally termed as ‘beels’) (Talchabhadel et al. 2018a). Although several studies have reported the increasing problems of surface water inundation inside polders, there has not been any scientific evidence on the

extent to which the construction of polders has contributed to increasing pluvial flood hazard.

2.2.3. A lack of scientific understanding of the impacts of historical flood interventions

The unavailability of a long time-series record of hydro-meteorological trends can limit the understanding of the impacts of historical flood interventions. A few studies have assessed the impacts of flood interventions such as polders empirically, using the hydro-meteorological gauge data with a long time-series record (Choudhury et al. 2004, Heine and Pinter 2012). For instance, Heine and Pinter (2012) evaluated the hydrological response to levee construction in Illinois and Iowa, using hydrological gauge records of more than 50 years. A long time-series data enabled the study to quantify the stage changes between the pre-levee and post-levee scenarios. The availability of hydrological observations for the pre-levee periods is ideal for conducting such a study. Other studies conducted a benefit-cost analysis to evaluate flood investments (Ramirez et al. 1988, Palanisami and Easter 1984), which similarly require a long time-series of flood damage estimates, particularly from the pre-investment scenario.

In relation to flood risk management in the coastal region of Bangladesh, there has been a lack of scientific understanding on beneficial and/or harmful effects of historical flood interventions. Most of the studies focusing on coastal flooding have concentrated on predicting floods, particularly under present and future climate change scenarios (Haque et al. 2018). A few studies have been conducted to quantify (i) the impact of Tidal River Management (TRM) on agricultural production (Masud et al. 2020); and (ii) the impact of coastal embankments on land elevation (Auerbach et al. 2015). None of these diagnosed what flooding might have been had these interventions not been implemented. For instance, Masud et al. (2020) evaluated the impact of TRM on flooding by comparing land use before and after the implementation of TRM in a few locations. They concluded that the

implementation of TRM resulted in a reduction of the percent share of areas underwater. This result is based on a major assumption that hydro-meteorological conditions were similar before and after the implementation of TRM. Evaluating the impact of such interventions is a complex process because flooding is an outcome of various combinations of geomorphological, hydrological, and anthropogenic processes (Tehrany et al. 2014a, Khosravi et al. 2016, Pradhan et al. 2010).

2.3. Challenges in understanding flood risk

The scope of flood risk assessments can range from global (Ward et al. 2017, Neumann et al. 2015, Vousdoukas et al. 2018, Ward et al. 2015) to national (Hall et al. 2003a, Hall et al. 2003c, Hall et al. 2006), city (Hallegatte et al. 2011, Lin et al. 2010, Hall et al. 2019), and local scales (Youssef et al. 2011). The implications of flood risk assessments vary according to the scale and scope. For instance, global assessments enable understanding of the risks at a country scale, where the impacts of projected global climate change can be better understood. National flood risk assessments aim to assess the relative adverse consequences of flooding across the country, which inform the identification of those areas most vulnerable to the impacts of flooding, is required to formulate policies (e.g. spatial planning) to guide future development (Penning-Rowsell et al. 2019, Hall et al. 2003a). Local-level risk assessments enable one to understand risks to a community or building (Ward et al. 2015).

The traditional approach of a risk assessment considers risk as a product of hazard and vulnerability, where risk is expressed in terms of the expected loss (of lives, persons injured, property damaged, and economic activity disrupted). The methods used in research and practice for quantifying flood hazard and vulnerability range from simple approaches (with numerous simplifying assumptions) up to very complex applications, which are data-intensive and computationally expensive (Apel et al. 2009). There are multiple sources of

uncertainties in flood risk analyses (Beven and Hall 2014), which add to its complexity, as for instance:

(i) Natural variability in loadings (e.g. rainfall, marine waves, and river discharge), which make their future predictions uncertain (Sayers et al. 2002, Chandler et al. 2014);

(ii) Inaccurate measurements and limited record lengths of gauged data on hydro-meteorological parameters create uncertainty in flood event identification through flood frequency analysis (Kjeldsen et al. 2014);

(iii) Uncertainty in flood inundation modelling from errors in the model and input data (Bates et al. 2014); and

(iv) Data issues, model biases, and conceptual misunderstandings could create uncertainty in flood loss assessments (Chatterton et al. 2014).

This section provides a discussion on the complexities in flood risk assessments in relation to (i) quantifying hazard; (ii) analysing vulnerability; (iii) temporal dynamics of land-use change; and (iv) extent of societal impacts of flood hazard.

2.3.1. Methods to quantify flood hazard

Flood hazard analyses provide an estimation on the extent and magnitude of floods, given the hydro-meteorological conditions, and identify assets that would be exposed to flooding (Apel et al. 2009). Flood frequency analysis is a simple approach to represent flood hazard, where the probability of exceeding a certain degree of hydro-meteorological conditions is estimated. The availability of a long time-series of hydro-meteorological observation data is essential for the application of this approach. To analyse flood hazard over a large region with homogenous characteristics, regional frequency analysis can be done (Rao and Hamed 2000). Through the application of this approach, uncertainties can be generated due to the unavailability of station data over a large domain, small data series,

heterogeneity of a region studied, the inappropriateness of the extreme value functions applied, and large standard deviations in the extrapolated range (Salman and Li 2018, Apel et al. 2009).

Generally, flood hazards are represented by hazard maps, which could include information on the depth and extent of inundations, flow velocity, and duration of inundations (Ward et al. 2011). For flood vulnerability assessments, two categories of hazard models are generally used: deterministic and probabilistic. Deterministic models consider a direct relationship between geomorphological factors and hydro-meteorological conditions while developing flood hazard maps (Thompson and Frazier 2014, Lian et al. 2013). Depending on the degree of complexities, deterministic models could range from a simple linear interpolation approach to 1D and 2D hydraulic models (Apel et al. 2009), as well as 3D numerical models (Haque et al. 2018). Whilst the deterministic models analyse the physical characteristics of flooding in relation to '(a) the hydraulic loading and failure behaviour of structural and non-structural coastal flood defences, and; (b) the hydraulic propagation of floodwaters into the landward floodplain' (Narayan et al. 2012), they do not analyse a range of scenarios, such as changing topological and anthropogenic influences on flooding (Thompson and Frazier 2014). Deterministic models are criticised because, even if well-calibrated, the model could perform poorly when it is used to predict floods with different input parameters (Di Baldassarre et al. 2010). Therefore, this approach is not suitable as a decision support system for planning future adaptation measures in a large and dynamic coastal system (Narayan et al. 2012). Nonetheless, deterministic models could be useful in the understanding of ex-post evaluation of flood interventions (Ramirez et al. 1988).

On the other hand, probabilistic models estimate the degree of flood susceptibility in an area. These models assume that areas at lower risk of flood hazard could still be

susceptible to flooding, provided it has similar characteristics of flood causative factors to that of a high-risk area. Probabilistic models are useful in sequencing and prioritising flood adaptation measures, as they characterise an area according to various degrees of flood risks (Thompson and Frazier 2014). Various probabilistic models have been used in the existing literature (Di Baldassarre et al. 2010, Thompson and Frazier 2014, Apel et al. 2006).

The emergence of high-resolution remote sensing data has advanced statistical models and machine learning techniques in flood hazard mapping (Tehrany et al. 2019a, Tehrany et al. 2019b). Machine learning techniques include approaches such as decision trees (DT) (Tehrany et al. 2019a), support vector machine (SVM) (Tehrany et al. 2019a, Tehrany et al. 2014b, Mojaddadi et al. 2017), and artificial neural networks (ANNs) (Kia et al. 2012). These methods could be disadvantageous, as they are computationally expensive and establishing these models is complex. Bivariate statistical analysis (BSA) and multivariate statistical analysis (MSA) are also widely used in flood hazard mapping. Weight of Evidence (Tehrany et al. 2014b, Khosravi et al. 2016, Tehrany et al. 2017), Frequency Ratio (Khosravi et al. 2016, Tehrany et al. 2017, Mojaddadi et al. 2017), and Evidential Belief Functions (EBFs) are a few examples of BSA, while Logistic Regression (Tehrany et al. 2014a, Pradhan 2010) is one of the most popular MSA approaches (Tehrany et al. 2019b). A qualitative approach such as the analytical hierarchy process (AHP) has also been used recently in flood mapping (Khosravi et al. 2016, Kabenge et al. 2017). Combination of different methods can yield a better prediction accuracy. For example, various studies applied a combination of FR and LR models, as using an ensemble of two models reduces variance-error and provides reasonable prediction accuracy (Althuwaynee et al. 2014).

2.3.2. Methods to quantify flood vulnerability

Flood vulnerability analyses aim to quantify the detrimental effects on human lives and assets by flooding. Like hazard models, vulnerability models also vary according to the degree of complexity (Apel et al. 2009). Methods used in research and practice for vulnerability assessments range from a simple stage-damage function to comprehensive assessments of flood effects (including inundation depth and duration, flow velocity, and resilience) (Shah et al. 2018). The complexity of stage-damage functions, however, varies according to the scales considered. For instance, meso-scale stage-damage functions consider the relationship between flood damage and flood depth in a linear function. Meso-scale flood loss estimation models calculate flood losses at the land-use level for a few discrete categories of flood depths. These models can also be used at the individual building level, a process called micro-scale flood loss estimation (Apel et al. 2009).

Accurate measurement of flood losses is one of the main challenges when assessing flood risk comprehensively. Poor understanding of the impacts of floods could lead to an underestimation of risk (Chatterton et al. 2014). An increase of complexities in vulnerability assessments can be associated with an increase in heterogeneity of population, economy, land-use, and ecology of the studied region (Gao et al. 2014). However, according to Meyer et al. (2009), the choice of risk assessment approach is a trade-off between accuracy and effort. Although micro-scale approaches enable the estimation of flood losses accurately, this method is not applicable to a large area such as a river basin, where meso- or macro-scale approaches could be more useful. But, the application of a meso- or macro-scale approach could lead to considerable uncertainties in the results, as damage functions in such approaches are simplified for different broad categories of land uses (Meyer et al. 2009).

2.3.3. Temporal dynamics of land-use change

Land-use change influences both the probability of occurrence of flood events and their consequences (Szwagrzyk et al. 2018, Beckers et al. 2013). Land use and/or land cover (LULC) impacts runoff, affecting elements of the water balance, particularly evapotranspiration. The amount of runoff generated upstream of a river basin determines the peak discharge of the river (Szwagrzyk et al. 2018). At the local level, in the absence of adequate drainage, excess runoff generated from a precipitation event can cause pluvial flooding (Diaz-Nieto et al. 2011). The presence of forest cover, for instance, may reduce catchment discharge by increasing rainfall interception, transpiration, and soil permeability and reducing soil moisture (Rogger et al. 2017, Wheater and Evans 2009). A change of LULC could also alter flood exposure; mangroves and saltmarshes provide protection to inland populations during surge events. Continued accidental (destruction from hazard) or planned (encroachment) land-use change could significantly influence flood risk during future events (Narayan et al. 2012).

There are many driving forces for LULC change in floodplains. Socio-economic changes have been attributed as one of the main drivers of increased flood exposure in coastal cities (Hallegatte et al. 2013). The presence of flood control measures could also promote LULC changes. The notion of the 'levee effect' (White 1945) is well understood in research, that the presence of flood control measures causes an increased vulnerability, due to a false sense of security (Logan et al. 2018, Di Baldassarre et al. 2013). A change of LULC due to flood control measures could also alter the pattern of livelihoods in floodplains, exacerbating poverty. For instance, the CEP in Bangladesh has promoted a rapid LULC change, causing a transformation of agricultural lands into aquaculture (e.g. brackish water shrimp cultivation). Such transformation of lands could lead to a loss of ecosystem

services (Akber et al. 2018), forced migration of rural inhabitants (Rahman et al. 2017), and a poverty trap in the coastal region of Bangladesh (Borgomeo et al. 2017, Islam et al. 2015).

The dynamics of LULC changes increases uncertainties when predicting future scenarios of flood risk (Shah et al. 2018). Many models quantifying flood risk consider the relationship between LULC and flood risk as static (Narayan et al. 2012). Capturing these dynamics within flood risk assessments is complex, and requires accurate predictions of LULC changes and estimations of flood risk in relation to predicted changes.

2.3.4. Societal impacts of flood hazards

There is a general consensus that risk of natural hazards does not depend solely on the magnitude and intensity of hazards, but rather that risk is an outcome of the dynamic interactions of hazardous events with changing natural and anthropogenic environments (Ebert et al. 2010). Floods have a large variety of spatio-temporal impacts on society, which range from direct to indirect as well as from tangible (market goods) to intangible (non-market goods) impacts (Bubeck et al. 2017, Penning-Rowsell et al. 2005). The current state-of-the-art socio-economic flood damage estimation involves two integral steps: (1) determination of flood hazard, which includes modelling the depth and extent of inundation of a flood of a specific frequency, and (2) estimation of damage potential by applying the depth-damage function to flood vulnerable properties or land uses (Messner and Meyer 2006). Whilst measuring direct economic impacts of flood hazard is very common in research and practice, the social impacts of the flood are often ignored or considered in a very limited manner (Chatterton et al. 2014, Meyer et al. 2009).

Direct tangible damage can be measured in a comparable way (e.g. monetary) and is widely assessed by researchers and insurance companies (Bubeck et al. 2017), but intangible impacts are difficult to quantify (Penning-Rowsell et al. 2005). Floods can have long-term impacts on the affected people and communities (Bubeck et al. 2017). Flooding and poverty

coexist particularly within rural communities, as damages caused by recurring flood events can lower quality of life in the communities (Dube et al. 2018). The correlation between flood risk and poverty can go in both directions (Winsemius et al. 2018). For instance, poor people tend to settle in remote low-lying floodplains, due to their access to relatively cheaper lands (Dasgupta 2007). On the other hand, households affected by recurring floods have a higher probability of falling into poverty (Winsemius et al. 2018). Existing studies related to flooding and poverty are mostly qualitative, while a few studies quantified the negative influence of flooding on poverty (e.g. income) (Borgomeo et al. 2017). Studies that have been conducted at a local scale, mainly utilised household survey data to quantify such relationship (Kawasaki et al. 2020). But, at a regional scale, this method would not be feasible, since the collection of household-level data is very expensive and time-consuming. This issue could be addressed by characterising an area according to an indicator of poverty (e.g. income, wealth index) (Winsemius et al. 2018). Nevertheless, spatial correlation between flood risk and poverty has not yet been quantified at a regional scale, particularly in a region like coastal Bangladesh. Whilst understanding the societal conditions is central to decision-making, particularly with respect to effective flood risk management, knowledge on this topic at a catchment or coastal cell-wide scale is limited (Schanze 2006).

2.4. Challenges in understanding the impact of potential risk reduction measures

When flood risk is intolerable, risk reduction measures are implemented. Globally, it is now accepted that a single option is not adequate to reduce risk entirely; a combination of various risk-reducing measures is essential (Shah et al. 2018). The risk reduction options range from physical flood interventions to measures influencing human behaviour (Schanze 2006, Hall et al. 2003c), whilst the scope of flood risk management decisions range from national-level policies to local level operations of risk reduction measures (Hall et al. 2003a). The decision to adopt effective risk reduction measures is subject to uncertainty (Hall 2014).

For example, the construction of polders in coastal Bangladesh resulted in increased agricultural production until the 1980s (Nowreen et al. 2014), but they simultaneously disconnected the floodplain from the river channel network, which has promoted land subsidence in the embanked areas. As a result of increased subsidence and inadequate drainage, the embanked region has been experiencing increased flood inundation (Van Staveren et al. 2017, Auerbach et al. 2015, Alam et al. 2017).

Historically, flood management practices in coastal Bangladesh emerged from the willingness to live with floods. Between the 1960s and the 1980s, flood risk management practices largely concentrated on hard-engineering structures. But biophysical changes resulting from structural measures and increased flood risks create a doubt about the effectiveness of such interventions (Shah et al. 2018). Thus, in practice, researchers and policymakers have been concentrating on finding alternative adaptation measures, encouraging people to adapt to floods. For instance, TRM in Bangladesh, which aims to restore sediments within polders in coastal Bangladesh through controlled flooding (Warner et al. 2018). However, the decision to implement TRM yielded both positive and negative impacts on local communities and environments. Whilst implementation of TRM led to an increase in land elevation in a few locations, the unplanned operation caused riverbank erosion, salinity intrusion, and inundation in built-up areas elsewhere (Gain et al. 2017). Understanding the effectiveness of TRM is particularly complex, as tidal rivers and environments resilience, floodplain ecosystems, human health, and communities all interact on different spatial and temporal scales, impacting the effectiveness of TRM (Masud et al. 2018).

2.5. Possible ways forward

Understanding the impacts of different flood adaptation options in complex coastal systems requires new research that (1) captures the complexities of flood processes and assesses the impacts of historical flood interventions; (2) links the biophysical components

of flood risk with societal impacts; and (3) enables spatial and temporal evaluation of the effectiveness of future adaptation options.

2.5.1. Ex-post evaluation of flood interventions

Ex-post analysis of historical flood interventions can help to understand their effectiveness against complex coastal flood systems. The retrospective analysis provides insights from the past, which could be of significance in understanding the dynamics of flood risk and identifying uncertainties when predicting the impacts of decisions (Penning-Rowsell and Korndewal 2019, Schanze 2006). It indicates how much a decision might have been changed had more information been available at the time of implementation. Such information can help improve decisions on future flood interventions (Ramirez et al. 1988). Short term success of flood control measures does not necessarily ensure risk management in the long run (Shah et al. 2018); ex-post evaluation of flood interventions can provide the necessary information required to make informed decisions on future flood risk management measures.

The emerging remote sensing technology and Geographic Information Systems (GIS) have become an integral part of flood hazard assessment. The availability of high-resolution remote-sensing data enables researchers to monitor floods both spatially and temporally (Rahman and Di 2017). Whilst GIS and remote sensing techniques can detect inundation extents during or after flood events, a lack of information on hydro-meteorological preconditions triggering floods creates difficulties in classifying flood types. However, one can apply statistical hydrology to analyse the flood frequency caused by extreme hydro-meteorological events. This approach could, therefore, be applied when identifying different sources of floods such as extreme rainfall, river discharge, or storm surges (Rao and Hamed 2000). Although flood frequency analysis indicates the magnitude of a flood event, it does not estimate the flood extent. Therefore, integrating remote sensing

and statistical hydrology can provide an understanding of the sources, magnitudes, and extents of historical floods.

As discussed previously, unavailability of flood observation data before the implementation of flood interventions could create a challenge for understanding the effectiveness of historical flood interventions. To conduct an ex-post analysis of flood interventions in areas where data at pre-intervention scenario are unavailable, a deterministic flood model can be established for a counterfactual scenario, for which flood interventions such as coastal embankments will not be considered. This approach requires an accurate simulation of hydrological and geomorphological characteristics of an area, in the absence of flood interventions. For example, in coastal Bangladesh, an absence of polders might have promoted natural sedimentation in low-lying areas, which might have resolved the issue of land subsidence.

The conventional approach of pluvial flood modelling includes analysis of rainfall-runoff under the effects of precipitation at a local scale (Schmitt et al. 2004), where drainage systems are represented using sewer network models. More recently, the availability of high-resolution Digital Elevation Models (DEM) facilitates the evolution of overland flow models, which interpret complex morphological characteristics for accurate delineation of pluvial inundation (Diaz-Nieto et al. 2011). In Bangladesh, a high-resolution DEM, created from Lidar (Light Detection and Ranging) remote sensing, and spatial data on drainage channels are not available. In that case, an open-source DEM from sources such as Shuttle Radar Topography Mission (SRTM) (https://www2.jpl.nasa.gov/srtm/) and Advanced Land Observing Satellite (ALOS) (https://www.eorc.jaxa.jp/ALOS/en/index.htm) can be used. To simulate flood inundations for a counterfactual scenario (without polders), land subsidence data from Brown and Nicholls (2015) is essential. However, whilst Brown and Nicholls (2015) documented point measurements of net subsidence rates in 205 locations across the

Ganges–Brahmaputra–Meghna delta, uncertainty related to the methodologies employed to measure subsidence could hinder the accurate delineation of pluvial inundation.

2.5.2. Quantifying the interactions between LULC change, flood risk, and societal impacts

Studies aimed at quantifying flood risk should consider LULC change dynamics and societal impacts of flooding. The influences of LULC change on water resources is well documented in the existing literature (Choi et al. 2017, Szwagrzyk et al. 2018). But, when considering the societal impacts of flood hazards, the spatial interactions between LULC change, flood risk, and socio-economic drivers are poorly understood. Methodologies for LULC change modelling are well developed, as many studies aimed to analyse historical LULC changes to simulate future LULC (Arsanjani et al. 2013, Shahbazian et al. 2019). However, there are only a few studies that quantified the impacts of LULC change on flood risk. For instance, Szwagrzyk et al. (2018) investigated the impacts of projected LULC changes on future flood risks, in terms of peak discharge and monetary flood losses. But the study did not evaluate the societal impacts of the estimated flood risks. Due to the spatial heterogeneity of LULC change, flood risks can result in different impacts on socio-economic parameters such as assets, consumption, and income-based measures of wellbeing. An inexpensive but comprehensive model is essential for quantifying the societal impacts of LULC changes and flood risks.

2.5.3. Ex-ante evaluation of future flood interventions

The ex-ante analysis addresses the challenges in understanding the impacts of future flood interventions, by assessing future impacts of a decision which has been made under uncertainty (Penning-Rowsell and Korndewal 2019). As it is essential to understand how systems (e.g. flood defences) respond to loads (e.g. rainfall, storm surges), models should

represent spatial interactions between flood defences, hydrology, and topography (Hall 2014). Such interactions could be considered while planning for future flood interventions.

As discussed above, flood risk-reducing measures change the geomorphological and hydrological conditions of floodplains. Therefore, a flood model that captures such changes after implementation of risk-reducing measures could help understand the effectiveness of such approaches. For instance, as mentioned, there is not enough scientific evidence on the effectiveness of TRM in coastal Bangladesh, which has been proposed and tested as a means of partially recovering from the lack of sediment deposition, land subsidence, channel siltation, and salinity intrusion. It is accepted that the implementation of TRM elevates land surface, although the rate of change in land elevation varies spatially (Amir and Khan 2019). A change in land elevation impacts various geomorphological components that could influence flooding, such as, slope, curvature, flow accumulation, stream power index (SPI), and topographic wetness index (TWI) (Tehrany et al. 2019a). A dynamic modelling framework, that can quantify all potential geomorphological and hydrological changes due to the implementation of TRM, could enable comparative evaluation of flooding before and after the implementation of this approach.

2.6. Conclusion

This chapter has reviewed a diverse range of literature to identify various challenges in evaluating the impacts of flood interventions in complex coastal systems. Flood processes in the coastal region of Bangladesh are poorly understood because floods occur from multiple sources. Together, the presence of coastal embankments alters the floodplain geomorphology and hydrology. This chapter has identified several gaps in the academic literature which resulting in a lack of scientific understanding of the impacts of historical flood interventions, societal impacts of flooding, and potential future flood adaptation

options. To address these gaps, this chapter identifies three broad research themes. The following chapter 3, 4, and 5 have been developed based on these research themes.

Chapter 3 Have coastal embankments reduced flooding in Bangladesh?

Abstract

From the 1960s, embankments have been constructed in south western coastal region of Bangladesh to provide protection against flooding, but the success of the polder programme is disputed. We present analysis of floods during the years 1988-2012, diagnosing whether the floods were attributable to monsoonal precipitation (pluvial flooding), high upstream river discharge into the tidal delta (fluvio-tidal flooding), or cyclone-induced storm surges. We find that pluvial flooding was the most frequent, but typically resulted in less flooded area (11% of the region on average) compared with the other forms of flooding. The greatest area of inundation (48% of total area) occurring in 2001 as a consequence of fluvio-tidal and surge flooding, whilst cyclone Sidr in 2007 flooded 35% of the area. We modelled these different forms of inundation to estimate what flooding might have been had the polders not been constructed. For the 'no embankment' counter-factual scenario, our model demonstrated that because of a combination of subsidence and inadequate drainage, construction of the polders has increased the pluvial flooded area by 6.5% on average (334 km^2). However, during the 1998 fluvio-tidal flood, the embankments protected an estimated 54% of the area from flooding. During the cyclone Sidr storm surge event, embankment failure in several polders and pluvial inundation resulted in 35% area inundation, otherwise, the total inundation would have been 18% area. We conclude that whilst polders have provided protection against storm surges and fluvio-tidal events of moderate severity, they have exacerbated more frequent pluvial flooding and promoted potential flooding impacts during the most extreme storm surges.

3.1. Introduction

Structural flood defence systems are one response to flood hazards (Bamberg et al. 2017). While embankments, levees and dykes usually provide flood protection up to a given severity of flooding, these structures are costly and may exacerbate flooding under some circumstances, as well as potentially encouraging the build-up of exposed people and assets (Hui et al. 2016).

Due to the deltaic geographical setting and high population density, Bangladesh is well-known as being vulnerable to flooding (Moniruzzaman 2012, Islam et al. 2016a). The coastal region is subject to multiple flood hazards, including pluvial floods, which are inundations induced by monsoon precipitation, fluvio-tidal floods and storm surge-induced floods (Abedin and Shaw 2015, Alam et al. 2017, Brouwer et al. 2007, Haque and Nicholls 2018, Islam et al. 2016b). The impact of several catastrophic floods impelled the then government to construct coastal embankments in the 1960s to protect agricultural land and communities (Nishat et al. 2010, Paul and Rashid 2017, Rahman and Salehin 2013). Coastal embankments have compartmentalized a portion of coastal region into polders. Their construction was accompanied by the excavation of drainage channels and sluice gates to impede saltwater intrusion in the dry season, drain excessive rainwater, and allow fresh river water flow to polders in the wet season for irrigation purposes (Masud et al. 2018).

The coastal embankment programme had a profound influence on the geomorphology of the coastal zone, as well as contributing to a transformation in human settlement patterns. The embanked region experienced rapid land use change (Abdullah et al. 2019, Akber et al. 2018). In the last couple of decades, a substantial growth in shrimp farming, replacing agricultural lands, is reportedly associated with soil salinity promoted by the intrusion of saline water in polders (Mukhopadhyay et al. 2018). Moreover, storm surges and pluvial flooding inundated agricultural lands, which has been reflected in a net reduction

in land use for agriculture (Khan et al. 2015). In this naturally dynamic sediment system, reducing flow in the channels of the delta, due to the separation of upstream river 'Mathabhanga' from the river Ganges, caused siltation in the riverbed (Alam et al. 2017). Polders simultaneously also impeded sedimentation within embanked region and resulted in land subsidence inside the polders (Auerbach et al. 2015). As a result of reduced sediment supply or irregular sedimentation, compaction of sediment, and anthropogenic activities (e.g. shrimp farming) (Brammer 2014, Brown and Nicholls 2015), the coastal region on average experienced about 2-3 mm/year of land subsidence (Brown and Nicholls 2015). In addition, physical deterioration and unreliable operation of the sluice gates caused prolonged inundation during the monsoon period (Auerbach et al. 2015, Choudhury et al. 2004, Van Staveren et al. 2017). The earthen embankments are subject to riverbank erosion which can breach the polders, a process that can be exacerbated by tropical cyclones and lead to extensive flood damage (Bhuiyan and Dutta 2012, Haque and Nicholls 2018). The polders have also been criticized for their impact on coastal habitats and ecology (Roy et al. 2017).

Though these criticisms of polderization are widely reported (Alam et al. 2017, Auerbach et al. 2015, Tareq et al. 2018), it has proved difficult to provide quantified evidence of the effect of the coastal embankment programme because (i) the flooding processes are complex and derive from many sources and (ii) it is difficult to establish what the extent and severity of flooding might have been had the coastal embankments not been constructed. This paper seeks to address both of these challenges by (i) analysing past events to diagnose different types flooding and (ii) estimating the extent of flooding that could have occurred had the polders not been constructed. The first challenge is addressed through empirical analysis of the hydrometeorological factors that can explain the severity of observed floods, whilst the second is tackled by constructing models of different types of flooding.

3.2. Materials and methods

This research was conducted in two stages (Figure 3.2). First, a series of flood observations for the years 1988-2012 were obtained from remote sensing imagery. Records of rainfall, river water level, and surge levels for the same period were used to identify the main type of flooding for each observed event. Second, the counter-factual scenario without the construction of coastal embankments was modelled in order to hypothesise how the flooding might have been different without the polders.

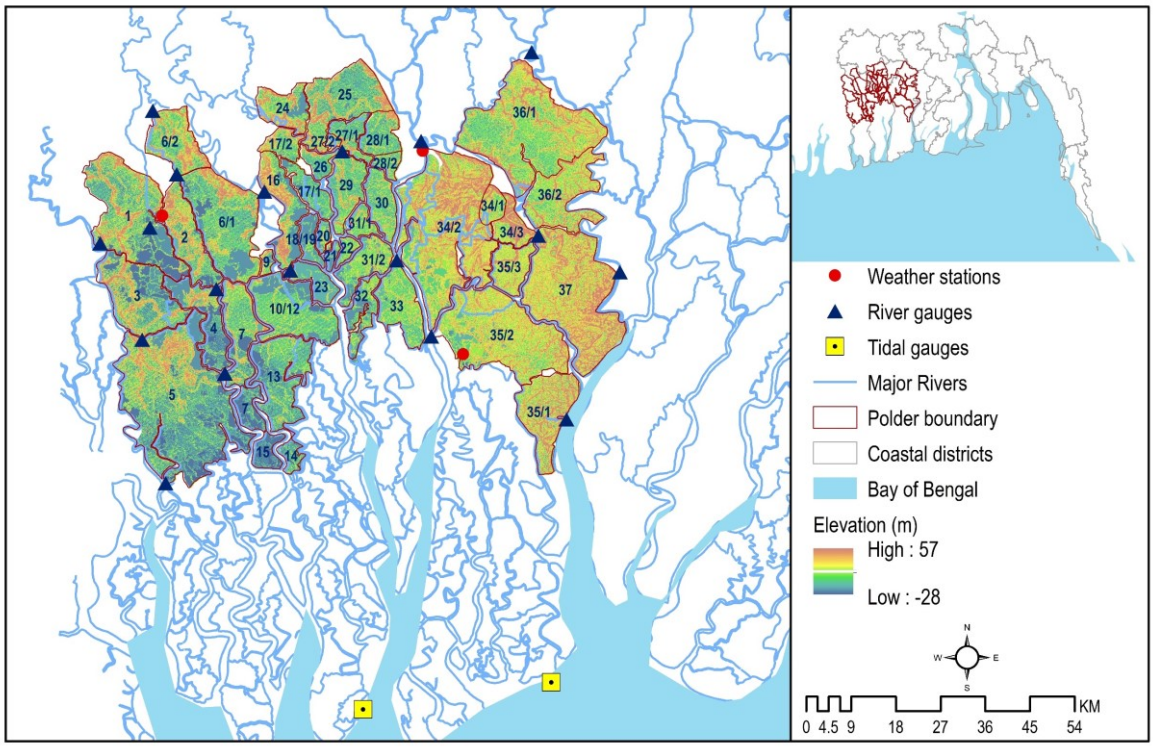

Figure 3.1 South western embanked region of Bangladesh

3.2.1. Flood hazard of south western coastal region of Bangladesh

The study addresses the south western coastal region of Bangladesh (Figure 3.1) which is vulnerable to fluvio-tidal flooding, monsoonal precipitation induced pluvial flooding, and storm surges (Bhuiyan and Dutta 2012, Gain et al. 2017). In the dry season, tidal oscillations dominate the low flows in the river channel in this region, making it susceptible to saltwater intrusion. Before polder construction, a common practice from local

people was to build temporary earthen embankments in the dry season to protect the land from salinity and remove those in wet season to enable sedimentation. Starting in 1960 a total of 44 polders were built in the Coastal Embankment Project (CEP) (Nowreen et al. 2014, Paul and Rashid 2017), protecting 5187km^2 (WARPO 2018). Polder construction transformed the coastal region into an agriculturally productive zone and encouraged people to settle within the polders (Nowreen et al. 2014). Conversely, polder construction de-linked the floodplain (Talchabhadel et al. 2016b) and induced several problems including river flow reduction, siltation in tidal channels, drainage congestion, waterlogging, land subsidence, polder breaching, soil salinity, etc. (Auerbach et al. 2015, Choudhury et al. 2004, Gain et al. 2017, Nowreen et al. 2014, Paul and Rashid 2017). For instance, polder construction has resulted in 1.0-1.5m of land subsidence inside an embanked area (Polder 32), whereas the outside of this embankment, the neighbouring Sundarban mangrove forest, has remained comparatively unchanged (Auerbach et al. 2015).

In response to multifaceted problems related to polders, over the years the government of Bangladesh, in cooperation with various international donor agencies, have implemented several projects. The World Bank, who supported the CEP project, has started the Coastal Embankment Improvement Project (CEIP) Phase I in 2015, which is rehabilitating and/or reconstructing several polders, as well as upgrading the drainage channels and structures (Paul and Rashid 2017). Meanwhile, the Blue Gold project, funded by Government of the Netherlands (GoN) and operated by the Bangladesh Water Development Board (BWDB), has been responsible for rehabilitation of water control structures within 26 polders districts (http://www.bluegoldbd.org/). In addition, Tidal River Management (TRM) has been adopted in an attempt to restore sedimentation within the polders through selective flooding (Van Staveren et al. 2017), gaining attention as a potential measure to alleviate pluvial flooding (Gain et al. 2017). The idea of TRM is to allow river

flow into low-lying bowl-shaped depressions (termed as 'Beel') within polder for sediment deposition to fill those depressions (Masud et al. 2018, Van Staveren et al. 2017). Though historically a community driven approach, BWDB implemented TRM in several 'Beels' in 1991-2013 (Masud et al. 2018).

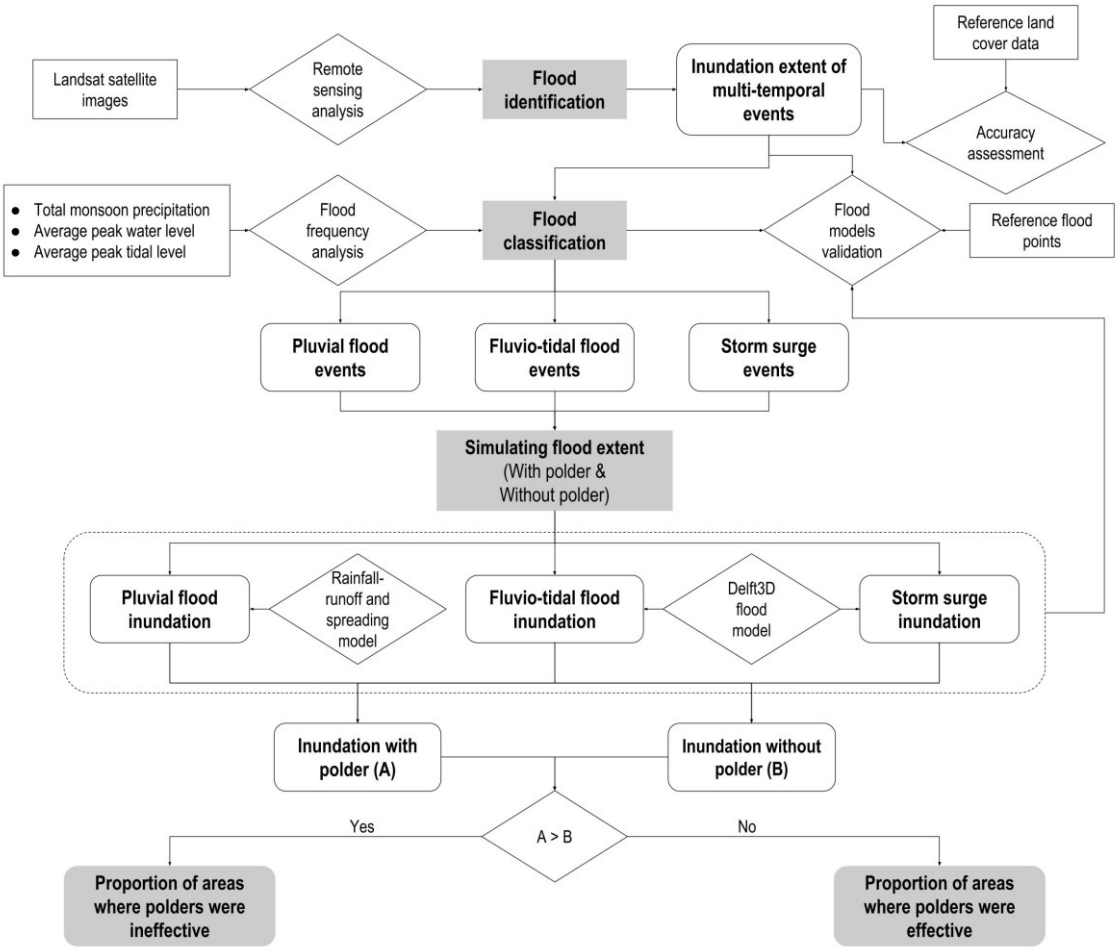

Figure 3.2 Analytical process of this study

Despite several initiatives, the challenges of providing sustainable flood risk management in the south western polder region are intensifying, with the threat of sea level rise, upstream modification of river flows and sediments from the Ganges Brahmaputra Meghna river system, and high population density providing little space for adaptation (Haque et al. 2018, Kay et al. 2018).

3.2.2. Identifying flood events

In last two decades (Hoque et al. 2011), water surface detection through remote sensing techniques has become an essential tool for various disciplines (Sanyal and Lu 2004, Sarp and Ozcelik 2017). Among various methods, water-indexing techniques have proved to be very useful for quick flood detection (Sarp and Ozcelik 2017). This study applied the Modified Normalized Difference Water Index (MNDWI) (Xu 2006) using ArcGIS 10.6.1 to detect water surfaces during pre (dry) and post (wet) monsoon period in a year. MNDWI uses green and middle infrared (MIR) bands of Landsat satellite images. It generates positive values for water surfaces and negative values for built-up areas, soil surfaces and vegetation. Then a change detection algorithm was used in Geographic Information System (GIS) to identify cells that changed from being normally dry to wet, which were classified as flood cells for that year. Cloud cover during the monsoon period (May to September) (Ahmed and Akter 2017) meant that the analysis was applied to compare pre and post monsoon images. The image database is summarised in Supplementary Table 3.2.

The major cyclone Sidr in 2007 caused prolonged flooding within the polders (Tareq et al. 2018), which lasted into 2008. Hence using pre-monsoon images of 2008 could cause under estimation of flood extent in 2008, so dry season images from 2007 we employed to detect flood extent in both 2007 and 2008.

The accuracy of MNDWI based classified images was assessed, for three different years (1989, 2001, and 2010), against reference land cover data (classified and validated images) collected from Mukhopadhyay et al. (2018) (Supplementary Table 3.1), producing an error matrix to estimate the overall accuracy and kappa statistics. The overall accuracy depicts a percentage agreement of pixels correctly classified (Lillesand et al. 2014). The kappa statistics (κ) is a measure for inter-raster reliability testing, whose value can range from -1 to +1, where ‘values ≤ 0 as indicating no agreement and 0.01–0.20 as none to slight,

0.21–0.40 as fair, 0.41– 0.60 as moderate, 0.61–0.80 as substantial, and 0.81–1.00 as almost perfect agreement' (McHugh 2012). The reference land cover data were converted into binary images (water, dry) and classified dry season (pre-monsoon) images of those three years were employed to estimate the indices of classification consistency. In this study, 'substantial agreement' within pixels between reference and classified land cover images were found for 1989 and 2010, and 'almost perfect agreement' was achieved for 2001 image classification (Supplementary Table 3.3). The processed flood maps were used to estimate the severity of observed flooding and also to validate the flood simulation outputs in the second phase of the study. The reference land cover maps included 12 land-use classes, in which general waterbodies are separated from aquaculture, mixed agriculture/aquaculture and agricultural lands. These maps were further used to analyse the types of land uses exposed to pluvial flooding.

3.2.3. Flood event classification

To attribute the observed floods to different sources of flooding, we analysed the severity of monsoon rainfall and elevated water levels within the region. Extreme value analysis was conducted by fitting to a generalized extreme-value (GEV) distribution using the L-moment method (Coles et al. 2001, Gilleland and Katz 2016). The cumulative distribution function of the GEV distribution is:

$$G(z) = \exp\left[-\left\{1 + \varepsilon\left(\frac{z-\mu}{\sigma}\right)\right\}_{+1}^{-1/\varepsilon}\right] \quad (3.1)$$

where, z is the random variable (monsoon precipitation/peak river water level/peak surge level) and ε, μ, and σ are the shape, location, and scale parameters respectively. The return period (T) was estimated by following formula:

$$T = \frac{1}{1 - G(z)} \quad (3.2)$$

The precipitation frequency analysis was based on 10-days gridded precipitation data from the Bangladesh Meteorological Department, aggregated into yearly monsoonal total precipitation and computed the regional average from 1948-2012. Fluvio-tidal flood attribution was based on annual peak water level (Rao and Hamed 2000), averaged across 18 river gauges. Finally, tidal surges were identified though analysis of peak tidal water level averaged across two tidal gauges in the Bay of Bengal, i.e. Hiron point and Khepupara (Figure 3.1). Data used for flood frequency analysis are summarised in Supplementary Table 3.1.

In each year the return period of pluvial rainfall, fluvio-tidal water level and surge water level were estimated according to Equation 3.2, denoted T_p, T_f and T_s, respectively. We then sought to classify each year, estimating thresholds T_p', T_f' and T_s' above which a flood of the given type was said to have occurred and a flooded area A_f' which represented the threshold between 'flood' and 'non-flood' events. The thresholds were optimised according to the following criteria, applied in this order of priority:

1. The separation between 'flood' and 'non-flood' events should not be contradictory i.e. events cannot be classified as being a version of 'flood' (i.e. pluvial, fluvio-tidal or surge) and 'non-flood'.
2. If an event with multiple types flood is identified, the classification of flood event should be consistent with the ordering of severity of T, i.e. the classification should be of the event type with the greatest T.
3. All events with above average flooded area should be classified as a version of 'flood'.
4. The number of multiple classifications should be minimised.

If it is not possible to meet criteria 1-3 the number of constraint violations should be minimised.

3.2.4. Modelling flood events

3.2.4.1. Pluvial flood model

To simulate the effect of polders on pluvial flood severity, a simple pluvial flood rainfall-runoff and spreading model was established. The model was then adjusted to simulate the effects of subsidence and drainage system.

Pluvial flooding materialises based on the interaction between precipitation, evapotranspiration, surface flow, local topography and drainage. It can occur either due to intense downpours (Falconer et al. 2009, Houston et al. 2011) or by prolonged moderate to heavy rainfall (Falconer et al. 2009). In low-lying areas like the polder region of south western Bangladesh, these processes are extremely complex, so we have developed simplified GIS-based water balance and flood spreading model to estimate inundated areas.

The Thornthwaite and Mather (TM) water balance model was used to produce monthly excess precipitation grids. The water balance model takes gridded monthly total precipitation (*P*), monthly mean temperature, monthly mean daylight hours, soil texture to estimate monthly potential evapotranspiration (equation 3.3), monthly water deficit or excess precipitation, actual evapotranspiration (equation 3.4, 3.5, 3.6, 3.7), and excess precipitation (equation 3.8, 3.9, 3.10). Raster layers of potential evapotranspiration (PE) and monthly water deficit or surplus (P-PE) in mm were calculated as follows:

$$PE_m = 16\ C\ \left(10\frac{T}{I}\right)^a \tag{3.3}$$

where, T is the monthly average temperature (˚C), I is the annual heat index for the year in concern, calculated as $I = \sum_1^{12} i$, where the monthly heat index $i = [T/5]^{1.514}$, $a = 6.75\times10^{-7}I^3 - 7.71\times10^{-5}I^2 + 1.792\times10^{-2}I + 0.49239$; the correction factor $C = m/30.d/12$, where m is the number of days in the month and d is the monthly mean daylight hours (Singh et al. 2004). The estimated monthly PE was then subtracted from the monthly P to find out the water excess (+) or deficit (-). After that, the soil budget was estimated to find the actual

evapotranspiration. At this stage, a raster layer of available water capacity ($SOIL_{max}$) was created following Thornthwaite and Mather (1957) principles. As Dingman (2002) demonstrated,

If $P_m \geq PE_m$, $$SOIL_m = min\{[(P_m - PE_m) + SOIL_{m-1}], SOIL_{max}\} \quad (3.4)$$

$$AET_m = PE_m \quad (3.5)$$

If $P_m < PE_m$, $$SOIL_m = SOIL_{m-1}\left[exp\left(\frac{P_m - PE_m}{SOIL_{max}}\right)\right] \quad (3.6)$$

$$AET_m = P_m + SOIL_{m-1} - SOIL_m \quad (3.7)$$

where, AET_m is the actual evapotranspiration of the month in concern; $SOIL_{m-1}$ is the soil moisture content of previous month. To solve this recursive equation, the GIS toolset started running from the first month (when P-PE <0) after the monsoon, considering that the soil moisture storage in previous month (last month of monsoon) was full, i.e. equal to the estimated available water capacity. Next, the following conditions and equations were followed to estimate the monthly and monsoonal total excess precipitation (SUR).

If $(P\text{-}PE)_m<0$, $$\mathrm{SUR_m} = 0 \quad (3.8)$$

If $(P\text{-}PE)_m \geq 0$ and $SOIL_m=SOIL_{max}$, $$\mathrm{SUR_m} = (\mathrm{P} - \mathrm{PE})_\mathrm{m} \quad (3.9)$$

If $(P\text{-}PE)_m \geq 0$ and $SOIL_m \neq SOIL_{max}$, $$\mathrm{SUR_m} = (\mathrm{P} - \mathrm{AET})_\mathrm{m} + \mathrm{SOIL_m} \quad (3.10)$$

Monsoon total excess precipitation, $$\mathrm{SUR_Y} = \sum \mathrm{SUR_{May\ to\ September}} \quad (3.11)$$

The flood extent was estimated by considering a series of surface depressions, whose catchments are nested (Diaz-Nieto et al. 2011). The SRTM DEM was analysed to identify surface depressions, their exit points (points through which water will pass to next level depressions when a depression is full), and catchment areas. While identifying exit points, the model followed the single-direction flow algorithm (D8), where one cell routed into the next steepest of eight neighbouring cells (Seibert and McGlynn 2007), and eliminated cells which drained back to the same depression. After that it selected depression points to define

respective depressions catchments and nest levels were assigned for depression catchments. The total volume of monsoon excess water from the water balance model was assigned to each depression. The water accumulation algorithm (equation 3.12) was started from the highest nest level depressions to accumulate water and subsequently passes to next level depressions. At this point, the model routes additional water, after filling previous level depressions (if remains), to the existing catchment(s). This iterative process continued until the model distributed water to the lowest sink catchment (Diaz-Nieto et al. 2011):

$$P_{P=0 \rightarrow P<0} = \sum P_{j=1,n} + E - V \quad (3.12)$$

where, P = water volume passed down from depression, E = access volume after filling the depression, V = depression volume, j = counter of nested depressions from 1 to n.

For each year (1988-2012), the model was used to simulate pluvial inundation with and without polders. For pluvial inundation 'with' polders the observed DEM was used. Drainage from the polder was constrained due to inadequate maintenance of drainage channels and deterioration of sluice gates. In this scenario, the excess precipitation was estimated by subtracting evapotranspiration from the total precipitation.

Brown and Nicholls (2015) documented 205 points measurements of net subsidence. Yearly land subsidence rates used in this study ranging from 0.24mm to 10mm per year. Using these point measurements, a raster of yearly subsidence rate was created, using Inverse Distance Weighted (IDW) interpolation. Multiplying this raster with subsequent number of years starting from 1960 (commencing year of polder construction) was added to the existing DEM to reconstruct past land elevations. The reconstructed DEM was used to delineate potential flood locations (surface depressions) in the 'without' polder scenario. The estimated total excess precipitation in each year was accumulated in the depressions and nested catchments. We further developed a scenario in which drainage channels within

the polders were effectively maintained. These channels were identified by hand from the satellite image. Catchments that contained these channels were permitted to drain.

We performed sensitivity analyses for (a) the method used to interpolate land subsidence rate (b) the rate of land subsidence, which was used to establish pluvial flood model for the counterfactual scenario. First, using the observed land subsidence data we generated three additional layers of land subsidence rates, applying kriging, spline, and natural neighbour methods (Supplementary Figure 3.9) in GIS (Childs 2004). These layers were incorporated to generate pluvial flood inundation simulations for the 25 years studied for the counterfactual scenario. We tested for significant differences in annual pluvial inundation in the counterfactual scenario (Supplementary Figure 3.1). This was done applying one-way analysis of variance (ANOVA) test. An ANOVA test could be performed to measure the sensitivity of input parameters (e.g. DEM) in hydraulic modelling and floodplain mapping (Raber et al. 2007). The estimated *p*-value 0.22 indicated that the difference in inundation for four types of land subsidence rates is not significant. The insignificant p-value and a smaller value of F-ratio than the critical F-ratio (Supplementary Table 3.4) confirmed the absence of sensitivity in the pluvial flood model in relation to method applied to interpolate the rate of land subsidence.

In addition, we generated raster layers of two land subsidence rates, randomly splitting the observed 205 points measurements of net subsidence rate into two groups. The first group contained a subset of 70% points, whereas the second group was comprised of the remaining 30% points. Yearly land subsidence rates in the two groups ranging from 1mm to 10mm and 1mm to 6mm, respectively. We applied IDW interpolation method to obtain two layers of subsidence rates, which were added (multiplying by the difference of modelled year from 1960) separately on the existing DEM to generate two different surfaces. We incorporated these surfaces in pluvial flood model to estimate the inundated area across

delineated depressions. Here, we modelled the pluvial events of 2004 and 2006, when a higher amount of excess precipitation was estimated (Figure 3.6). Supplementary Figure 3.2 in supplementary document exhibits a similar pattern of individual depression behaviour for a change in land subsidence rate. Again, ANOVA test was performed to analyse the difference in inundation during two events in individual depression, for different rates of land subsidence. The obtained p-value 0.27 and F-ratio 1.3 (< critical F-ratio 2.01) indicated that the difference in inundation in different depressions insignificant.

The pluvial flood model was validated based on a field survey that was conducted on May 2018 to collect GPS locations of pluvial floods and non-floods (Supplementary Figure 3.3). An error matrix was produced (Supplementary Table 3.5) to verify the accuracy of modelled potential flood/non-flood pixels, comparing to observations. An overall accuracy of 95% and spatial statistical κ statistics value 0.87 suggest an 'almost perfect agreement' (McHugh 2012) between observed and modelled flood pixels.

The observed total inundation in years that were identified as pluvial flood events were plotted against the modelled inundation of corresponding years for 'with polder' scenario, yielding a coefficient of determination R^2=0.98 (Figure 3.3). However, the validation process also included 2005 event, despite it was classified as 'no flood' event. The reason for using this event to validate the pluvial flood model is explained in Section 3.3.3.

3.2.4.2. Fluvio-tidal and storm surge inundation model

The Delft 3D hydrodynamic model (Haque et al. 2018) was used to estimate inundation extent from fluvio-tidal (1998) and storm surge flooding (2007) for 'with' and 'without' polder scenarios. The model domain was bounded by border with India in the west (type of boundary is not fixed), Lower Meghna estuary in the east, three major rivers (the Ganges, Brahmaputra and Upper Meghna) in the north and Bay of Bengal in the south. The

discretized model domain contains 896,603 grid points, where grid size varies from 186m to 1704m. Coarser grid size is provided in the ocean and finer grid size is provided in the river channels to capture the details of the river/estuarine systems and topographic variation. The model was set up for all rivers and estuaries with a width of at least 100m. Measured flow data was provided from BWDB for three the major rivers, from which fluvial flow enters the model. In absence of measured sea level data, the model takes simulated sea level data from the GCOMS model (Kay et al. 2015), which generated the tidal (ocean) boundary. As morphological changes were considered static (except subsidence) – no additional sediment input is provided. A rate of 2.6 mm/year (Brown and Nicholls 2015) of subsidence is considered in the area bounded by the polders including the polder itself. A DEM with a spatial resolution of 50m was provided by WARPO (2018). The ocean bathymetry data was obtained from General Bathymetric Chart of the Oceans (GEBCO) while river bathymetry data was collected from BWDB at 294 locations in coastal rivers/estuaries. Channel planforms were assumed to remain the same over the model simulation period. Similar assumption was made for channel bed level and floodplain levels of rivers / estuaries.

The model indirectly considered impacts of land-use and land cover through resistance in the floodplain. Different resistance values were specified for sea, rivers/estuaries, floodplain and forest (Sundarban). These resistance values were determined during model calibration. The calibrated Manning's roughness coefficient was spatially variable having values of 0.00025 in the ocean (considered as large water body), 0.015 to 0.025 in rivers /estuaries (a value generally considered to be valid for rivers / estuaries in the region), 0.025 to 0.040 in the floodplain, and 0.08 to 0.1 in forests including mangrove and natural plantation. The model simulated 103 polder areas (out of 139) using design heights of embankments collected from BWDB. Present day observations are only available for 61 polders (some of which are outside the study region) that show that actual polder heights

can vary from 3m to 7m (Huq et al. 2010). Where actual embankment heights are not available, an average design embankment height of 4.75m is used in the model (CEIP 2013). Storm surge modelling was based on a reconstructed cyclone track for the 2007 cyclone Sidr (Supplementary Figure 3.4) that passed by the study area. Consideration of reconstructed cyclone track was based on the premise that modelled result could ideally explain the observed flood inundation. Resulting simulated inundation data was masked for the south western polder region. Further details on model setup, calibration, and validation can be found in Haque et al. (2018) and Haque and Rahman (2016).

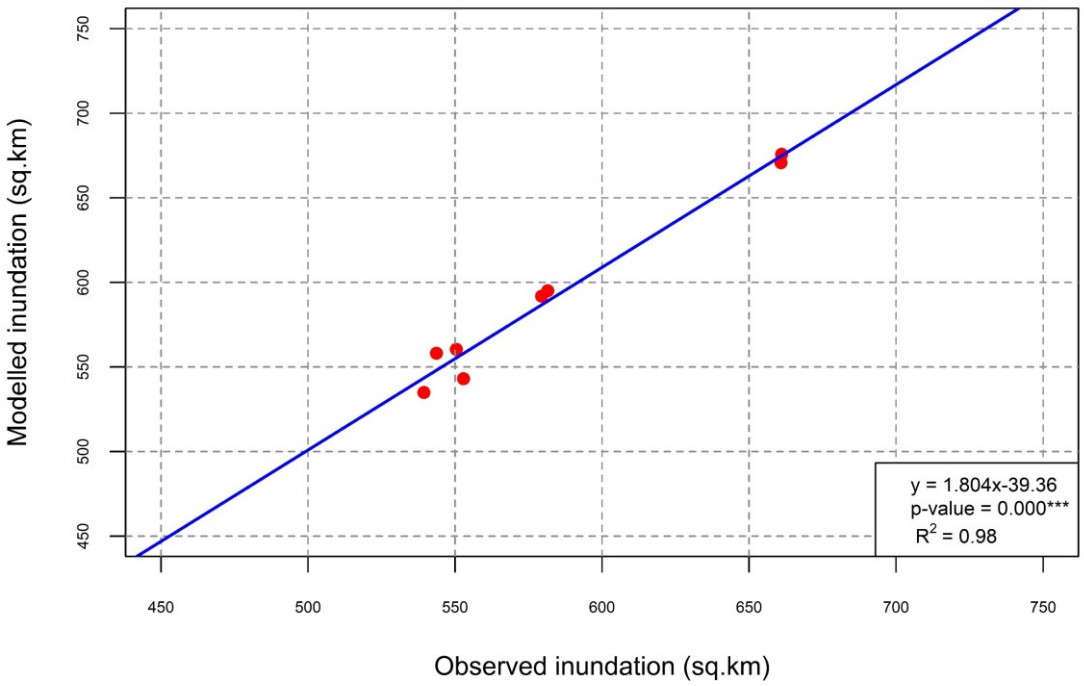

Figure 3.3 Modelled versus observed pluvial flood inundation plot

3.3. Results and discussion

3.3.1. Identification of flood events

In 25 observed years, the inundated area ranged from 6% (in 2010) to 48% (in 2001). The mean flood footprint was 13% of the total embanked region. The patterns of inundation were heterogeneous spatially and temporally, with different parts of the embanked region

flooded in different years. Six polders were flooded by more than 13% (average flood area) of their respective area, on average. The largest extent of inundation occurred in polder 34/1, whereas the polder 28/2 and 30 experienced the lowest level of inundation (Supplementary Figure 3.5).

Figure 3.7 (a) shows a typical inundation footprint for the year 2004 obtained from remote sensing data analysis. Here, major inundation occurred in the northern segment of embanked region. Generally, flooding in the south western part of the region was less frequent and the extent of inundation in that segment was relatively low during various events.

3.3.2. Classification of flood events

3.3.2.1. Frequency analysis

Figure 3.4 portrays the frequency analysis of total monsoon precipitation, peak river water level, and peak surge level respectively to classify them into pluvial, fluvio-tidal, and surge induced floods. The estimated return periods of these three hydrological parameters varied annually, indicating different types of floods in different years. For instance, within 25 observed years, the highest monsoon precipitation was in 2002, whereas the highest peak river water level and surge level were in 1996 and 2007 respectively. The relationship between flood conditioning factors and flood type is complex (Nied et al. 2014), in this study, we provide a simplified flood classification system estimating minimum thresholds T_p', T_f' and T_s'.

3.3.2.2. Flood event classification

Table 3.1 presents the return period of each type of flood in each year. The optimisation of return periods of three hydrological parameters yielded the following minimum flood thresholds: T_p'= 5.2 years, T_f'= 5.9 years and T_s'= 7.9 years and threshold between ‘flood’ and ‘non-flood’ events was 10.3% of the area. According to this criterion,

floods were identified as occurring in 14 different years and three compound events were detected. The estimated thresholds generated one false negative and one false positive flood event. The event in 1996 was classified as 'F' even though the flood area was 9.2%. The highest T_f during that event was responsible for such attribution. Besides, 2005 event was classified as 'N' despite about 11.5% area was inundated. In 2005, the region received a lower level of monsoon precipitation, in addition to low peak river water level and surge level. The outcome of pluvial flood model explained the reason for a higher level of inundation in 2005 (Section 3.3.3).

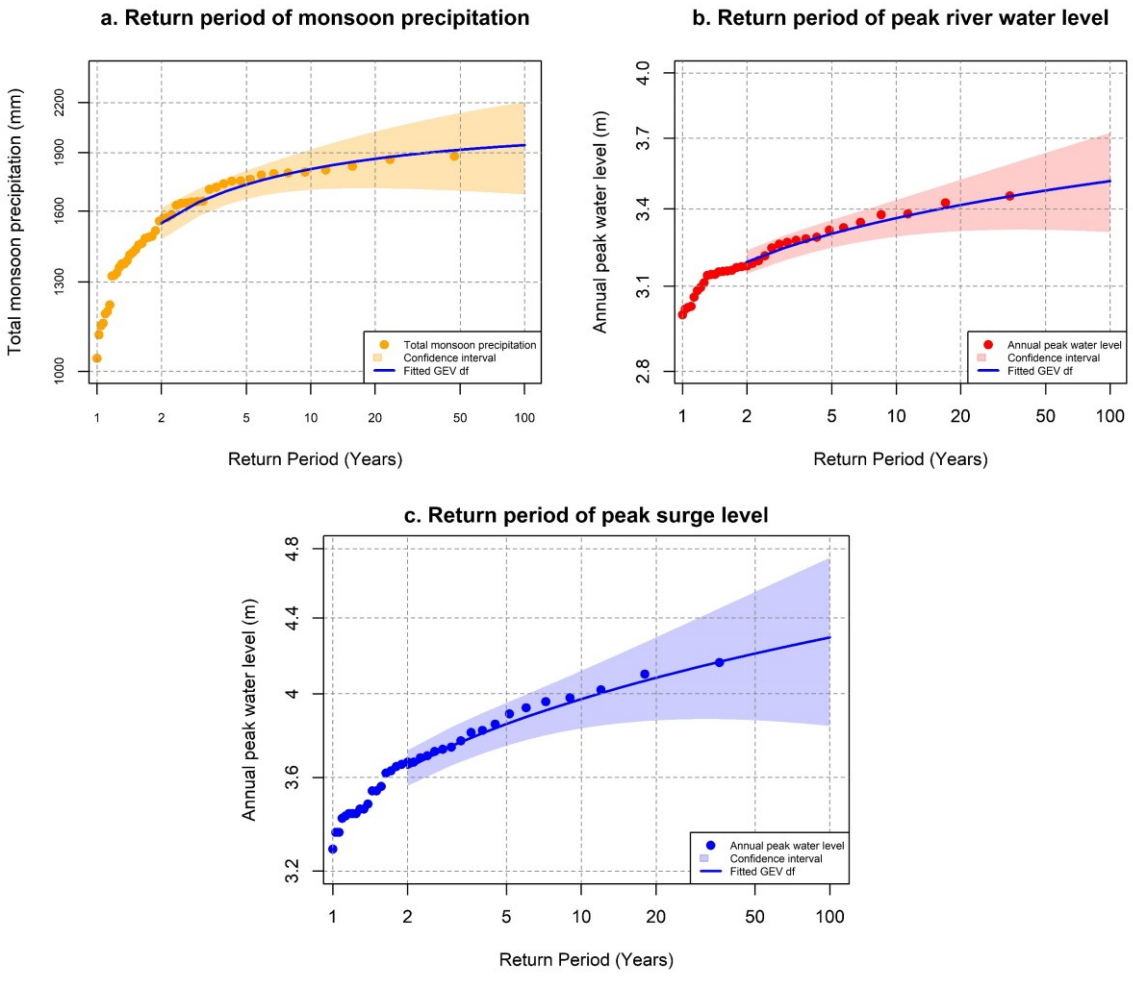

Figure 3.4 Return level plots with fitted GEV df and 95% confidence bands

We find that pluvial flooding was the most frequent, but typically resulted in less flooded area (11.4% of the region on average) compared with the other forms of flooding.

The fluvio-tidal and surge induced floods caused more extensive inundation than the pluvial floods: 21.8% and 30.2% on average, respectively. The greatest area of inundation (48% of total area) occurring in 2001 as a consequence of fluvio-tidal and surge flooding, whilst cyclone Sidr in 2007 flooded 35% of the area.

Figure 3.5 (a) illustrates the identified pluvial floods. We classified seven pluvial flood events considering 5.2-year return period as the minimum threshold level. The region received the highest monsoonal precipitation of 1861.91mm in 2002 leading to an 18.8-year return level of pluvial flood. The highest two precipitation events in 2002 and 2011 caused approximately 11% of total polder area inundation, while 2004 resulted in the highest pluvial inundation (13% area).

Table 3.1 Flood attribution in south western polder region

Year	Precipitation return period (T_p)	Return period of peak river water level (T_f)	Surge peak return period (T_s)	Percentage of area inundated (A_f)	Flood type (P-Pluvial, F-Fluvio-tidal, S-Surge, N-No flood)
1988	9.5	3.9	6.5	10.3	P
1989	1.4	1.5	2.7	6.5	N
1990	2.1	2.1	2.4	9.3	N
1991	1.7	1.6	1.9	8.2	N
1992	1.3	3.4	2.5	7.8	N
1993	8.1	1.8	1.5	11.4	P
1994	1.3	1.2	1.2	5.9	N
1995	2.8	6.4	13.4	16.5	F, S
1996	1.4	34.6	4.3	9.2	F
1997	2.2	1.9	2.1	9.3	N
1998	3.0	11.8	2.0	22.8	F
1999	7.9	3.6	1.8	10.8	P
2000	2.9	8.2	5.0	10.9	F
2001	1.7	22.7	9.2	48.1	F, S
2002	18.8	12.3	1.5	10.7	P, F
2003	1.1	5.8	2.2	7.9	N
2004	5.2	1.3	1.0	13.1	P
2005	1.2	1.2	1.1	11.5	N
2006	5.7	1.6	1.2	13.0	P
2007	3.0	2.4	34.9	35.0	S
2008	1.4	1.5	2.8	10.1	N
2009	1.6	4.4	22.8	21.2	S
2010	1.1	1.0	1.2	6.1	N
2011	11.8	1.1	1.2	10.8	P
2012	1.1	1.1	1.1	7.0	N

The six events that were classified as fluvio-tidal happened in 1995, 1996, 1998, 2000, 2001, and 2002. The highest regional average peak water level of 3.45m was observed in 1996, leading to a 34.6-year event (Figure 3.5 (b)). But the most extreme event did not result in the highest extent of inundation. For instance, whilst in 1996 the inundation area was 9%, the highest percentage of total area (48%) was inundated in 2001 when the region experienced a 23-year fluvio-tidal flood which breached various polders. However, the 2001 event was attributed to both the fluvio-tidal and surge event, though fluvio-tidal flood was the dominant force (as higher return period) leading to the inundation. Fluvio-tidal floods mostly occurred in between 1995 and 2002. After 2003, relatively a lower mean discharge in upper Ganges River was observed (Supplementary Figure 3.6), contributing to a lower peak river water level.

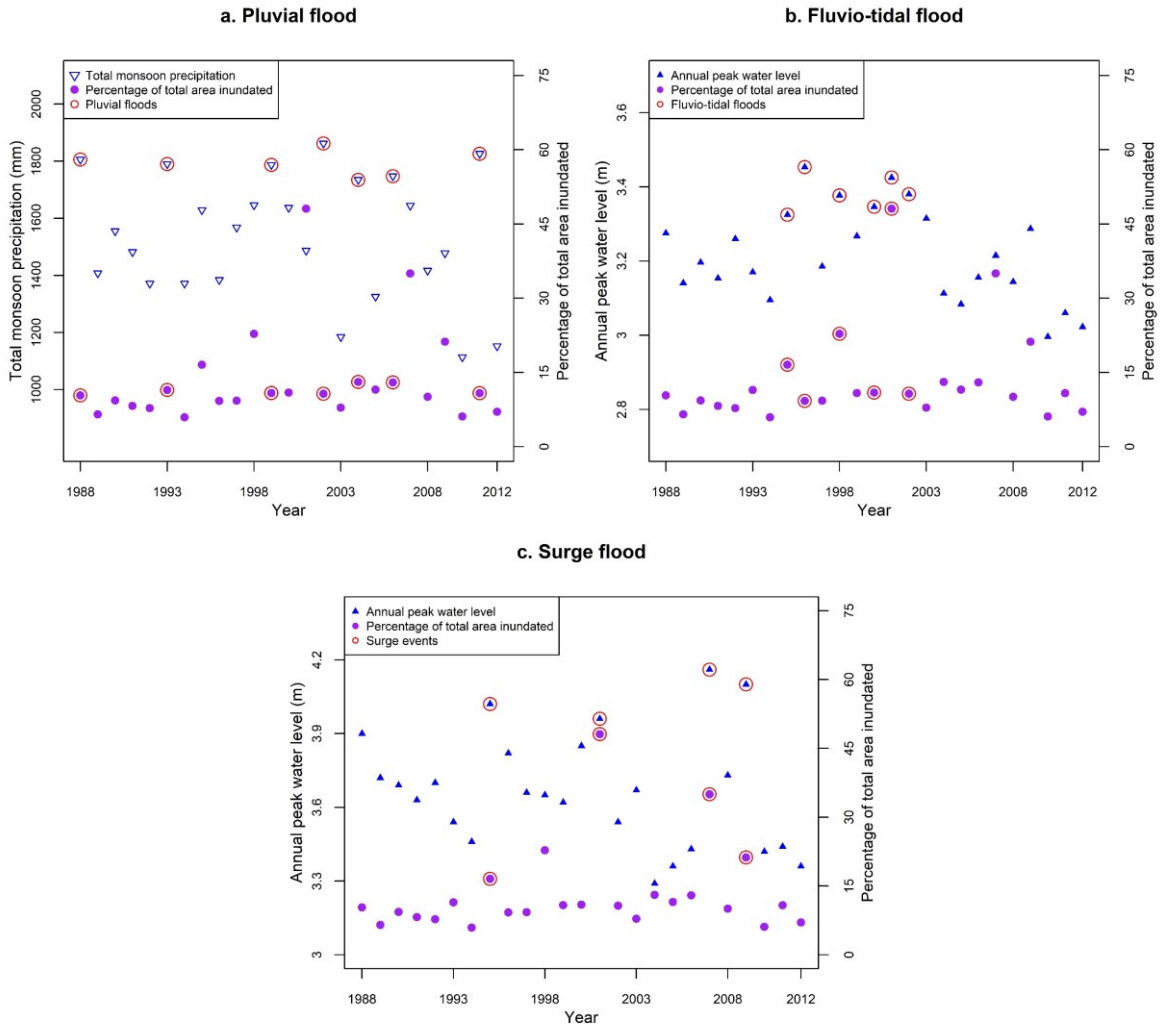

Figure 3.5 Classified flood events in relation to values corresponding hydrological parameters

Four surge induced floods were attributed, considering the estimated 7.9-year return period as minimum threshold limit (Figure 3.5 (c)). The most extreme surge occurred in 2007 during the cyclone Sidr, when the peak surge height reached to 4.16m (35-year return period), causing 35% of the total area inundation. Another major cyclone Aila affected the study area in 2009 with a peak surge of 4.10m, leading to 21% area inundation. Both fluvio-tidal and surge flooding formed the compound event of 1995, when the impact of surge was the highest.

3.3.3. Modelling flood inundation with and without polders

The outcome of pluvial flood model indicated that the study area was prone to pluvial inundation annually, since excess precipitation of different magnitude was estimated in all studied years (Figure 3.6). The extent of inundation has a strong positive correlation with the amount of excess precipitation (correlation coefficient = 0.90). Among the classified seven pluvial flood events (Table 3.1), the lowest level of monsoon precipitation was observed in 2004. But, the greatest extent of pluvial inundation was estimated in 2004, due to presence of the highest amount of excess precipitation caused by a lower level of evapotranspiration. In 2005, the modelled pluvial inundation was 11.2% area, which is similar to observed flood inundation (11.5%) for that year. The lowest level of evapotranspiration was estimated in 2005, leading to a higher amount of excess precipitation. Therefore, the extent of inundation in 2005 was greater than A_f' (10.3%), despite the region received a 1.2-year return level precipitation. Thus, we included this event to validate the outcome of pluvial flood modelling (Section 3.2.4.1). The results from pluvial flood modelling further demonstrated that a greater extent of inundation was the outcome of polder construction and inadequate drainage systems. The extent of pluvial inundation would have been substantially lower in absence of polders.

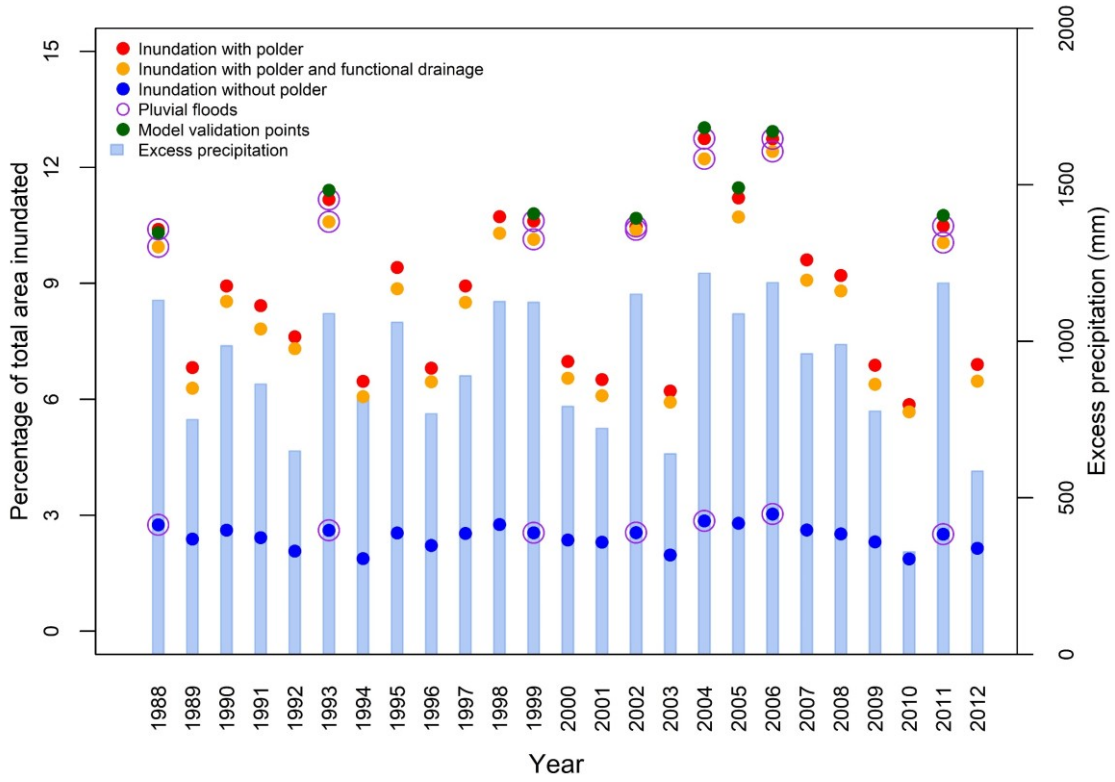

Figure 3.6 Simulated pluvial flood inundation for three scenarios

Typical results from the pluvial flood model are shown in Figure 3.7 (b, c), which illustrates how a combination of land subsidence (a maximum of approximately 0.5m relative to locations where polders were not constructed) and inadequate drainage, has exacerbated pluvial flooding. We estimate that on average over the modelled period the extent of flooded area was 334km^2 (i.e. 6.5% of total area) larger because of the land subsidence, generated from the construction of polders, and inadequate drainage. The extent of inundation primarily depends on the number of surface depressions generated due to land subsidence. Polder construction increased the number of shallow depressions (<1m in depth), which are prone to flooding. Without polders flooding in those areas might have been alleviated, as sedimentation would have transformed the geomorphology of the region and reduced the number of shallow depressions. Flooding in that case would have only occurred in areas characterized as deep surface depressions. Hence, our modelled pluvial inundation for the counter-factual scenario showed relatively a small year-to-year difference

in the extent of inundation (Figure 3.6), although the total inundated area was positively correlated with the estimated excess precipitation.

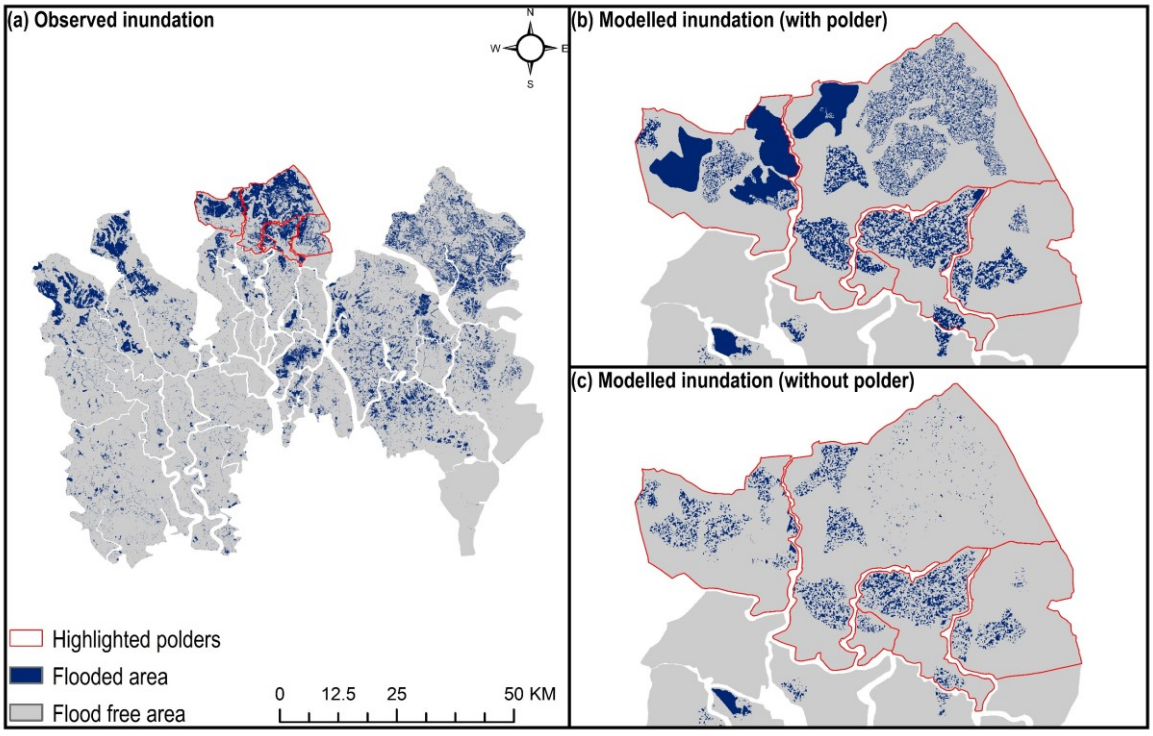

Figure 3.7 Impact of polders on pluvial flooding (2004 event)

Results from the pluvial flood model further indicated that if the observed drainage system were maintained adequately, it would have been able to reduce pluvial flooding by about 4.9%. This number is relatively small because there are many catchments that were not observed to have a drainage channel. The pluvial flood prone area comprises about 50% aquaculture land (shrimp culture and freshwater fish culture), which is not necessarily harmfully affected by flooding. However, 40% of the flood-prone area is agricultural land (rice field, other croplands, mixed rice and shrimp culture) which can be more adversely impacted by pluvial flooding, whilst 10% is comprised of settlement areas with homestead vegetation where pluvial flooding is directly harmful.

Simulations of fluvio-tidal and surge flooding demonstrate the effectiveness of embankments in reducing inundation due to elevated water levels. For example, during the 1998 fluvio-tidal flood, majority of the region would have been flooded without polders.

The presence of polders resulted in an estimated 27% of total area being flooded in this fluvio-tidal flood, compared to 79% for the 'without polder' counter-factual. Complete inundation occurred in 14 polders for 'with' polder scenario, which would have been escalated to 31 polders for the counter-factual scenario (Figure 3.8 (a)). Overlaying the inundated areas for both scenarios, we found that the embankments protected an estimated 54% area from flooding.

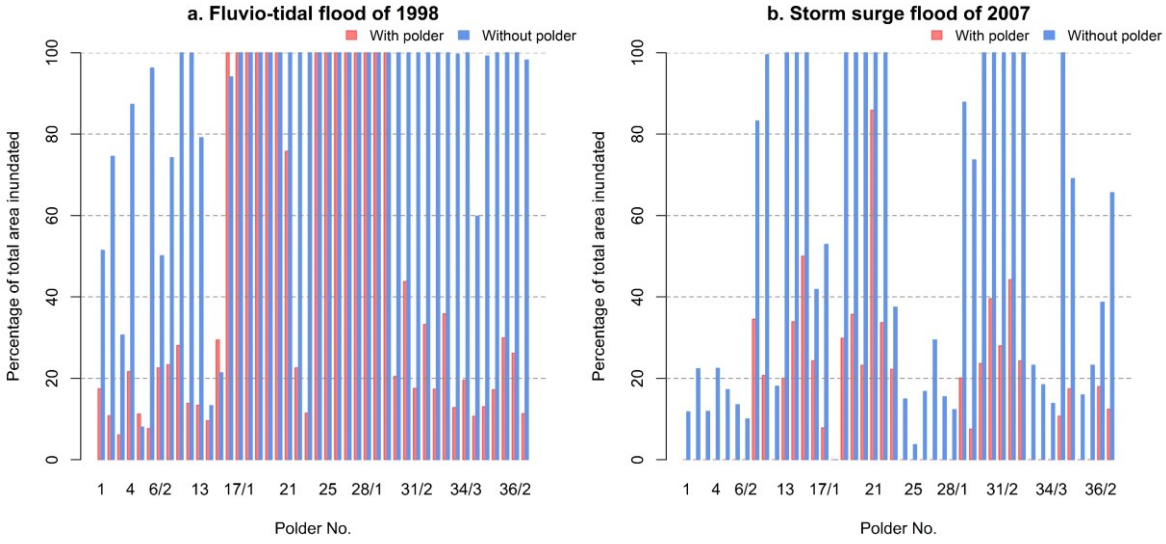

Figure 3.8 Polder wise inundation in two scenarios during (a) fluvio-tidal flood of 1998, and (b) storm surge flood of 2007

Simulation results for surge event Sidr suggests that, in presence of polders (without breaching), about 18% of the total area might have been inundated. Without polders, the extent of inundation would have been increased to approximately 35% area. Seventeen different polders that were partially at risk of flooding would have been inundated by more than 80% area without embankments (Figure 3.8 (b)). However, our modelled total inundation for counter-factual scenario is similar to the observed inundation of 35% area. When simulating inundation for 'with polder' scenario, the model considered overtopping as the flood mechanism in polders. Therefore, the number of flood-affected polders were substantially lower under this scenario. But, embankment failure in several polders, both in

form of damage and overtopping, increased the extent of inundation. Furthermore, the observed inundation in 2007 is a compound inundation of pluvial and surge induced flooding. The estimated pluvial inundation in 2007 was about 10% area. Subtracting (spatially) the pluvial inundation from the observed inundation, we found that surge induced flood solely contributed to the inundation in 25% area.

3.4. Conclusion

Creation of polders by construction of embankments in coastal Bangladesh has been a controversial process. The creation of polders enabled large increases in agricultural production and reduced the impacts of storm surges and fluvio-tidal floods. However, blocking off the coastal floodplain from channels practically eliminated annual deposition of sediments on the land, whilst compaction of sediment and anthropogenic activities exacerbated land subsidence. Over the years, drainage channels have not been adequately maintained, which has inhibited drainage of pluvial flood waters and exacerbated inundations. Moreover, construction of polders has provided an impression of security from flood hazards, encouraging human settlement in vulnerable locations.

In this paper we have empirically analysed the evidence for both the beneficial and harmful impacts of polder construction. We found that pluvial flooding occurs frequently, but the flood extent is usually less than in other forms of flooding. By modelling a counter-factual scenario in which polders had not been constructed we quantified a substantial (6.5% area) increase in pluvial flooding that can be attributed to land subsidence resulted from polder construction and poor management of drainage facilities.

On the other hand, the polders have provided protection against fluvio-tidal and storm surge events. In the worst fluvio-tidal flood in the ‘without polder’ scenario 79% of the area would have been flooded, compared with 27% which occurred with the polders. In the surge event Sidr, 18% of the polder area would have been flooded, without the breaching

to embankments. But, the extent of inundation was increased to 25% area due to the damage to embankments during the cyclone. Simultaneously, pluvial flooding exacerbated the flood impact, inundating a total 35% area in 2007.

The empirical analysis of past floods reported in this paper is subject to errors in observations of precipitation and water levels. In addition, the recognition of flooded areas from satellite imagery is also subject to error. The attribution of flood types is to some extent subjective, based on the criteria that were used to optimise the classification thresholds. Given the relatively short record of flood events, the complexity of the flooding process and the possibility of compound events, it would not be possible to establish a definitive classification method.

Flooding processes in low-lying coastal areas are complex, so the modelling we have used to analyse the 'without polder' counter-factual is inevitably approximate. This particularly applies to pluvial flooding, which is sensitivity to local rainfall patterns, topography, land surface and drainage and so would be extremely difficult to model with more accuracy on the spatial/temporal scale considered in this study. Nonetheless, these models have provided insights into the polders' effectiveness. Generally, this study is an attempt to estimate the impact of anthropogenic intervention (creation of coastal embankments) on the hydrology (inundation) of south western embanked region of Bangladesh.

Rehabilitation and reconstruction of embankments is now under way in the coastal zone of Bangladesh (Supplementary Figure 3.8). Further choices will need to be made in the face of rising sea levels. Alternative adaptation strategies are being examined as part of the Bangladesh Delta Plan. The empirical analysis of the benefits and impacts of embankment construction, which has been reported in this paper, should help to inform plans for

adaptation of Bangladesh's coastal zone to flood hazards, by helping to target and sequence investments for flood management.

Appendix A: Supplementary Materials to Chapter 3

Supplementary Tables

Supplementary Table 3.1 Datasets used in this research

Data	Description	Sources
Landsat satellite images	Landsat 4-5 Thematic mapper (TM) Landsat 7 Enhanced Thematic Mapper Plus (ETM+) 30m resolution	The United States Geological Survey (https://earthexplorer.usgs.gov/)
Reference land cover data	Land use / land cover data for 1989, 2001, and 2010 30m resolution	(http://www.espadelta.net/) (Mukhopadhyay et al., 2018)
Precipitation data	Gridded (5km grid points) precipitation data of 10-day temporal resolution from 1965-2012	Bangladesh Meteorological Department (www.bmd.gov.bd/)
River water level data	Daily river water level data from 1981 to 2014 across 18 gauges	Bangladesh Water Development Board (BWDB) (www.bwdb.gov.bd)
Tidal water level data	Hourly tidal water level data of two tidal gauges, i.e. Hiron point (21.78300, 89.46700) and Khepupara (21.83300, 89.83300)	University of Hawaii Sea Level Center (https://uhslc.soest.hawaii.edu/) and Bangladesh Inland Water Transport Authority (www.biwta.gov.bd/)
Climate data	Monthly average temperature, monthly average daylight hour data from 1988-2012, across four weather stations	Bangladesh Agricultural Research Council (http://www.barc.gov.bd/)
Soil texture data	Vector data of topsoil texture with attributes of texture types, such as 'silt loam', 'clay', 'silty clay', etc.	Bangladesh Agricultural Research Council (http://www.barc.gov.bd/)
Digital elevation model (DEM)	Shuttle Radar Topography Mission (SRTM) DEM of 30m spatial resolution	The United States Geological Survey (https://earthexplorer.usgs.gov/)
Spatial data	GIS vector data of polder region with the attributes of polder number, area etc.	The Water Resources Planning Organization (WARPO, 2018)

Supplementary Table 3.2 Landsat satellite images used to detect year wise flood extent

Year	Path, Row	Image acquisition date (dry season)	Image acquisition date (wet season)	Dataset
1988	137, 44	19-Feb-88	01-Nov-88	Landsat 4-5 TM C1
	138, 44	10-Feb-88	08-Nov-88	Level-1
	138, 45	25-Jan-88	24-Nov-88	
1989	137, 44	12-Jan-89	04-Nov-89	
	137, 45	12-Jan-89	04-Nov-89	
	138, 44	19-Jan-89	11-Nov-89	
	138, 45	19-Jan-89	27-Nov-89	
1990	137, 44	07-Jan-90	09-Dec-90	
	137, 45	24-Feb-90	09-Dec-90	
	138, 44	14-Jan-90	14-Nov-90	
	138, 45	14-Jan-90	14-Nov-90	
1991	137, 44	27-Feb-91	10-Nov-91	
	137, 45	27-Feb-91	10-Nov-91	
	138, 44	06-Mar-91	01-Nov-91	
	138, 45	18-Feb-91	30-Sep-91	
1992	137, 44	02-Apr-92	12-Nov-92	
	137, 45	02-Apr-92	12-Nov-92	
	138, 44	08-Mar-92	02-Oct-92	
	138, 45	08-Mar-92	02-Oct-92	
1993	137, 44	15-Jan-93	15-Nov-93	
	137, 45	15-Jan-93	15-Nov-93	
	138, 44	06-Jan-93	21-Oct-93	
	138, 45	22-Jan-93	21-Oct-93	
1994	137, 44	18-Jan-94	18-Nov-94	
	137, 45	18-Jan-94	18-Nov-94	
	138, 44	25-Jan-94	22-Sep-94	
	138, 45	25-Jan-94	22-Sep-94	
1995	137, 44	05-Jan-95	21-Nov-95	
	137, 45	05-Jan-95	05-Nov-95	
	138, 44	28-Jan-95	12-Nov-95	
	138, 45	28-Jan-95	28-Nov-95	
1996	137, 44	09-Feb-96	22-Oct-96	
	137, 45	09-Feb-96	22-Oct-96	
	138, 44	16-Feb-96	13-Oct-96	
	138, 45	16-Feb-96	13-Oct-96	
1997	137, 44	26-Jan-97	26-Nov-97	
	137, 45	26-Jan-97	26-Nov-97	
	138, 44	18-Feb-97	16-Oct-97	
	138, 45	01-Jan-97	01-Nov-97	
1998	137, 44	14-Feb-98	26-Sep-98	
	137, 45	02-Mar-98	26-Sep-98	
	138, 44	05-Feb-98	04-Nov-98	
	138, 45	05-Feb-98	22-Dec-98	
1999	137, 44	01-Feb-99	15-Oct-99	
	137, 45	01-Feb-99	15-Oct-99	

Year	Path, Row	Image acquisition date (dry season)	Image acquisition date (wet season)	Dataset
	138, 44	23-Jan-99	23-Nov-99	
	138, 45	08-Feb-99	25-Dec-99	
2000	137, 44	19-Jan-00	02-Nov-00	
	137, 45	19-Jan-00	02-Nov-00	
	138, 44	26-Jan-00	09-Nov-00	
	138, 45	26-Jan-00	09-Nov-00	
2001	137, 44	29-Jan-01	29-Nov-01	Landsat 7 ETM+ C1
	137, 45	29-Jan-01	29-Nov-01	Level-1
	138, 44	26-Apr-01	20-Nov-01	
	138, 45	26-Apr-01	20-Nov-01	
2002	137, 44	01-Feb-02	31-Oct-02	
	137, 45	01-Feb-02	31-Oct-02	
	138, 44	24-Feb-02	22-Oct-02	
	138, 45	13-Apr-02	22-Oct-02	
2003	137, 44	19-Jan-03	19-Nov-03	
	137, 45	19-Jan-03	19-Nov-03	
	138, 44	26-Jan-03	10-Nov-03	
	138, 45	11-Feb-03	10-Nov-03	
2004	137, 44	15-Feb-04	13-Nov-04	Landsat 4-5 TM C1
	137, 45	15-Feb-04	13-Nov-04	Level-1
	138, 44	26-Apr-04	19-Oct-04	
	138, 45	26-Apr-04	04-Nov-04	
2005	137, 44	16-Jan-05	16-Nov-05	
	137, 45	16-Jan-05	16-Nov-05	
	138, 44	07-Jan-05	07-Nov-05	
	138, 45	07-Jan-05	23-Nov-05	
2006	137, 44	08-Mar-06	03-Nov-06	
	137, 45	08-Mar-06	03-Nov-06	
	138, 44	27-Feb-06	12-Dec-06	
	138, 45	27-Feb-06	12-Dec-06	
2007	137, 44	27-Mar-07	16-Dec-07	Landsat 7 ETM+ C1
	137, 45	27-Mar-07	30-Nov-07	Level-1
	138, 44	05-May-07	21-Nov-07	
	138, 45	05-May-07	21-Nov-07	
2008	137, 44	27-Mar-07	31-Oct-08	
	137, 45	27-Mar-07	31-Oct-08	
	138, 44	05-May-07	07-Nov-08	
	138, 45	05-May-07	07-Nov-08	
2009	137, 44	19-Jan-09	05-Dec-09	
	137, 45	19-Jan-09	05-Dec-09	
	138, 44	10-Jan-09	25-Oct-09	
	138, 45	10-Jan-09	25-Oct-09	
2010	137, 44	07-Feb-10	06-Nov-10	
	137, 45	07-Feb-10	22-Nov-10	
	138, 44	29-Jan-10	28-Oct-10	
	138, 45	29-Jan-10	28-Oct-10	

Year	Path, Row	Image acquisition date (dry season)	Image acquisition date (wet season)	Dataset
2011	137, 44	25-Jan-11	09-Nov-11	
	137, 45	25-Jan-11	09-Nov-11	
	138, 44	01-Feb-11	15-Oct-11	
	138, 45	01-Feb-11	31-Oct-11	
2012	137, 44	13-Feb-12	11-Nov-12	
	137, 45	13-Feb-12	11-Nov-12	
	138, 44	04-Feb-12	04-Dec-12	
	138, 45	04-Feb-12	20-Dec-12	

Supplementary Table 3.3 Accuracy assessment of classified flood maps

Year	Overall accuracy	Kappa statistics	Remarks
1989	89%	0.78	Substantial agreement
2001	91%	0.81	Almost perfect agreement
2010	89%	0.77	Substantial agreement

Supplementary Table 3.4 Summary of ANOVA test for sensitivity analysis of pluvial flood model

Sensitivity test for	Groups	Number of observations	Mean inundation (km^2)	P-value	F ratio	F ratio (critical)
Interpolation method	IDW	25	126.9	0.22	1.49	2.69
	Kriging	25	123.7			
	Spline	25	119.8			
	Natural neighbour	25	119.2			
Subsidence rate	Subsidence 1 (2004 inundation)	277	26.6	0.27	1.3	2.61
	Subsidence 2 (2004 inundation)	277	26.6			
	Subsidence 1 (2006 inundation)	277	29.7			
	Subsidence 2 (2006 inundation)	277	29.6			

Supplementary Table 3.5 Pluvial flood model validation using field observation data

		Observed flood pixels		Row Total
		Flooded	Not flooded	
Modelled flood pixels	Flooded	276	8	284
	Not flooded	11	92	103
	Column total	287	100	387
	Overall accuracy		95%	
	Kappa coefficient		0.87	

Supplementary Table 3.6 Estimated GEV df parameters and return levels of different hydrological parameters

Parameters	**Estimated GEV df parameters**	**2.5% ci**	**95% ci**	**97.5% ci**
Monsoon total precipitation	Location	1390.83	1462.002	1540.96
	Scale	184.75	245.16	299.63
	Shape	-0.69	-0.44	-0.22
	Return levels			
	2-year	1473.962	1544.918	1616.129
	20-year	1783.559	1866.232	1938.832
	100-year	1833.738	1942.149	2067.480
River water level	Location	3.11	3.15	3.20
	Scale	0.08	0.11	0.13
	Shape	-0.42	-0.16	0.11
	Return levels			
	2-year	3.15	3.19	3.23
	20-year	3.34	3.42	3.49
	100-year	3.39	3.52	3.69
Tidal water level	Location	3.50	3.57	3.64
	Scale	0.15	0.20	0.26
	Shape	-0.40	-0.12	0.11
	Return levels			
	2-year	3.57	3.64	3.72
	20-year	3.92	4.08	4.24
	100-year	4.02	4.29	4.64

Supplementary figures

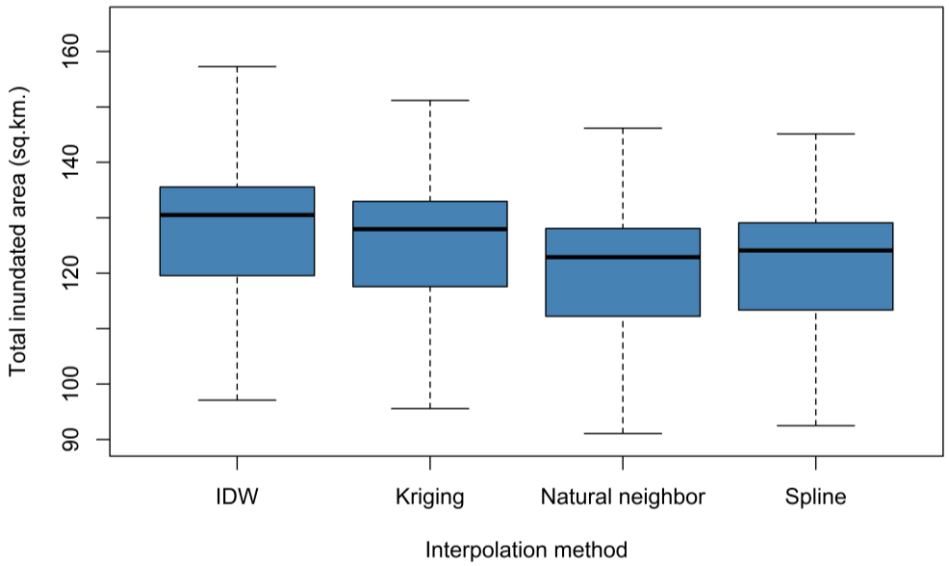

Supplementary Figure 3.1 Boxplot of annual pluvial inundation (for counterfactual scenario) based on subsidence rates derived applying four methods

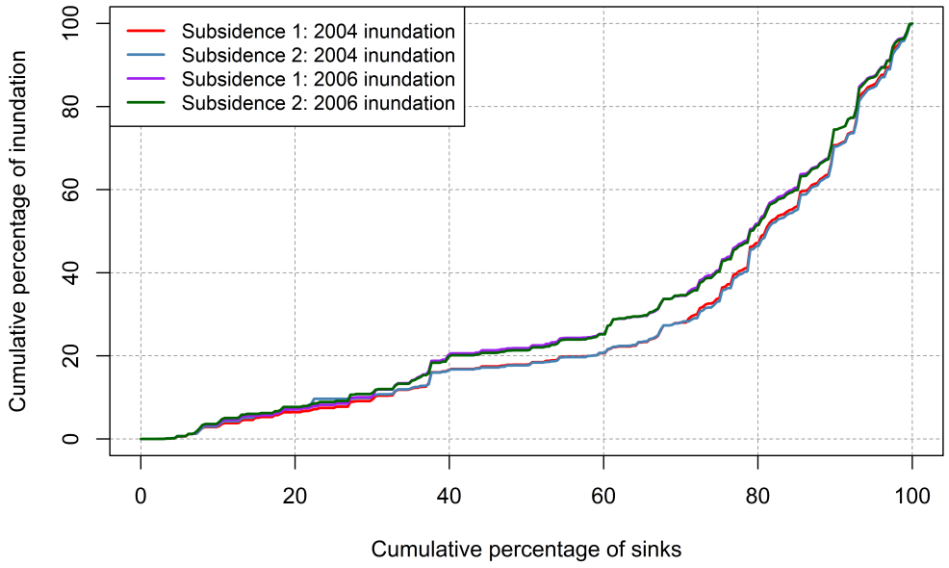

Supplementary Figure 3.2 Cumulative percentage change in inundation among various depressions for a change in land subsidence rates during two pluvial flood events

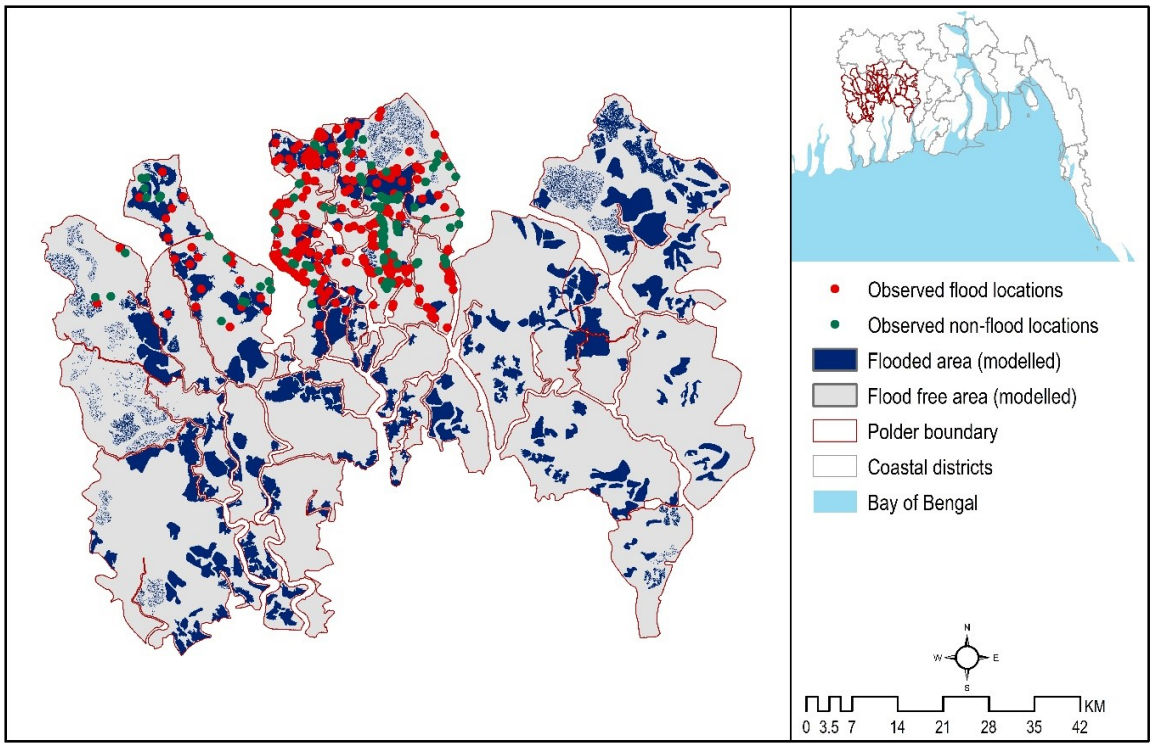

Supplementary Figure 3.3 Potential pluvial flood inundation areas (blue) and locations with field observations (circles)

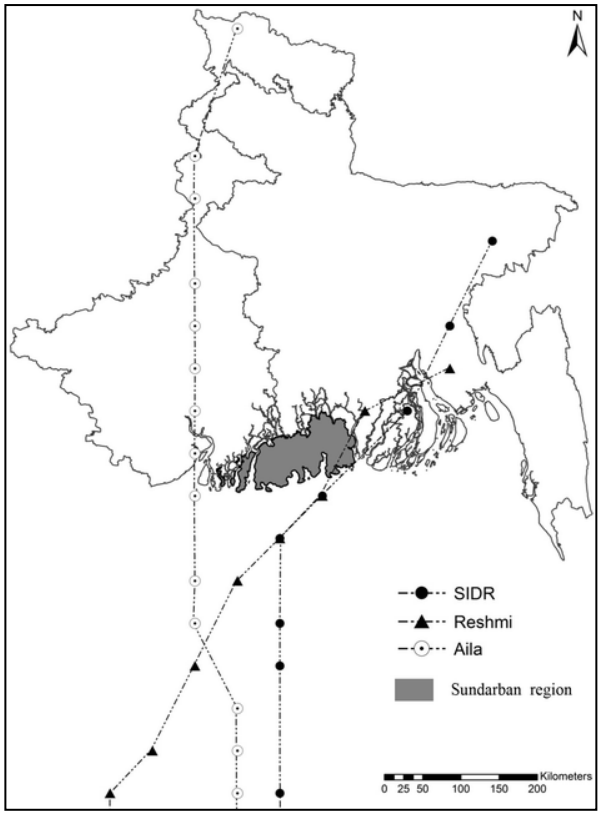

Supplementary Figure 3.4 Major cyclones from 2007-2009.

(In 2007, the track of cyclone Sidr crossed the south-central coast of Bangladesh. Since this study focused on south western region, we assumed that flood simulation based on reconstructed cyclone track (Reshmi) will explain the observed inundation. The unavailability of various hydrological data during the cyclone encouraged us to consider reconstructed cyclone track).

Source: (Dutta et al. 2015)

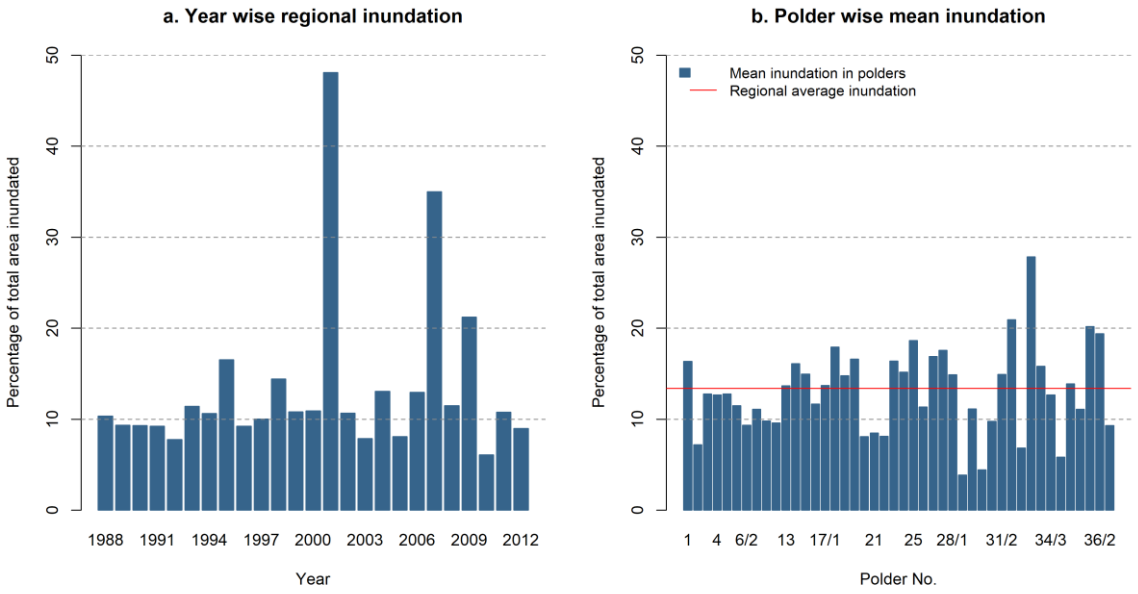

Supplementary Figure 3.5 Results from remote sensing-based flood identification

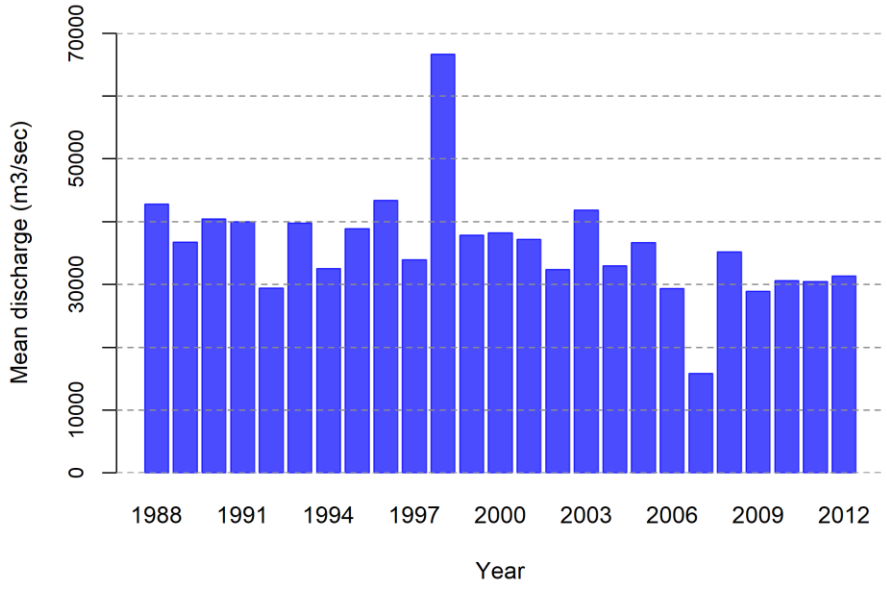

Supplementary Figure 3.6 Year mean discharge in Ganges River (Station: Baruria Transit)

Data source: Bangladesh Water Development Board (BWDB)

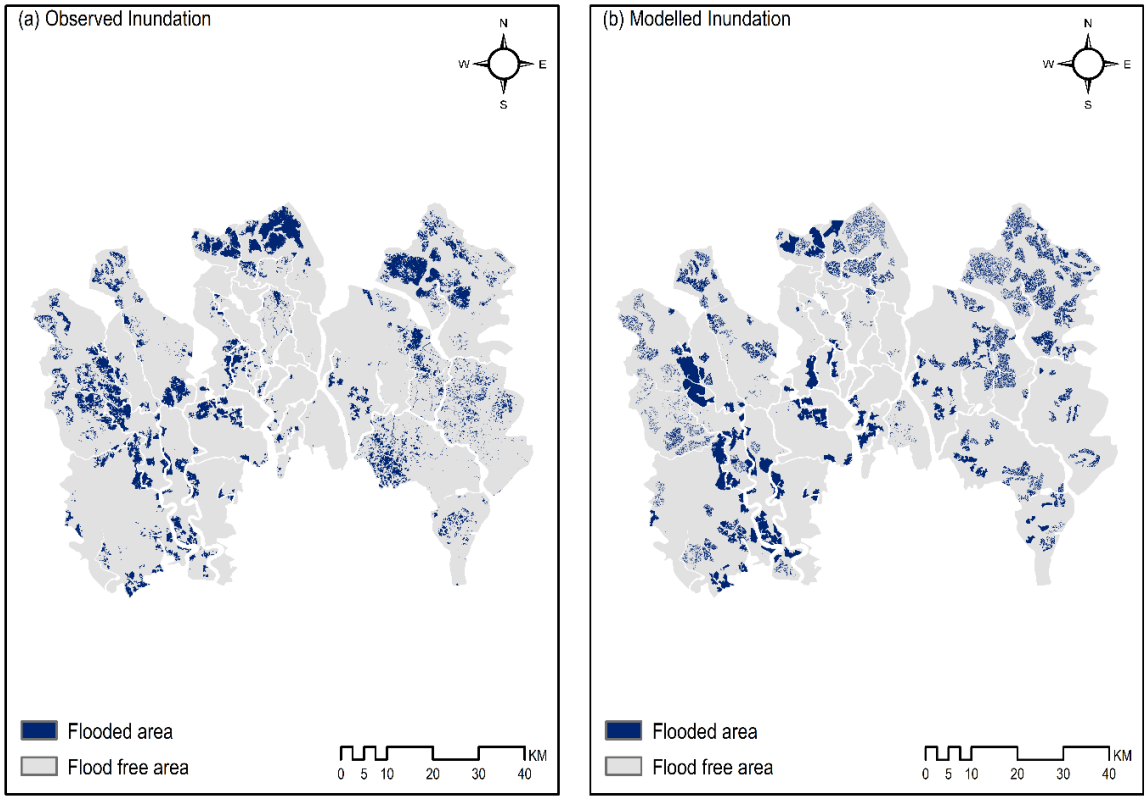

Supplementary Figure 3.7 Pluvial flood inundation in 1999. (a) observed inundation and (b) modelled inundation for 'with polder' scenario

a. Obsolete sluice gate (Polder 25)

b. Riverbank erosion damaging embank ment (Polder 30)

c. Excavation of drainage channel inside polder 29

d. Excavated Kobedak River

e. Rehabilitation of embankment (Polder 30)

Supplementary Figure 3.8 Snaps of polder observation.

(a, b. Poor structural conditions in polders. Water control structures including sluice gates and drainage channels could be utilized properly for pluvial flood reduction. Embankments are the major interventions against fluvio-tidal floods. Embankment breaching could cause significant inundation inside polders. c, d, e. Ongoing or implemented structural measures to minimize diversified problems in polders)

Source: (Field visit, 2018)

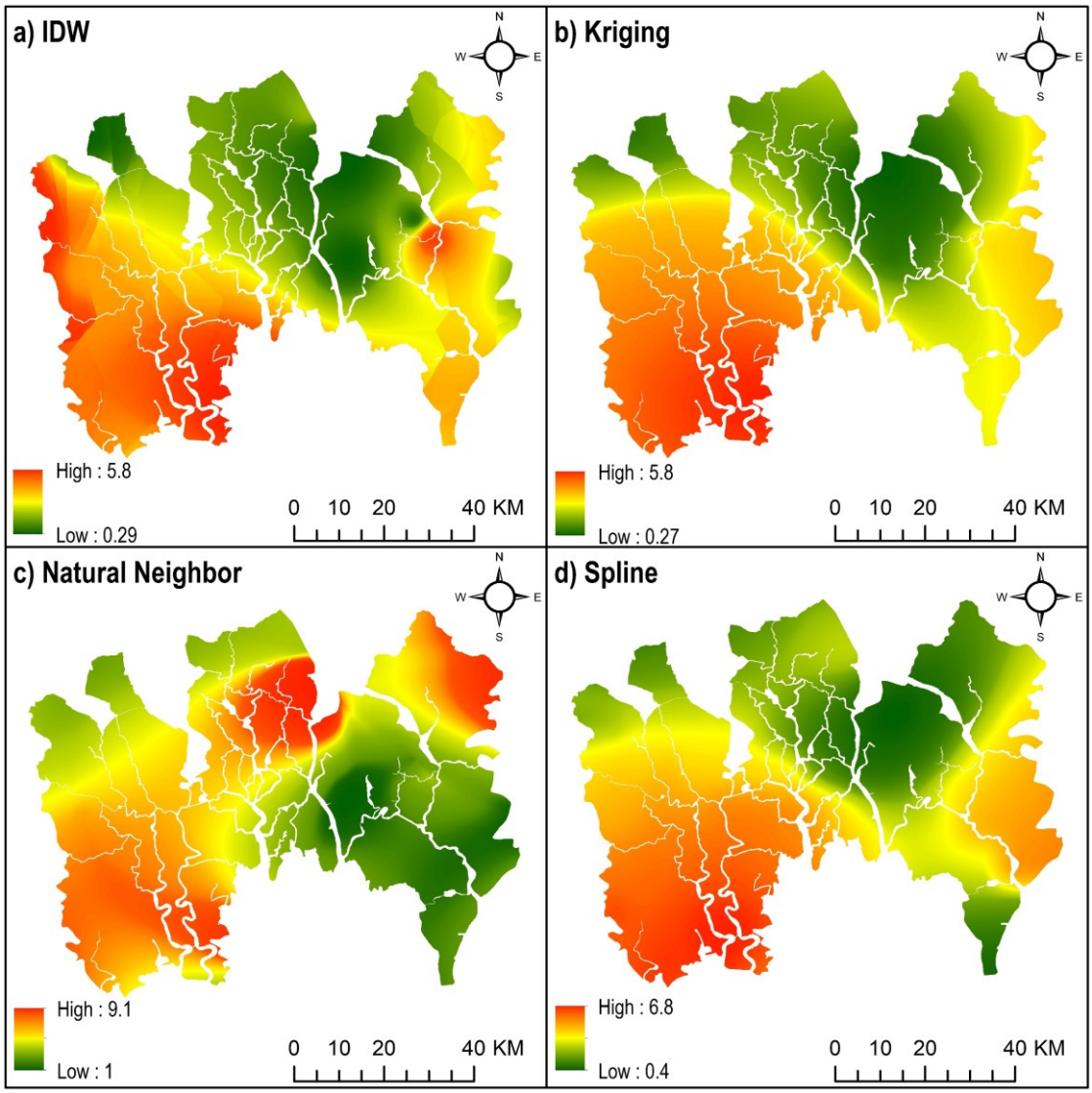

Supplementary Figure 3.9 Layers of annual land subsidence rates (mm/year) generated using various interpolation methods.

Chapter 4 The effects of changing land use and flood hazard on poverty in coastal Bangladesh

Abstract

The construction of polders in the coastal region of Bangladesh has significantly modified the patterns of flooding, as well as leading to significant land use/land cover (hereinafter, LULC) changes. The impact of LULC change and flooding on poverty is complex and poorly understood. This study presents a spatiotemporal appraisal of poverty in relation to LULC change and pluvial flood risk in the south western embanked area of Bangladesh. A combination of logistic regression (LR), cellular automata (CA), and Markov Chain models were utilised to predict future LULC based on historical data. Flood risk assessment was performed at present and for future LULC scenarios. A spatial regression model was developed, incorporating multiple parameters to estimate the wealth index (WI) for present-day and future scenarios. In the study area, agricultural lands reduced from 34% in 2005 to 8% in 2010, while aquaculture land cover increased from 17% to 39% during the same time. The rate of LULC change was relatively low between 2010 and 2019. Based on the recent trend, LULC was predicted for the year 2030. Flood risk was positively correlated with LULC and the expected annual damage (EAD) was estimated at $903 million in 2005, which is likely to increase to $2096 million by 2030, considering changes in LULC scenarios. The analysis further showed that the EAD and LULC change were negatively associated with the WI. Despite consistent national GDP growth in Bangladesh in recent years, the rate of increase of WI is likely to be low in the future because flood risk and patterns of LULC change have a negative effect on WI.

4.1. Introduction

It is widely recognised that poor people are disproportionately exposed to environmental hazards (Winsemius et al. 2018). There are several possible reasons for this. For instance, poor people tend to inhabit remote low-lying floodplains, due to the limited development opportunities and relatively cheaper lands (Dasgupta 2007). Their livelihoods and assets are less protected (Hossain et al. 2012, Bangalore et al. 2019), and thus, they have relatively a low capacity to cope with property losses resulting from flooding (Brouwer et al. 2007).

Bangladesh is located in the floodplain of three major rivers — the Ganges, Brahmaputra, and Meghna. The combined discharge generated of these three rivers is the highest in the world. The peak run-off depth is also the highest, which, combined with storm surges generated from the Bay of Bengal. This makes a major portion of the country is prone to flooding (Dasgupta 2007). Flood processes in the coastal region of Bangladesh are complex, as it can occur from multiple sources such as intense precipitation during the monsoon, high water levels in the rivers, and cyclone induced storm surges (Adnan et al. 2019b). Different environmental stresses create biophysical and socioeconomic challenges in the coastal region. For instance, frequent flooding and increasing soil salinity limit agricultural productivity, which is the main source of livelihoods in coastal Bangladesh (Rahman et al. 2020).

Flood management approaches in the coastal region of Bangladesh include both structural and non-structural measures (Rahman and Salehin 2013, Paul and Rashid 2017). Major surge events induced by cyclones in the 1950s forced the then government to invest in the Coastal Embankment Project (CEP) in the 1960s. The CEP aimed at increasing agricultural production to ensure food security, by preventing salinity intrusion in the coastal region particularly during the dry season. As a part of the CEP, 139 polders (enclosed coastal

embankments) were created in between the 1960s and 1980s (Warner et al. 2018, Islam et al. 2016b). The construction of the polders has brought both beneficial and harmful effects on society and the environment. The protection from flooding afforded by embankments led to an increase in agricultural productivity until the 1980s (Adnan et al. 2020). Embankments have demonstrably protected the polder area against storm surges and fluvio-tidal floods of moderate severity (Adnan et al. 2019b). However, the separation of floodplains from adjacent rivers caused geomorphological changes in the polder areas, exacerbating land subsidence inside polders (Auerbach et al. 2015). Accelerated land subsidence and inadequate drainage are accountable for frequent pluvial flooding (locally called 'waterlogging') (Adnan et al. 2019b).

Generally, the construction of structural flood control measures, such as polders, shapes the pattern of human settlements and land use, which in turn impacts the extent of flood risk. Such flood control measures create the so-called "levee effect" (White 1945). Whilst people tend to settle in less flood-prone areas, presence of structural flood defence system encourages floodplain development by engendering a sense of safety (Di Baldassarre et al. 2013, Montz and Tobin 2008). Therefore, the failure of structural systems in the form of overtopping or breaching of embankments may exacerbate flood damages (Hui et al. 2016).

The pattern of land use/land cover (LULC) in the coastal region of Bangladesh has experienced major changes over the past half-century, following the construction of polders (Rahman et al. 2017, Khan et al. 2015, Parvin et al. 2017, Huq et al. 2015, Abdullah et al. 2019). Such changes largely occurred due to frequent and diverse natural hazards (e.g., floods) and increases in inundation, soil salinity, and land erosion (Brouwer et al. 2007, Khan et al. 2015). For instance, about 25.9% increase in the proportion of wetland/shrimp farm area was observed in between 1989 and 2015 in a small administrative area of the south

western coastal zone (Rahman et al. 2017). The transformation of agricultural land to shrimp culture has been a common practice in the area since the 1980s as it can be more profitable (Khan et al. 2015). However, such land transformation has reportedly been leading to an increase in soil salinity, reducing agricultural production (Rahman et al. 2017, Khan et al. 2015).

Whilst anthropogenic drivers profoundly change the pattern of LULC, such transformation of land may affect local flooding processes (Wheater and Evans 2009). The pattern of LULC determines the amount of runoff generated during a precipitation event, thus, influencing the water balance in an area. Hence, LULC may affect both the probability of flooding and its consequences (Szwagrzyk et al. 2018, McColl and Aggett 2007). Flood losses are not only dependent on extreme hydro-meteorological conditions of a region, unplanned land use can multiply property damages (Lee and Brody 2018). In coastal Bangladesh, unplanned LULC change may lead to environmental degradation such as soil salinization, disappearance of seasonal lagoons, and deterioration of water quality by increasing salinity (Islam et al. 2015).

Generally, flooding and poverty coexist particularly within rural communities, as damages caused by recurring flood events deplete assets, negatively impact agricultural incomes and thus lower quality of life of communities (Dube et al. 2018). It has been hypothesised that increasing flood risk and unplanned LULC change may create a poverty trap in the coastal region of Bangladesh (Ahmed 2018, Borgomeo et al. 2017), inhibiting long-term development prospects (Parvin et al. 2017). Marginalised farmers could not generate adequate income through agricultural activities, whilst being unable to transform their agricultural land into aquaculture due to high cost associated with such change (Islam et al. 2015). As a result, they are unable to migrate out of such areas due to social and economic constraints and related costs (Dasgupta 2007).

Regulating LULC change is an intervention to reduce flood risk, which has been adopted in different coastal cities (Adnan and Kreibich 2016). Therefore, it is essential to understand the association between LULC and flood risk. Risk-based flood management approaches have received attention globally due to recent experience of several catastrophic events in many regions across the world (Hall et al. 2003c, Poussin et al. 2015, Hall et al. 2015), as well as the projected increase in the frequency and severity of flooding due to climate change-induced sea level rise (Koks 2018). An empirical analysis of flood risk can support decision-makers to appraise and sequence investments for flood management (Dawson et al. 2011, Hall et al. 2003a, Sayers et al. 2002, Hino and Hall 2017, Hall et al. 2019). The methods used in research and practice for quantifying flood hazard and vulnerability range from simple approaches (with numerous simplifying assumptions) to very complex applications, which are both data and time-intensive and computationally expensive (Apel et al. 2009, Dewan 2013).

In the existing literature, the association between flood risk and poverty has been comprehended primarily by estimating exposure of poor people to flooding at various geographical scales (Bangalore et al. 2019, Winsemius et al. 2018, Brouwer et al. 2007, Qiang et al. 2017). In the case of coastal Bangladesh, a few studies have applied quantitative approaches (based on household survey data) to show how poverty exacerbates flood vulnerability/risk (Brouwer et al. 2007, Akter and Mallick 2013). However, little is known about (i) how the pattern of LULC change influences flood risk at present and in the future; (ii) what is the association between LULC change and risk of flooding, and how they impact poverty spatially. We address these questions by estimating: (i) flood risk in relation to current and future LULC scenarios; and (ii) the change in poverty in relation to a change in LULC and flood risk.

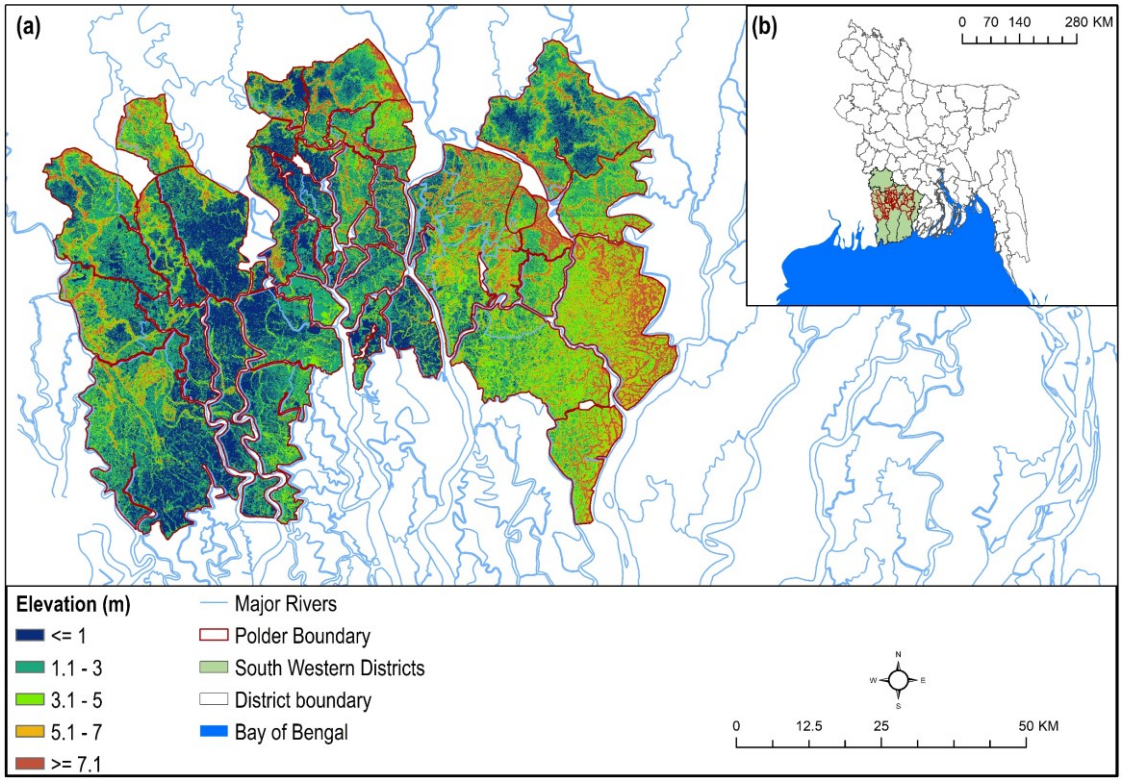

Figure 4.1 South western embanked area of Bangladesh

4.2. Materials and methods

This study was conducted in three stages. First, a model was established to analyse spatiotemporal patterns of LULC change and predict future LULC. Second, pluvial flood hazard was modelled to simulate the depth and extent of inundations for various return periods of monsoonal precipitation. Then flood risk was estimated at each LULC scenario (historical and future), for different flood return periods. Finally, a spatial regression model was developed to estimate poverty, incorporating geographical, environmental, and socio-economic parameters including LULC change and flood risk.

4.2.1. Description of the study area

This study focussed on polders in the south western coast of Bangladesh. The area includes a total of 44 polders, located in five coastal districts: Bagerhat, Jessore, Khulna, Pirojpur, and Satkhira (Figure 4.1). These polders were constructed to protect about 5187

km^2 of land, where approximately 5.3 million people inhabited in 2015 (WorldPop 2018). The area has a mean elevation of 3.5 m and is heavily intersected by tidal rivers. The area is prone to three types of flooding — pluvial, fluvio-tidal, and surge floods. Inadequate drainage channels and increasing land subsidence exacerbate frequent pluvial flooding during the monsoon months (May to September) (Adnan et al. 2019b), when the area receives the maximum amount of precipitation (Figure 4.2). A lack of sedimentation and accelerated compaction within the embanked area led to a loss of 1.0-1.5 m elevation since the construction of polders in the 1960s (Auerbach et al. 2015). Agriculture, shrimp farming, and the natural resources of the Sundarban mangrove forest (located in the south of the study area) are the major sources of livelihoods and economy of the inhabitants (Khan et al. 2015). Approximately 80% of the total shrimp ponds of Bangladesh are located in south western coast (Ahmed 2018). However, increased soil salinity resulting from the excessive shrimp farming has negatively impacted crop yield. The situation potentially affects the livelihoods of the poorest segments of society (Szabo et al. 2016). A risk-sensitive land use policy would help to alleviate the complex problems of the south western coast (Rahman et al. 2017). Thus, this study aimed to provide spatial information on land use change and flood risk, as well as their association with poverty.

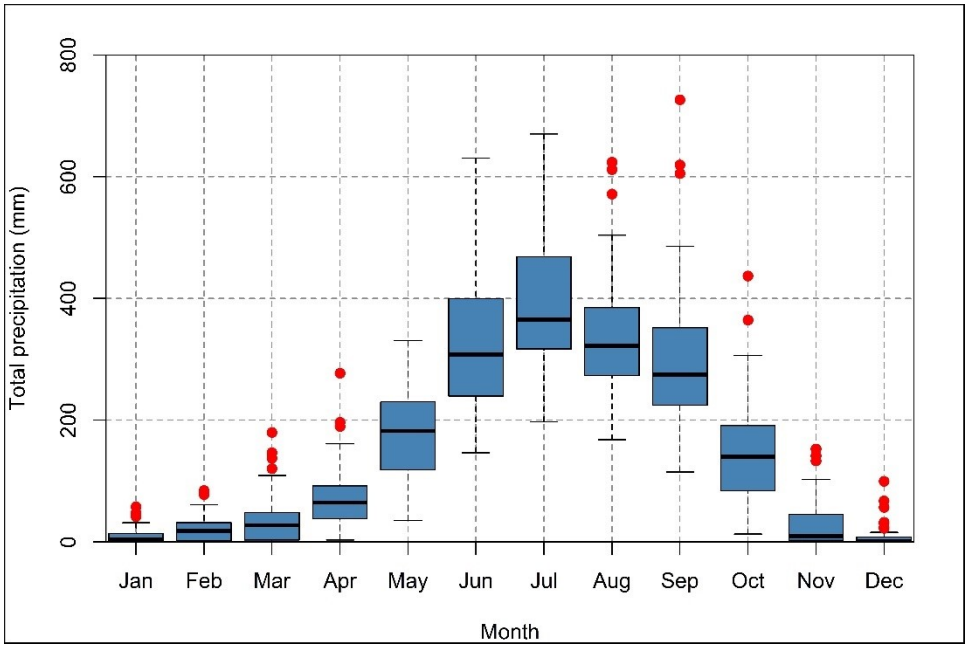

Figure 4.2 Box and whisker plot of monthly rainfall (1965-2012) for south western embanked area

4.2.2. Data

This study examined the effects of LULC change and flood risk on poverty. A range of spatial and hydrometeorological data were used to model LULC change, assess flood risk, and estimate poverty. A list of data is given in Table 4.2. The LULC dataset used in this study is an updated version of Abdullah et al. (2019). The dataset contains five classes: agricultural, aquaculture, bare land, built-up area (urban), vegetation with the rural settlement, and waterbody. The Advanced Land Observing Satellite (ALOS) digital elevation model (DEM) (JAXA 2015) at 30 m resolution used to derive maps of various geomorphological parameters (e.g. elevation, slope, curvature) and establish flood hazard model. The ALOS DEM was used as it is considered to be highly reliable and freely available DEM, which has a low root mean square error (1.78m) in vertical accuracy (Adnan et al. 2020). Hydrometeorological data were collected from various organisations including Bangladesh Meteorological Department (BMD), Bangladesh Agricultural Research Council (BARC), and Water Resources Planning Organisation of Bangladesh (WARPO). This study

considered the Wealth Index (WI) as an indicator of poverty. The WI data was obtained from Steele et al. (2017).

Table 4.1 Different data types used in this study

Data	Description	Source
1. LULC	LULC data of 2005, 2010, and 2019 at 30 m resolution	(Abdullah et al. 2019)
2. DEM	ALOS DEM of 30 m resolution	(JAXA 2015)
3. Precipitation	Gridded (5km grid points) precipitation data of 10-day temporal resolution from 1965-2012	(www.bmd.gov.bd/)
4. Climate	Monthly average temperature, monthly average daylight hour data from 1988-2012, across four weather stations	(http://www.barc.gov.bd/)
5. Poverty	Gridded Demographic and Health Surveys (DHS) Wealth Index (WI)	(Steele et al. 2017)
6. Soil salinity	Gridded soil salinity index	(Abdullah et al. 2018)
7. Population density	Total number of people per 100 m grid-cell	(https://www.worldpop.org)
8. Gross Domestic Product (GDP)	Gridded GDP data of 30 arc-sec (~900m) resolution	(Kummu et al. 2018)
9. Agricultural employment	Number of people employed in the agricultural sector	(De Bono and Chatenoux 2014)
10. Spatial data	GIS vector data of road network, river channels, and growth centre	(http://www.warpo.gov.bd)

4.2.3. Modelling LULC change

This study predicted LULC during 2030 using a combination of logistic regression (LR), cellular automata (CA), and Markov Chain models, following an approach by Arsanjani et al. (2013). A similar modelling approach has been used in several studies for detecting and simulating LULC change (Mitsova et al. 2011, Kityuttachai et al. 2013, Shahbazian et al. 2019, Wang et al. 2019, Ahmed et al. 2013). We applied this approach for following reasons: (i) it can incorporate both environmental and socio-economic variables;

(ii) the model can incorporate a wide range of spatial factors; (iii) the LR model can use data at different scales; and (iv) the CA model can control spatial dynamics of LULC changes (Arsanjani et al. 2013, Shahbazian et al. 2019).

The CA model uses a principle that areas tend to change to a state based on the state of their neighbouring areas (Arsanjani et al. 2013). A CA system includes four components such as cells, states, neighbourhoods, and rules (Shahbazian et al. 2019). Cells are defined as the smallest unit and the state of each cell is determined by its initial state, the conditions in the surrounding cells, and a set of transition rules (Arsanjani et al. 2013, Verburg et al. 2004). The CA model in this study incorporated a LULC change map, transition potential maps created using LR models, the change rate calculated in the change analysis step, and a transition probability matrix predicted for a future year (using Markov Chain model).

4.2.3.1. Analysing LULC change

LULC data of 2005, 2010, and 2019 were analysed to detect spatiotemporal changes. The model initially calibrated LULC change over the period 2005-2010. While developing a LULC change map, the transition areas less than 5 km^2 (~0.001% of total area) were ignored, otherwise, the modelling approach would have been computationally expensive. As a result, the 2005-2010 change map included a total of 12 LULC transition categories.

4.2.3.2. Driving forces for detecting change

The LR models were established for all 12 transitions, to estimate the degree of influence of different factors (driving forces) on a type of LULC (Shahbazian et al. 2019). LULC changes could be governed by various combinations of geographical, environmental, and socio-economic factors (Dewan and Yamaguchi 2009). Based on the knowledge attained from literature as well as expert knowledge on the study area, a total of 14 variables were selected (Table 4.2). For a LULC transition, the LR model incorporated a binary (change to a LULC class and no-change) dependent variable and different combinations of

independent variables (driving forces). Combinations of independent variables were selected in a way that yielded the highest relative operating characteristic (ROC) and adjusted odds ratio values, indicating performance of the models (Arsanjani et al. 2013).

The LR model created probability surface maps using the following equation (Hosmer Jr et al. 2013):

$$p = 1/(1 + e^{-z}) \tag{4.1}$$

where p ranges from 0 to 1 on an S-shaped curve, explaining the probability of a cell changing to a LULC class; z is the linear combination of independent variables (driving forces), which was estimated using the following equation:

$$z = b_0 + b_1x_1 + b_2x_2 + \cdots + b_nx_n \tag{4.2}$$

where b_0 is the model intercept, b_i (i = 1, 2, ..., n) indicates the coefficients of independent variables, and x_i (i = 1, 2, ..., n) represents the n number of independent variables.

4.2.3.3. Simulating future LULC

The CA-Markov Chain model was used to predict LULC change based on the estimated transition probabilities (Arsanjani et al. 2013, Shahbazian et al. 2019). The Markov Chain model predicted the quantity of change in each LULC transition. Based on the Bayes' theorem of conditional probability, LULC was predicted using the following formula (Sang et al. 2011):

$$S\,(t+1) = P_{ij} \times S(t) \tag{4.3}$$

where $S(t)$ and $S(t+1)$ are the LULC status at the time t and $t+1$, respectively; the transition probability matrix P_{ij} was estimated as follow:

$$P_{ij} = \begin{bmatrix} P_{11} & P_{12} & \cdots & P_{1n} \\ P_{21} & P_{22} & \cdots & P_{2n} \\ \cdots & \cdots & \cdots & \cdots \\ P_{n1} & P_{n2} & \cdots & P_{nn} \end{bmatrix} \tag{4.4}$$

$$\left(0 \leq P_{ij} < 1 \; and \; \sum_{j=1}^{n} P_{ij} = 1, (i, j = 1,2,3, \ldots n) \right)$$

where n is the total number of LULC classes. In this study, probability values of 2019 and 2030 were predicted based on transition matrices of 2005-2010 and 2010-2019, respectively. However, the spatial distribution of LULC in a Markov Chain model is unknown. Therefore, the CA model was integrated to provide a spatial dimension to the model (Arsanjani et al. 2013, Shahbazian et al. 2019, Corner et al. 2014).

4.2.3.4. Validating the outputs

The LULC change model was validated for the year 2019. Therefore, considering LULC maps of 2005 and 2010 as the initial and final state maps, the model predicted LULC map of 2019. We compared predicted LULC map with observed data of 2019. Kappa statistic was estimated to determine the degree of agreement between observed and modelled LULC maps (Mitsova et al. 2011).

4.2.4. Flood risk assessment

Flood risk assessment was carried out for various LULC scenarios to estimate temporal changes of direct economic damage due to floods of various magnitudes. The risk was defined as the product of flood hazard, exposure, and vulnerability. The expected annual damages (EAD) at different LULC scenarios were estimated to represent spatiotemporal pattern of flood risk (Rojas et al. 2013).

4.2.4.1. Flood frequency analysis

This study primarily focused on pluvial flooding, considering increased frequency and severity of this type of flooding in the study area. Although historically, three types of flooding (pluvial, fluvio-tidal, and storm surge induced flooding) affect the study area, occurrence of pluvial flooding is a relatively recent and frequent phenomenon. Adnan et al. (2019b) documented that monsoon precipitation caused inundation in the area every year

from 1988 to 2012. Persistent pluvial flooding damages crops and therefore impacts the livelihoods of people who inhabit the south western coast (Alam et al. 2017).

Flood frequency analysis was carried out to estimate return periods of monsoon precipitation, which is the main source of pluvial flooding in the study area (Adnan et al. 2019b). Seven recurrence intervals (i.e. 1, 2, 5, 10, 20, 50, and 100 years) of floods were considered here. Inundation depth was estimated at each cell within the study area. Since pluvial flood hazard model takes monthly precipitation as an input, we generated raster layers of monthly precipitation of seven return periods. To decide whether the climate in the near future (i.e. 2030) is likely to be in a 'changed' or 'unchanged' state, a precipitation trend analysis was performed. Therefore, linear regression models of monthly precipitation were established (Panda and Sahu 2019). We also applied an autocorrelation function (ACF) to estimate whether monthly total precipitation was autocorrelated between years (Feng et al. 2016). No significant autocorrelation was found between successive years. The linear regression models confirmed the absence of a significant trend in monthly precipitation. The results of precipitation trend analysis are summarised in Supplementary Table 4.3 and Supplementary Figure 4.1. To generate monthly precipitation layers of seven return periods, extreme value analysis was conducted at each grid cell by fitting a generalized extreme-value (GEV) distribution using the L-moment method, following Adnan et al. (2019b).

4.2.4.2. Flood hazard assessment

Flood hazard assessment included a hydrological simulation of floods of various return periods (Rojas et al. 2013). Inundation maps were also derived for seven recurrence intervals of monsoon precipitation — 1, 2, 5, 10, 20, 50, and 100 years — using a pluvial flood rainfall-runoff and spreading model established for the study area by Adnan et al. (2019b). The modelling process started with estimating monthly water balance. A Thornthwaite and Mather water balance model was accompanied by the flood model, which

estimated monthly excess precipitation at each grid cell, after subtracting evapotranspiration from monthly total precipitation. Monthly excess precipitation layers from May to September were aggregated to prepare excess precipitation layers during the monsoon. The inundation model incorporated the ALOS DEM to identify depressions and their catchments. During a flood event, the estimated total volume of excess precipitation was assigned to each depression according to the respective catchment position to represent both flood depth and extent. Further description of the model, validation process and sensitivity analysis can be found in Adnan et al. (2019b). The flood hazard mapping resulted in inundation maps of seven recurrence intervals.

4.2.4.3. Flood vulnerability analysis

Flood vulnerability assessment generally includes the estimation of direct or indirect damages due to floods. Direct damages, which primarily occurred because of physical contact of houses, building, and public infrastructures with floodwater, are estimated as a function of flood depth in different cells, the relationship between flood depth and LULC (or structural use), and total cell area (Apel et al. 2009). Indirect damages can be an outcome of the failures of critical infrastructure systems, such as transportation, production, and energy (Koks et al. 2019). The scope of the study was however limited to estimating direct flood damages. It was estimated for three types of LULC (i.e. agriculture, aquaculture, and residential) using the following equation (Islam et al. 2019):

$$D_j = \left(\sum_{i=1}^{n} x_i \times f(x_i) \right) \times A \tag{4.5}$$

where D_j is the total damage (in million USD ($)) during a flood return period of j, x_i is the flood depth (m) in cell i, $f(x_i)$ is the damage function for the flood depth level x in cell i, and A is the area of a cell. Global depth-damage curves, adopted from Huizinga et al. (2017), were used to estimate direct tangible flood damage to residential and agricultural

LULC. The depth-damage curve for aquaculture lands was obtained from Islam et al. (2019). The maximum damage values in depth-damage functions were given in Euro, which we converted into USD using a currency conversion rate of 1 Euro = 1.11 USD.

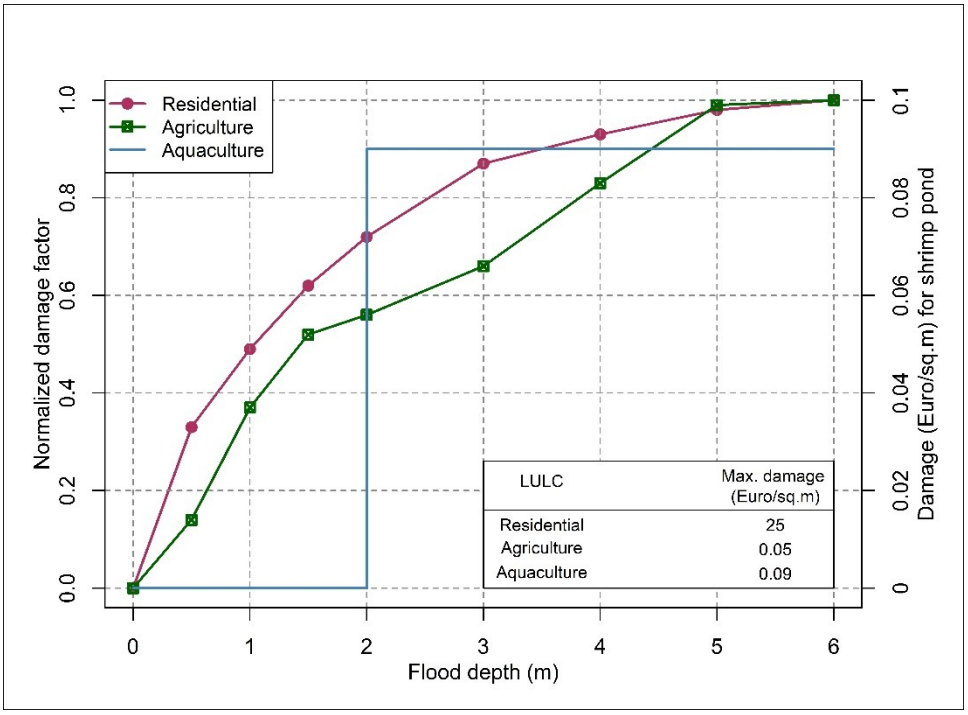

Figure 4.3 Depth-damage curves (adopted from Huizinga et al. (2017) and Islam et al. (2019))

Pixel-scale (30 m resolution) flood damage was estimated in a GIS for seven flood return periods (1, 2, 5, 10, 20, 50, and 100-year) at four LULC scenarios of 2005, 2010, 2019, and 2030. Inundation maps (see section 4.2.4.2) were overlaid on LULC maps to record flood depth and LULC according to each pixel. This dataset was imported in an R package and integrated with equation 5.5 to estimate pixel-scale flood damage, as well as total damage of the study area.

4.2.4.4. Estimating flood risk

Following flood hazard and vulnerability assessments, risks were estimated in the form of expected annual damage (EAD) for four LULC scenarios (2005, 2010, 2019, and 2030). The EAD can be estimated using the following equation (Olsen et al. 2015):

$$EAD = \iint_{A\,p} D(p)dpdA \tag{4.6}$$

where *D(p)* is the damage occurred during an event with the annual probability of exceedance *p* (approximated by the inverse of the flood return period (*T*)), *A* is the total area of the region under study. Since the choice of return periods influences flood risk estimates, a consideration of all return periods between the low and high probability floods enables an accurate estimation of risk (Ward et al. 2011). The probability space of flood risk for each integer year flood return period between 1 and 100 is discretised into 100 equal intervals, by interpolating flood damages estimated between seven recurrence intervals (Rojas et al. 2013). An exceedance probability curve was developed by plotting flood damages against corresponding exceedance probabilities. The exceedance probabilities of 0.01 (100-year) and 1 (1-year) were considered correspondingly as the lower and upper limits of the probability curve. The EAD was estimated as the area under the curve (AUC), applying the trapezoidal rule given in equation 4.7 (Olsen et al. 2015).

$$EAD = \frac{1}{2}\sum_{i=1}^{n}\left(\frac{1}{T_i} - \frac{1}{T_{i+1}}\right)(D_i + D_{i+1}) \tag{4.7}$$

where *n* is the total number of return periods which is 100; T_i is the return period of the i^{th} event; D_i is the estimated flood damage during the i^{th} event.

4.2.5. Downscaling poverty data

Flood damage may exacerbate the degree of poverty in a region, whilst poor people may be compelled to live in riskier locations (Dube et al. 2018). This study aimed at investigating the spatiotemporal distribution of poverty, diagnosing its association with flood risk and LULC change. Steele et al. (2017) developed a gridded poverty dataset for Bangladesh, combining data from multiple sources such as mobile phone, satellite, and traditional survey. The spatial scale of the database was determined by developing the

service area coverage of a cellular network using the Voronoi polygons. The spatial resolution of the data varies from 60 m to 5 km, where poverty was represented as asset, consumption, and income-based measures of wellbeing. In this study, we considered the asset-based measure, i.e., Demographic and Health Surveys (DHS) Wealth Index (WI), because the WI yielded the highest accuracy of predictions than other poverty metrics (Steele et al. 2017). The WI is a measure of household's living standard that is calculated using survey data on household characteristics (e.g. material used for housing construction), ownership of selected assets (e.g., television, bicycles), and access to different facilities such as water supply and sanitation (https://www.dhsprogram.com). The values of the WI can be either positive or negative, where a higher value implies higher socioeconomic status (Steele et al. 2017).

We downscaled the gridded WI data obtained from Steele et al. (2017), establishing a GIS-based ordinary least square (OLS) model (equation 4.8) based on ten spatial parameters (Table 4.4). The south western embanked area is comprised of 303 Voronoi polygons. The polygons were used to extract the values of all parameters.

$$y = \beta_0 + \beta_1 X_1 + \beta_2 X_2 + \cdots + \beta_n X_n + \varepsilon \quad (4.8)$$

where y is the WI, X_n is the value n^{th} parameter, β is the regression coefficient, and ε is the random error in prediction or residuals.

Spatial parameters included soil salinity, elevation, EAD, relative flood frequency, distance from northing and easting coordinates, LULC change, population density, GDP, and the number of people employed in the agricultural sector. The selection of parameters was based on their (i) role in influencing poverty (ii) availability as gridded data. Soil salinity impacts poverty as increasing salinity in the coastal region hinders agricultural activity (Szabo et al. 2016). A map of relative flood frequency was collected from Adnan et al. (2020). To represent ground elevation, ALOS DEM was used. The EAD map developed in

this study (see section 4.2.4.4) was included in the regression model. A binary (change or no-change) LULC change map from each previous time step was incorporated. Two layers, representing the Euclidean distance from northing and easting lines were produced, to understand the spatial distribution of WI. GDP indicates the extent of human and economic development of a country, may influence WI. Gridded GDP data was extracted for the study area from a global dataset developed by Kummu et al. (2018). The dataset has a spatial resolution of 30 arc-sec (~900m) and generated for years 1990, 2000, and 2015. Using the GDP data of 2015, we projected the GDP of 2010, 2019, and 2030, incorporating existing and projected GDP growth rates provided by the World Bank and the International Monetary Fund (IMF), respectively. Sources of gridded soil salinity, population density, and agricultural employment data are given in Table 4.1.

The year 2010 was considered as a base year for this analysis, as WI data was developed based on 2011 DHS and 2010 Household Income and Expenditure (HIES) survey data. Performance of the model was determined by estimating the coefficient of determination (R^2). The generated OLS regression equation was used to predict WI for the year 2019 and 2030. Therefore, four independent variables were adjusted accordingly: The EAD, LULC change, population density, and GDP, while other variables were assumed to be constant.

4.3. Results

4.3.1. LULC change modelling

4.3.1.1. Temporal change of LULC

Figure 4.4 (a) shows temporal changes of observed LULC from 2005 to 2019 and their spatial variations are presented in Supplementary Figure 4.2. From 2005-2010, a significant decrease in agricultural land was observed, while the proportion of aquaculture category increased substantially. More than 50% of agricultural lands transformed into

aquaculture use, with another 25% into rural settlements. Contrarily, LULC change from 2010-2019 was relatively stable, when the main transformation took place in bare land; about 23% bare land area transformed into rural settlements. Stable growth in rural and urban settlements was observed between the years 2005 and 2019.

4.3.1.2. Driving factors

Various combinations of geographical, environmental, and social factors account for different types of LULC transition. Table 4.2 shows regression coefficients of different factors influencing the transformation of agricultural lands into aquaculture, rural, and urban use within 2005-2010. The probability of LULC change from agricultural to aquaculture use is higher in areas characterised by low elevation, concave curvature, frequently affected by flooding, located in proximity to existing aquaculture lands, roads, and drainage channels, high level of soil salinity, and located in the northern portion of the study area. Notably, we found a positive correlation of flood frequency with LULC change from agriculture to rural and urban settlements. About 57% of the study area was inundated by at least two historical flood events from 1988 to 2012 (Adnan et al. 2020). Therefore, substantial development of the residential area took place in the flood-prone zones. A summary of LR models of the remaining nine LULC transitions is given in Supplementary Table 4.1.

Table 4.2 Driving factors of LULC change from 2005 to 2010

Factors	**Regression coefficient**		
	Agriculture to aquaculture	**Agriculture to rural settlement**	**Agriculture to built-up area (urban)**
Intercept	1.41	1.25	9.53
Elevation	-0.02	0.11	-0.37
Slope	$-1e^{-04}$	$2e^{-05}$	$-2e^{-04}$
Curvature	0.05		
Flood frequency	0.69	0.19	0.43
Distance from aquaculture land	-0.34		
Distance from existing road	-0.04	-0.05	-0.06

Distance from residential area		-0.07	-2.42
Distance from adjacent river	-0.11		
Distance from drainage channel	-0.35		
Distance from growth centre		0.07	0.11
Soil salinity	0.39	0.25	
Distance from northing coordinates	-0.19	-0.31	-0.09
Distance from easting coordinates		-0.003	0.10
Population density	-0.21	0.05	0.18

The performance of each LR model is indicated by the estimated ROC and odds ratio (Table 4.3). A ROC value 1 indicates a perfect fit and ROC value 0.5 represents a random fit. Also, a higher adjusted odds ratio indicates a better performance of a model (Arsanjani et al. 2013). In this study, the LR model for LULC transformation from agriculture to aquaculture cover obtained highest estimates of these performance indicators.

Table 4.3 ROC and adjusted odds ratio values of LR models

*Transitions	ROC	Adjusted odd ratio
LULC -1 to LULC -2	0.93	81.27
LULC -1 to LULC -3	0.71	5.23
LULC -1 to LULC -4	0.91	24.67
LULC -1 to LULC -5	0.73	4.60
LULC -1 to LULC -6	0.89	17.82
LULC -2 to LULC -3	0.74	8.10
LULC -3 to LULC -1	0.67	4.28
LULC -3 to LULC -2	0.89	14.38
LULC -3 to LULC -5	0.68	2.96
LULC -5 to LULC -1	0.63	2.07
LULC -5 to LULC -2	0.93	35.74
LULC -5 to LULC -3	0.82	9.81

** LULC -1= Agriculture; LULC -2 = Aquaculture; LULC -3 = Bare land; LULC -4 = Built-up area (urban); LULC -5 = Vegetation with rural settlement; LULC -6 = Waterbody*

4.3.1.3. Predicting LULC

The combination of LR and CA-Markov chain model determined LULC quantitatively, where the LR model generated probability surfaces of different transitions, the Markov chain model predicted the quantity of change in each LULC transition, and the

CA model controlled the spatial dynamics the projected LULC. The Markov chain model estimated the transition probability of 2030 based on the transition matrix 2010-2019 (Supplementary Table 4.2). The simulation suggests that the proportion of agricultural land, bare land, and general waterbody is likely to decrease, while aquaculture lands, as well as rural and urban settlement areas, would increase (Figure 4.4 (a)). In the case of the spatial distribution of different categories of LULC, aquaculture is likely to remain as the dominant type of LULC in northern and western segments of the study area given its economic return. Agricultural activities would mostly take place in the eastern segment, where "vegetation with rural settlement" is likely to be the dominant LULC category (Supplementary Figure 4.2). The validation process yielded a kappa coefficient of 0.87, which indicates an acceptable degree of accuracy. However, the choice of driving forces affects the accuracy of the model (Wang et al. 2019). Although different environmental and socio-economic factors were considered in this study, a limited number of driving forces may have resulted in some errors in the predicted LULC.

4.3.2. Association between LULC change and flood risk

4.3.2.1. Flood damage

Flood damages are associated with the type of LULC in the study area. Figure 4.4 (b) shows estimated damages during floods of different recurrence intervals, under four LULC scenarios. An increasing trend of flood damages was estimated, with changes in recurrence intervals and LULC scenarios. The estimated average damage (across all recurrence intervals) of $1180 million in 2005 is likely to increase by the year 2030 to $2601 million. From 2005-2010, the highest increase of flood damage was estimated at $839 million for a flood event with a 50-year return period. Within this period, a significant transformation of LULC was observed, which resulted in a decrease in agriculture lands and an increase in aquaculture land (Figure 4.4 (a)).

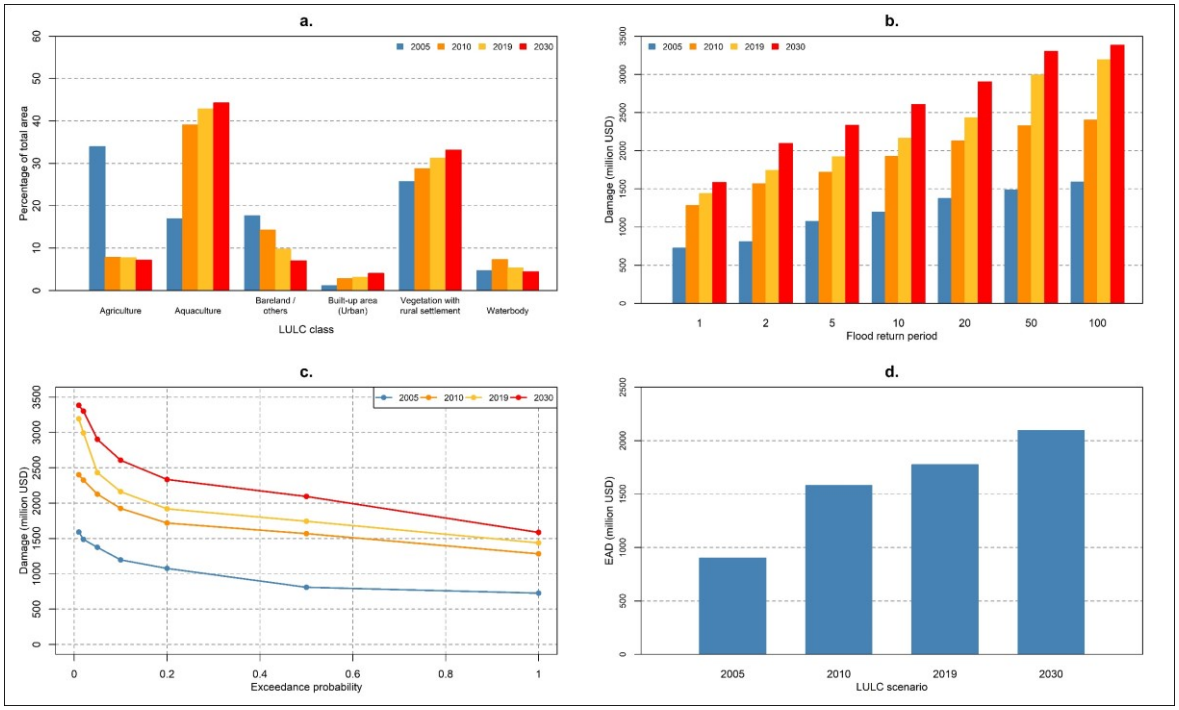

Figure 4.4. a. Trend of LULC change from 2005 – 2030; b. Estimated damages during floods of different return periods under four LULC scenarios; c. Exceedance probability distribution curve; d. Comparison of EAD among four LULC scenarios

4.3.2.2. Flood risk for various LULC scenarios

An exceedance probability curve in Figure 4.4 (c) and estimated EAD in Figure 4.4 (d) indicate the contribution of LULC change to flood risk. Notably, in Figure 4.4 (c), the difference of flood losses between the highest and the lowest exceedance probabilities does not vary greatly. In 2005, damage of $809 million was estimated for the median annual maximum flood event (an event with a 2-year return period). The damage increased to $1591 million when the exceedance probability reduced to 0.01. In 2030, damages may range from $1586 million to $3384 million for floods with annual exceedance probabilities from 1 to 0.01, respectively. A relatively small difference in estimated damages between the low and high probability floods is because even frequent floods (e.g. the median annual maximum) cause a substantial extent of inundation, and thus, significant damages (Figure 4.4 (b)). With an increase in the magnitude of precipitation, depths in the inundated areas tend to increase

substantially, rather than the extent of inundations. We estimate that the extent of inundation may range from 5% area (for the 2-year return period flood) to 15% area (for the 100-year flood).

LULC change has resulted in increased exposure primarily of residential (rural and urban) and aquaculture lands, which may result higher flood risk in the future. The EAD of the year 2005 was estimated to be approximately $903 million, which may be more than twice ($2096 million) by the year 2030 (Figure 4.4 (d)), assuming persistent LULC change in the future.

4.3.3. Association among LULC change, flood risk, and poverty

Table 4.4 summarises the results of the OLS regression model, developed to explain the degree of influence of different parameters on WI in the study area. Among the ten factors included, nine were found to be statistically significant. The estimated regression coefficients indicate that the WI was relatively higher in areas where land elevation, population density, and GDP are high, as well as a larger number of people employed in agriculture. Conversely, higher soil salinity, EAD, flood frequency, and LULC change negatively affected the WI. The regression coefficients were incorporated in equation 4.8 in a GIS to estimate WI at each pixel, encompassing the study area. The estimated R^2 in Figure 4.6 (c) exhibits the performance of the model. The R^2 value of 0.81 indicates an acceptable level of agreement between observed versus modelled WI values for 2010.

Table 4.4 Estimated regression coefficients for downscaling wealth index (WI) data

Variables	Coefficient	Standard error	*t*-value	VIF	*p*-value
Intercept	-2.984	0.536	-5.572		0.000^{***}
Soil salinity	-0.125	0.136	-0.925	2.70	0.317
Land elevation	0.042	0.009	4.472	3.08	$7e^{-06***}$
EAD	-0.016	0.007	-2.153	1.14	0.0373^{*}
Relative flood frequency	-0.324	0.181	-1.791	1.81	0.059▪
Distance from northing coordinates	-0.132	0.018	-7.481	1.59	0.000^{***}

Distance from easting coordinates	0.151	0.028	5.345	3.07	0.000***
LULC change	-0.213	0.091	-2.336	1.40	0.003**
Population density	0.182	0.012	14.754	1.68	0.000***
GDP	0.012	0.005	2.520	1.31	0.013*
Agricultural employment	0.298	0.039	7.342	1.40	0.000***
R^2: 0.81	Significance level: 0 '***' 0.001 '**' 0.01 '*' 0.05 '▪' 0.1 ' ' 1				

The WI of the study area was classified according to five categories using the Jenks scheme (Figure 4.5). During the base year of 2010, most of the south western zone (about 58%) was classified as areas with 'low' and 'very low' level of WI. Relatively, a higher WI was observed in the northern and western segments of the study area (Figure 4.5 (a)). The simulation showed a potential increase in WI in the year 2019 and 2030 (Figure 4.5 (b and c)). Supplementary Figure 4.3 compares the spatial distribution of WI in 2010 between the disaggregated data created in this study and the WI grid developed by Steele et al. (2017).

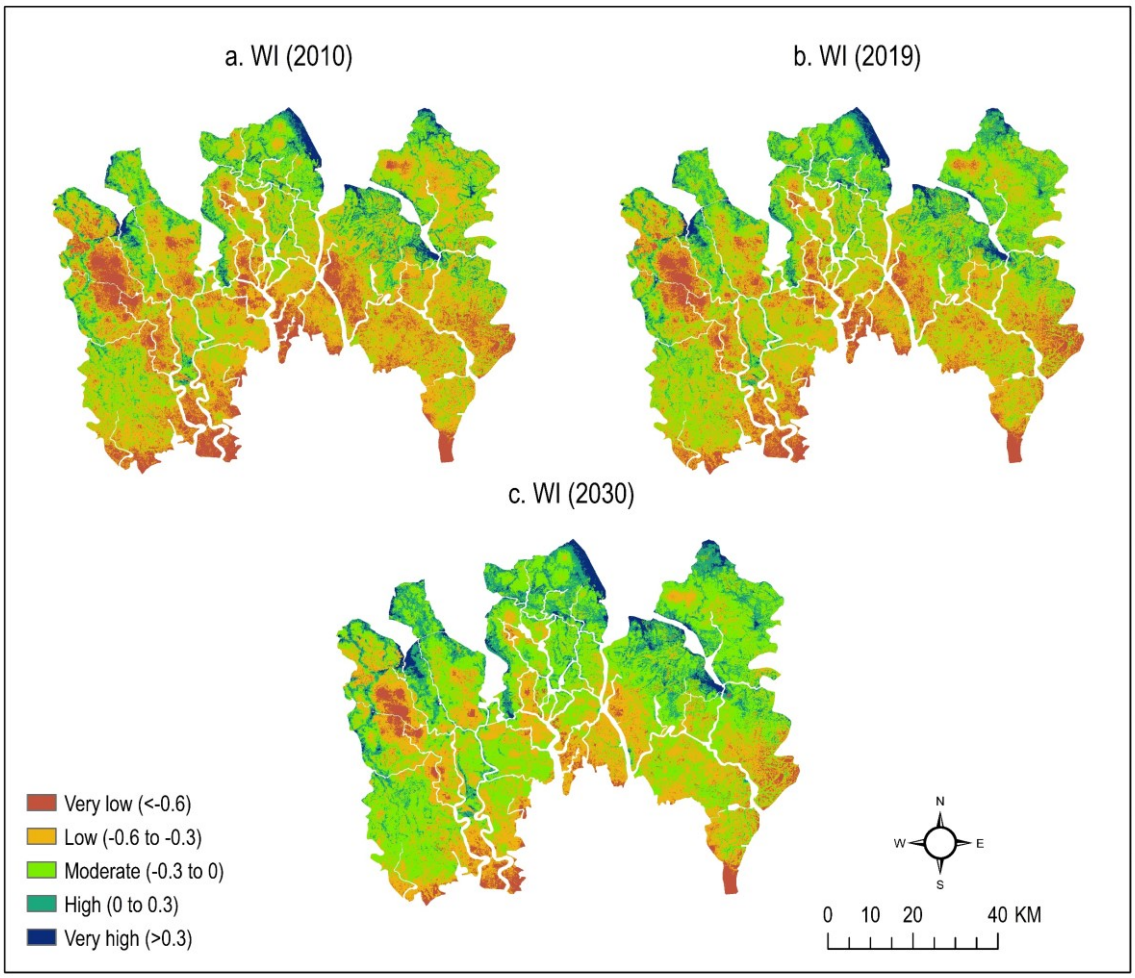

Figure 4.5 Spatiotemporal change of wealth index (WI) in the study area

Areas classified as 'very low' WI would potentially decrease from 15% area in 2010 to about 6% area in 2030, while the proportion of areas with 'moderate' WI may increase from 30% to 46%, respectively. However, the rate of increase in the proportion of areas classified as 'high' and 'very high' WI was estimated to be insignificant (Figure 4.6 (a)). The proportion of total area with positive WI ('high' and 'very high' categories) is likely to increase from 11% in 2010 to 18% in 2030. Bangladesh has an increasing GDP per capita growth, which was about 6.9% annually, on average, from 2010-2019. Population density has also been projected to increase in the future. Although these two variables exhibited a positive correlation with WI, LULC change and increasing EAD may hinder the growth of the WI in 2030. The estimated WI of 2010, 2019, and 2030 were disaggregated at the polder

scale to identify marginalised polders at present and in future (Figure 4.6 (b)). In general, more than 50% of the total area in most of the polders were classified as zones with 'low' and 'very low' WI. In 2010, there were 19 polders where more than 50% area was classified as 'moderate' to 'very high'. Nonetheless, the numbers increased in 2019 and 2030 for which correspondingly 21 and 34 polders were identified, with the majority of the area (>50%) classified as 'moderate' to 'very high' WI.

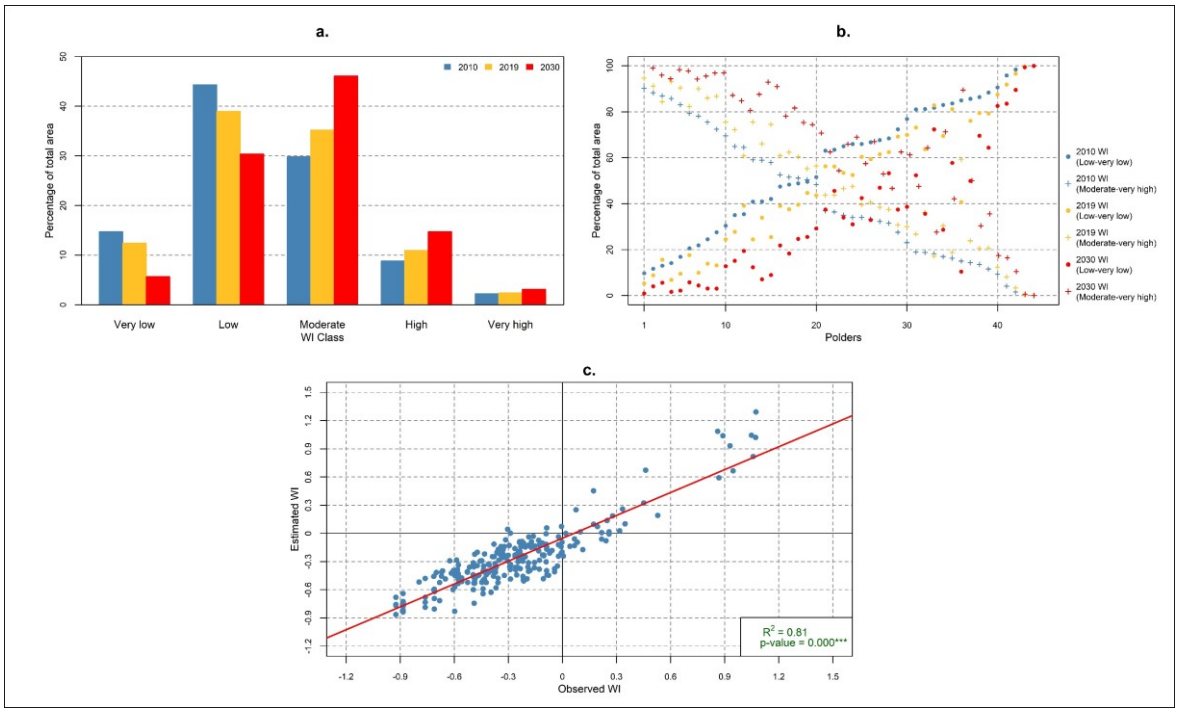

Figure 4.6 Temporal change of wealth index in: (a) South western embanked area and (b) Polders; (c) Association between observed and estimated WI in 2010

4.4. Discussion

Monitoring and managing LULC changes have been recognised as an essential geographic phenomenon for guiding socio-economic development (Shahbazian et al. 2019, Corner et al. 2014). This study analysed and simulated LULC changes in the south western embanked area of Bangladesh to understand their association with flood risk and poverty. The study results indicated that the proportion of agricultural lands decreased significantly between 2005 and 2019. This result is similar to a few other studies that focused on LULC

changes in south western Bangladesh (Islam et al. 2015, Khan et al. 2015, Rahman et al. 2017). A significant reduction of agricultural lands is reportedly associated with growing prevalence of shrimp farming, which reflects a socio-economic trend whereby land-owners near existing shrimp farms are more likely to convert to shrimp, together with the effect of salinity intrusion, in particular following surge flood events, which forced farmers to transform their agricultural lands into aquaculture use (Islam et al. 2015, Khan et al. 2015). The projection of future LULC indicated a potential increase in settlement areas, while bare lands are likely to decrease. Such LULC transformation may follow a pattern which was observed from 2010-2019. Rahman et al. (2017) also predicted a similar pattern of LULC change by 2028 in a small administrative unit (‘*upazila’*) of the south western coast. They explained that the natural increase of settlement and vegetation may lead to such changes in LULC.

Simulating future LULC is subject to uncertainty (Szwagrzyk et al. 2018). Although combined LR and CA-Markov Chain model considers a wide range of driving forces, it does not incorporate exogenous covariates such as personal preferences and government regulations (Arsanjani et al. 2013). For instance, lower market price, higher production cost, and increased frequency of diseases caused a decline in benefits in brackish water shrimp farming in the last decade (Akber et al. 2017). Although aquaculture was perceived as one of the few options for economic development (Akber et al. 2017), intensive aquaculture and subsequent salinity intrusion may result in poverty, promoting rural unemployment, social unrest, conflicts and forced migration (Johnson et al. 2016). Despite a reduction in brackish water shrimp cultivation in recent years, mixed cultivation of sweet water shrimp and fish has proved to be beneficial, which may persist in future. Therefore, in the current study, we considered the trend of LULC change in the last decade to predict future LULC. An alternative to the current LULC change model, an Agent Based Model (ABM) can

incorporate individual-related factors, an approach which has been followed in recent studies to model LULC change (Arsanjani et al. 2013). However, the main limitation of the ABM is that it requires a large sample of empirical data to parameterise the model (Valbuena et al. 2010). In summary, LULC change modelling is a complex process and therefore, results should be used with caution (Wang et al. 2019). For example, areas predicted to be transformed into settlements by the LULC model should be interpreted as areas most suitable for future settlement development, rather than the precise locations of future change (Szwagrzyk et al. 2018).

Notably, this study found a positive association between LULC change and losses caused by floods for various recurrence intervals. A lack of risk-oriented residential development might be associated with increased flood risk. The majority of rural houses are temporary or semi-permanent structures (Akter and Mallick 2013). Exposure of those areas to floods results in significant damages. Similar evidence of residential development in wetlands in recent years can be found in the existing literature (Akber et al. 2018). Aquaculture lands, comprised of shrimp or freshwater ponds, can withstand a certain depth of floodwater (i.e. < 2 m). However, when the depth increases, shrimp or fish may escape and cause financial losses (Islam et al. 2019).

We found that pluvial floods that occur each year cause substantial damage in the south western embanked region. This more or less inevitable flood damage is attributed to geomorphological characteristics of the study area. Land subsidence in the embanked region created depressions, which are prone to frequent pluvial flooding. Therefore, annual monsoon precipitation causes a substantial extent of inundation. For instance, a monsoon precipitation event of 2.1-year return period in 1990 inundated about 9.3% of the total area (Adnan et al. 2019b). From 2009-2014, pluvial flooding in Khulna Division (where the study area located) caused greater damage than any other natural hazards (BBS 2015). Frequent

pluvial flooding in the south western embanked region causes both damages to crops and delay to winter crop cultivation (Alam et al. 2017).

This study further presented a spatially explicit regression model to estimate poverty in terms of the WI. The results indicated a positive correlation of GDP and population density with the WI. A similar pattern of association of these parameters with poverty was reported elsewhere (Dasgupta 2007). The results of poverty modelling in this work highlighted that the rate of increase of WI is likely to be low in the future because of the pattern of LULC change and associated increase in flood risk. Few other studies have quantified the association between poverty indicators and flood risk/vulnerability (Brouwer et al. 2007, Akter and Mallick 2013). Those studies were based on household-level survey data, where poverty was considered as an indicator of flood risk.

4.5. Conclusion

This study quantified the degree of influence of LULC change and flood risk on poverty in the south western embanked area of Bangladesh. Poverty was estimated, in terms of WI, for the present-day and for future LULC and flood risk scenarios. The analysis indicated that the region has been experiencing a rapid LULC change, resulting in a significant decrease in agricultural lands, while the proportion of aquaculture lands increased consequently. Based on the recent pattern of changes, LULC was predicted for the year 2030. The study further demonstrated that losses due to floods of various recurrence intervals have increased with LULC change. The exposure of residential areas (rural and urban) was predicted to increase in future. A lack of attention to flood risk in land development decisions may explain the increased flood loss. Likewise, the expected annual flood damage (EAD) was also estimated to increase in the future LULC scenario. Moreover, we further estimated that LULC change and EAD negatively influence WI, which may restrict the growth of the WI in the future. The area with negative WI is predicted to decrease

from 89% area in 2010 to 82% area in 2030, which is slower than one might expect given Bangladesh's predicted GDP growth. This is because flood risk and patterns of LULC change have a negative effect on WI. Among 44 polders analysed, more than 50% area in 11 polders would potentially have 'low' and 'very low' WI.

When interpreting the findings of this study, uncertainty related to flood damage functions and values of input parameters for poverty estimation should be considered. We considered global flood depth-damage functions for different LULC, due to the unavailability of micro (local)-level functions. We estimated flood losses for different categories of LULC, as building-level land use data are not available for all of the study area. While describing uncertainty in flood depth-damage function, Huizinga et al. (2017) highlighted that materials of structures primarily determine the maximum damage that may occur during a flood. In this study, the accuracy of the projected WI depends on the accuracy of input parameters. Parameters value (e.g. soil salinity and flood frequency) which were assumed to remain constant in may change in the future. The dynamics in soil salinity may also change in future climate change scenarios. Although few studies focused on modelling soil salinity in coastal Bangladesh under future climate change scenario (Dasgupta et al. 2015, Payo et al. 2017), the coarser resolution of their results restricted this study to incorporate such data in estimating WI. However, the statistical significance of salinity remains low. Also, GDP and population density were projected for the future year considering national-level growth rates, which may vary at the local scale such as polder level.

This study highlights that the absence of risk-oriented land use planning is potentially increasing flood risk in the coastal region. Various national and regional level policies of Bangladesh have addressed this issue and express the need to formulate land use plans following a risk-based approach. For instance, the Coastal Development Strategy

focused on developing a coastal land use plan. More recently, the Bangladesh Delta Plan (BDP) 2100 emphasised the adoption of measures to mitigate flood risk, to achieve a long-term goal of reducing poverty and ensuring sustainable livelihoods (Khan 2018). Spatial information on flood risk and land use changes provided in this study should inform stakeholders such as the Ministry of Land in identifying areas required land use policy intervention. Also, the proposed methodology to assess the implications of changing land use and flood risk for poverty should be of interest to land use planners. The results can help target policies in areas with greater poverty at present and in future scenarios. To the best of our knowledge, this study is the first attempt to model spatiotemporal change of poverty with changes in land use and flood risk. Although many studies focused on land use change modelling and/or flood risk assessment, there is a dearth of studies that quantify their combined influence on local level poverty.

Appendix B: Supplementary Materials to Chapter 4

Supplementary tables

Supplementary Table 4.1 Extent of influence of various driving forces on LULC change

Factors	LULC 1 to LULC 3	LULC 1 to LULC 6	LULC 2 to LULC 3	LULC 3 to LULC 1	LULC 3 to LULC 2	LULC 3 to LULC 5	LULC 5 to LULC 1	LULC 5 to LULC 2	LULC 5 to LULC 3
Intercept	2.38	-2.01	-0.57	-3.92	-5.86	-1.35	0.50	-1.51	2.14
Elevation	-0.32	-0.49	-0.03	0.32	0.03	0.10	-0.10	-0.51	-0.63
Curvature		0.39		-0.20	-0.01	-0.03			
Flood frequency	0.01	0.79	-0.41	0.13	0.72	0.17	-0.22	0.61	-0.18
Distance from aquaculture land								-0.10	
Distance from existing road	-0.06			0.08		0.02	0.02	0.02	0.03
Distance from residential area						-0.22			
Distance from adjacent river			0.004						
Distance from drainage channel			0.006	0.04				-0.03	
Distance from growth centre						0.03			
Soil salinity	-0.08			0.05	0.31	0.11	-0.18	0.17	-0.06
Easting coordinates	0.16		0.07	0.07	0.21	0.05	$2e^{-04}$	-0.17	
Northing coordinates	-0.11	-0.02	0.02		-0.11			0.16	
Population density									
Slope	$-1e^{-04}$		$7e^{-05}$						
ROC	**0.71**	**0.89**	**0.74**	**0.67**	**0.89**	**0.68**	**0.63**	**0.94**	**0.82**
Adjusted odds ratio	**5.23**	**17.82**	**8.10**	**4.28**	**14.38**	**2.96**	**2.07**	**35.74**	**9.81**

LULC 1= Agriculture; LULC 2 = Aquaculture; LULC 3 = Bare land; LULC 4 = Built-up area (urban); LULC 5 = Vegetation with rural settlement; LULC 6 = Waterbody

Supplementary Table 4.2 Markov Chain transition probability matrix of LULC change

	LULC class	Agriculture	Aquaculture	Bare land	Built-up area (urban)	Vegetation with rural settlement	Waterbody
Transition probability of 2019 based on the transition matrix of 2005-2010	Agriculture	0.0571	0.4943	0.0713	0.0425	0.2160	0.1189
	Aquaculture	0.0112	0.6845	0.0310	0.0198	0.0492	0.2044
	Bare land / others	0.0983	0.2865	0.2527	0.0227	0.2853	0.0546
	Built-up area (urban)	0.0062	0.1078	0.0121	0.7319	0.0356	0.1063
	Vegetation with rural settlement	0.1226	0.2433	0.1075	0.0246	0.4708	0.0312
	Waterbody	0.0044	0.6815	0.0204	0.0079	0.0236	0.2622
Transition probability of 2030 based on the transition matrix of 2010-2019	Agriculture	0.2296	0.1756	0.2314	0.0189	0.3439	0.0007
	Aquaculture	0.0080	0.7358	0.0724	0.0355	0.0677	0.0806
	Bare land / others	0.0779	0.2742	0.4352	0.0266	0.1790	0.0071
	Built-up area (urban)	0.0007	0.0422	0.0128	0.9310	0.0081	0.0053
	Vegetation with rural settlement	0.0585	0.1897	0.0947	0.0264	0.6257	0.0051
	Waterbody	0.0000	0.7527	0.0569	0.0222	0.0261	0.1421

Supplementary Table 4.3 Diagnosing autocorrelation of monthly precipitation between years

Month	Autocorrelation	Significant
January	-0.12	FALSE
February	0.14	FALSE
March	-0.14	FALSE
April	0.02	FALSE
May	0.18	FALSE
June	-0.01	FALSE
July	0.09	FALSE
August	-0.14	FALSE
September	-0.14	FALSE
October	-0.21	FALSE
November	-0.24	FALSE
December	-0.17	FALSE

Supplementary Figures

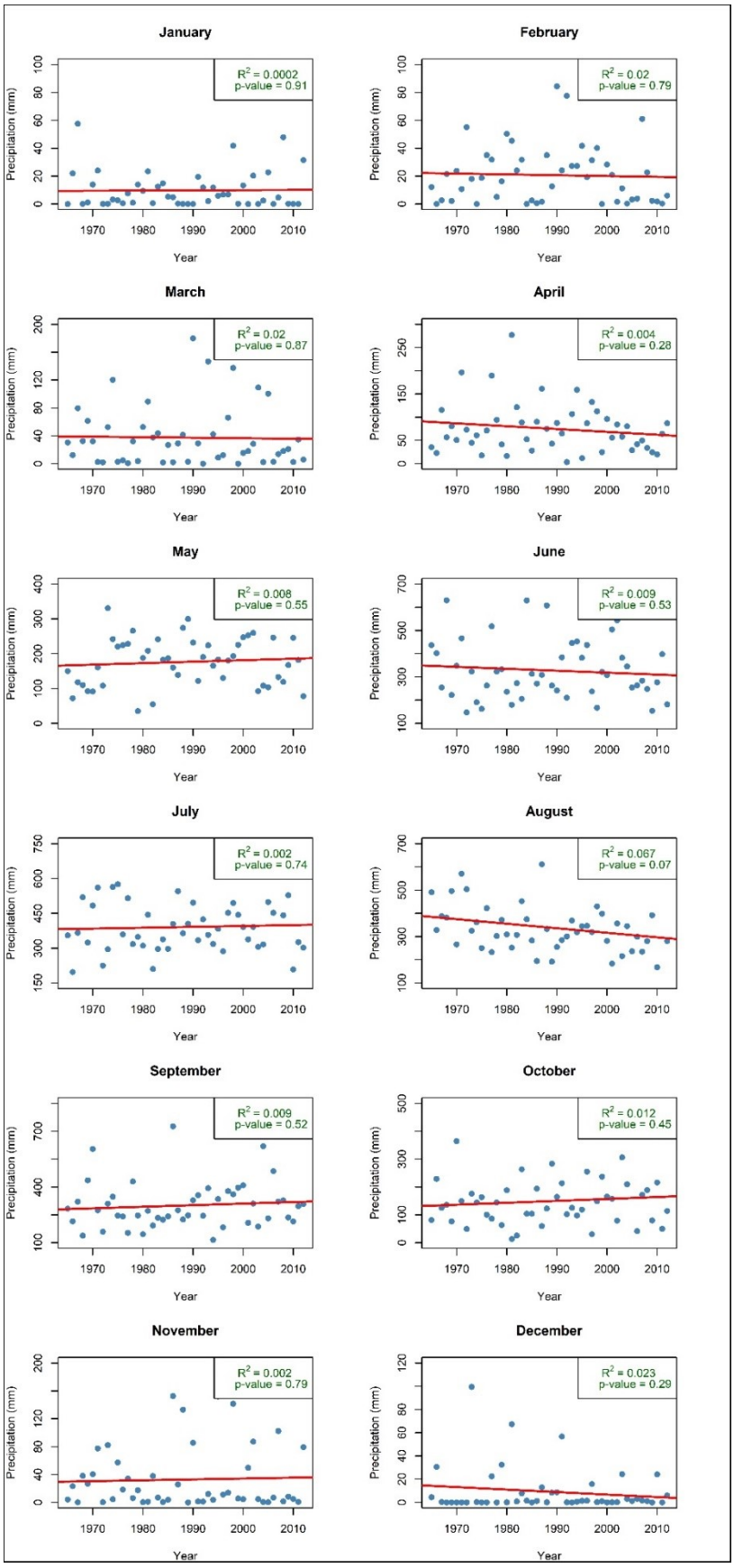

Supplementary Figure 4.1 Trend of monthly rainfall from 1965 to 2012

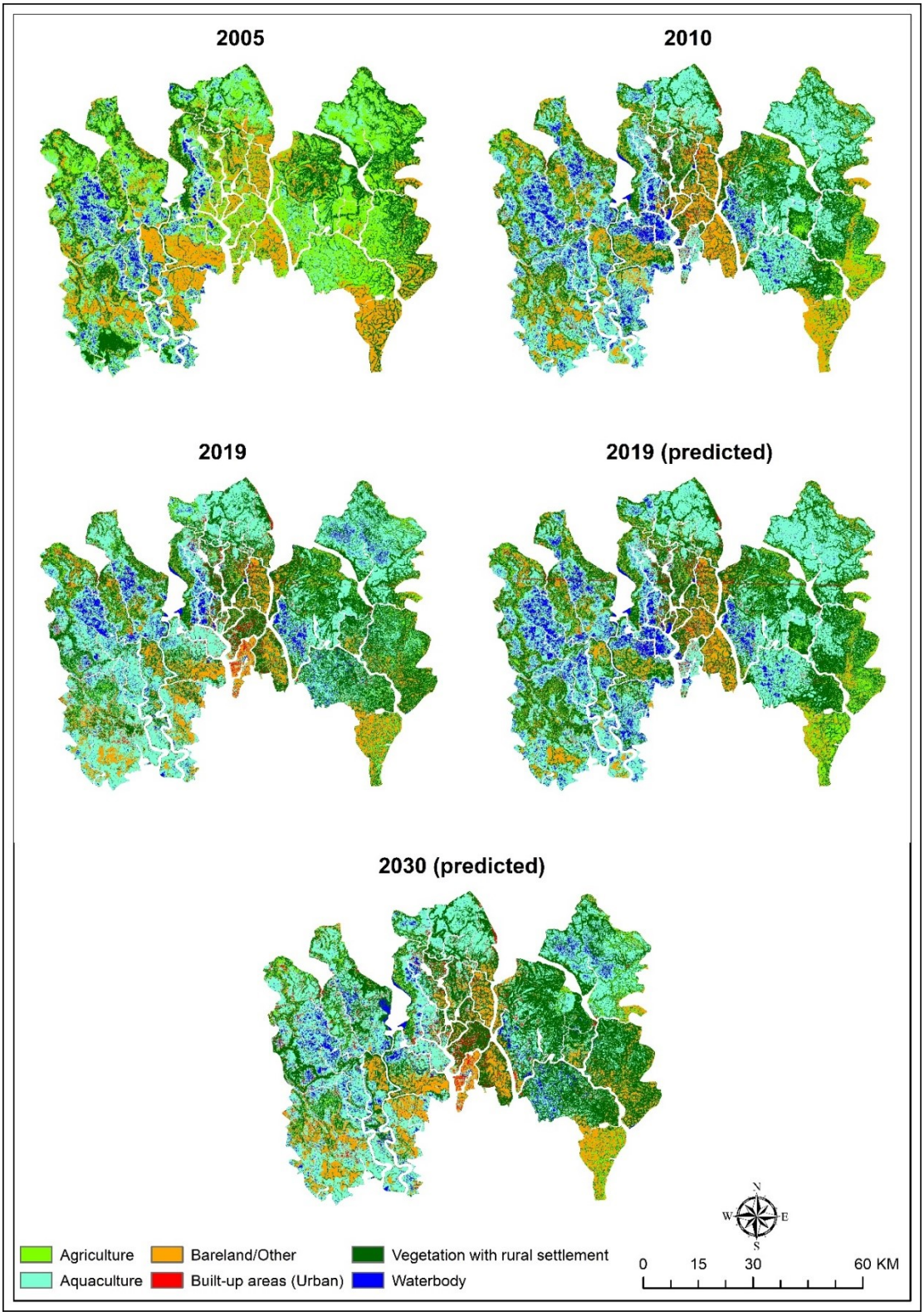

Supplementary Figure 4.2 Predicted and observed LULC change between 2005 and 2030

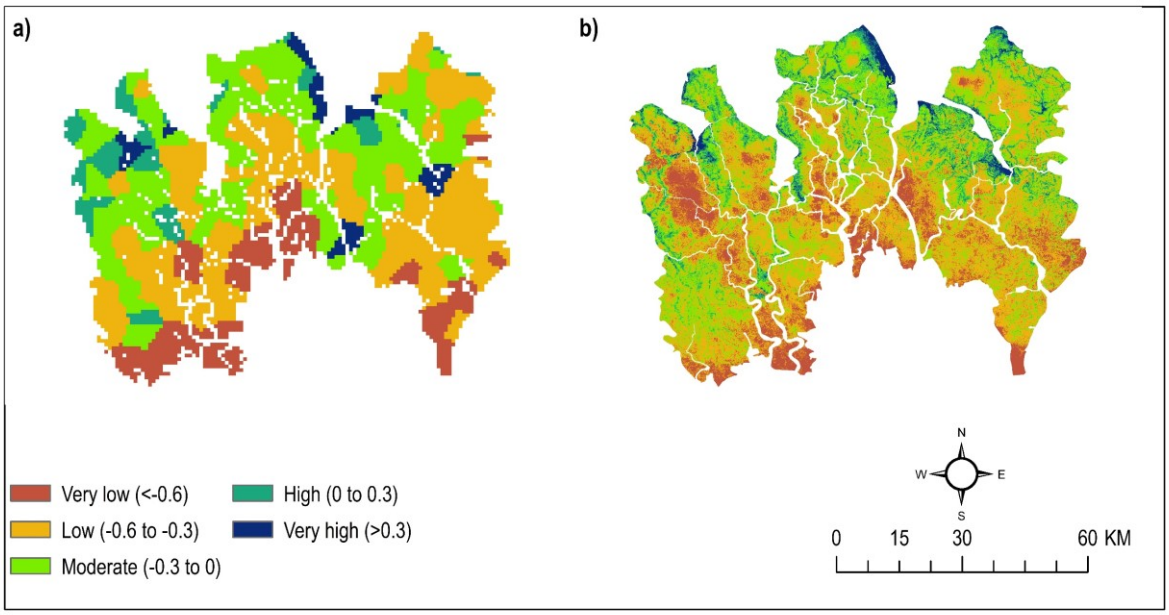

Supplementary Figure 4.3 Wealth Index in 2010: a) obtained from Steele et al. (2017); and b) downscaled for this study

Chapter 5 The potential of Tidal River Management for flood alleviation in South Western Bangladesh

Abstract

Reduced sediment deposition, land subsidence, channel siltation, and salinity intrusion has been an unintended consequence of the construction of polders in the south western delta of Bangladesh in the 1960s. Tidal River Management (TRM) is a process that is intended to temporarily reverse these processes and restore sediment deposition and land elevation at the low-lying sites, known as 'beels', where TRM is carried out. However, there is limited evidence to prioritise sites for TRM on the basis of its potential effectiveness at alleviating flooding. In this study, the south western delta of Bangladesh was classified according to different flood susceptible zones. In south western Bangladesh, the major portion of agricultural and aquaculture land is located within flood susceptible zones (65% and 81%, respectively). 44.5% of the total population in embanked regions live in areas classified as being flood susceptible. This study identified 106 'beels' suitable for TRM. Modelling of potential sediment deposition predicted that the consequent increase in land elevation could be up to 1.4 m in five years, which would alleviate land subsidence and modify several geomorphological factors such as aspect, slope, curvature, and Stream Power Index (SPI). Implementation of TRM at these sites could potentially reduce the probability of annual flooding from 0.86 (on average) to 0.57 (on average). Therefore, TRM could lower the flood susceptible area by 35% in suitable 'beels'. Whilst during the implementation of TRM agriculture has to cease for a few years, a systematic programme of TRM could result in a long-term increase in agricultural production by reducing flood susceptibility of agricultural lands in delta regions.

5.1. Introduction

Pluvial flooding during the monsoon period affects the south western coastal region of Bangladesh annually (Warner et al. 2018), inundating agricultural lands and damaging people's livelihoods (Awal 2014, Alam et al. 2017). This form of flood occurs either due to a short term intense or prolonged low to moderate level precipitation (Falconer et al. 2009). Pluvial flooding has become much more severe in this region because of land subsidence, siltation in riverbeds restricting drainage, and land-use change e.g., the encroachment of drainage channels (Alam et al. 2017).

Following a major cyclone and storm surge flood in 1953, the East Pakistan Water and Power Development Authority (now the Bangladesh Water Development Board (BWDB)) invested in a major Coastal Embankment Project (CEP). Since 1960, a total of 139 polders (enclosed coastal embankments) were constructed throughout the coastal region, with the stated objective of preventing inundation by saline water of agricultural lands during surge tides and cyclones, increasing agricultural production and ensuring food security (Warner et al. 2018, Islam et al. 2016c). The construction of polders resulted in increased agricultural production until the 1980s (Nowreen et al. 2014). On the other hand, the polder system disconnected the delta floodplain from the river channel network, which had the consequences of promoting land subsidence in the embanked areas (Van Staveren et al. 2017, Auerbach et al. 2015, Alam et al. 2017). The embanked region in the south western coast of Bangladesh has lost 1.0 - 1.5 m of land elevation since the construction of the polders (Auerbach et al. 2015). The polder system restricted silts from rivers being deposited onto 'beels' (a local term referring to surface depression), whilst accelerating sedimentation in riverbeds and increasing river water levels. In turn, this prevents gravity drainage systems within the embanked region from functioning properly (Mutahara et al. 2018). As a result, runoff generated from monsoon precipitation accumulates in and floods,

polders (Choudhury et al. 2004, Auerbach et al. 2015, Talchabhadel et al. 2018a). Projected sea level rise (Church et al. 2013) will increase the tidal water level within the adjacent Bay of Bengal, worsening drainage congestion and pluvial flooding in polders (Awal 2014). Pluvial floods lead to economic losses either by damaging crops or delaying cultivation of winter crops ('Boro' rice), affecting the livelihood of millions of people across the Ganges-Brahmaputra-Meghna (GBM) delta, and particularly poor and marginal farmers living inside polders (Alam et al. 2017). For instance, a pluvial flood in 2011 inundated more than 128,000 ha of croplands for 90 days in three south western coastal districts of Bangladesh: Khulna, Satkhira, and Jessore (Awal 2014).

Tidal River Management (TRM) has been adopted in an attempt to address the worsening impacts of pluvial flooding, salinity, and siltation in riverbeds, by restoring sedimentation in low-lying 'beels'. The idea of TRM is to bring sediment-carrying tidal water into selected 'beels' two times a day through a controlled breaching in polders, to allow sedimentation and elevate the land (Masud et al. 2018, Gain et al. 2017, Talchabhadel et al. 2018a, Seijger et al. 2019, Amir and Khan 2019). Although historically a community-driven approach, the BWDB has been responsible for implementing TRM since 1997. From 1991 to 2013, TRM has been implemented (either by local people or the BWDB) in 12 out of 35 designated 'beels' in the south western coastal zone (Masud et al. 2018, Gain et al. 2017). Implementation of TRM in the south western embanked region is still an ongoing process (Gain et al. 2017). However, governance issues (e.g. disagreement about TRM sites and issues with compensation) were reported during the implementation and operation of TRM projects (Gain et al. 2017, Mutahara et al. 2018). Since TRM makes the 'beel' unsuitable for crop production during the implementation period (Masud et al. 2018), an explicit engagement of different stakeholders (land owners and agricultural workers who are

fully or partially dependent on the land in TRM sites) is required from project planning to implementation phases (Mutahara et al. 2018).

Existing studies have described both positive and negative impacts of TRM projects on local communities and the environment (Amir and Khan 2019, Gain et al. 2017, Masud et al. 2018, Mutahara et al. 2018). For instance, the operation of TRM in 'beel' Bhaina (1997 - 2001) led to a raise in land elevation by 1 m on average and consequently increased the depth and width of the adjacent Hari River by 10-12 m and 2-3 times, respectively (Gain et al. 2017, Mutahara et al. 2018). On the other hand, an unplanned TRM operation could lead to riverbank erosion, salinity intrusion, and inundation in built-up areas (Talchabhadel et al. 2018a, Gain et al. 2017). For instance, in 'beel' Khuksia, an unplanned implementation of TRM, without sufficient cooperation between stakeholders and government agencies, resulted in several disruptions during implementation (2006 - 2012). Thus, inundation problems remained after the implementation of TRM in Khukshia (Figure 5.1 (c)) because of an uneven land elevation caused by an uneven distribution of deposited sediments (Gain et al. 2017). Also, various environmental and economic issues can arise during the implementation of TRM (Masud et al. 2018). These issues include an increase in salinity intrusion, inundation of agricultural lands, riverbank erosion, and disruption of transport services (Gain et al. 2017).

Evaluating the impact of TRM on flooding is a complex process because (1) the rate of sedimentation vary spatially and temporally (Gain et al. 2017) and (2) flooding is an outcome of various combinations of geomorphological, hydrological, and anthropogenic processes (Tehrany et al. 2014a, Khosravi et al. 2016, Pradhan et al. 2010). Although some benefits of TRM have been reported in the literature (Gain et al. 2017, Amir and Khan 2019), there remains a lack of evidence of how the implementation of TRM will change the actual mechanism of flooding, leading to a potential change in the extent of the flood susceptible

area in embanked regions. Care should be given to identify areas suitable for operating TRM to avoid adverse impacts on society and the environment. To address these challenges, (1) flood mechanisms in the south western embanked region of Bangladesh were analysed, estimating the influence of various flood causative factors on flood susceptibility, and (2) the impact of TRM on flood susceptibility was quantified, modelling sediment transportation and deposition in suitable TRM sites comparing flood susceptibility before and after TRM implementation, in order to prioritise suitable sites.

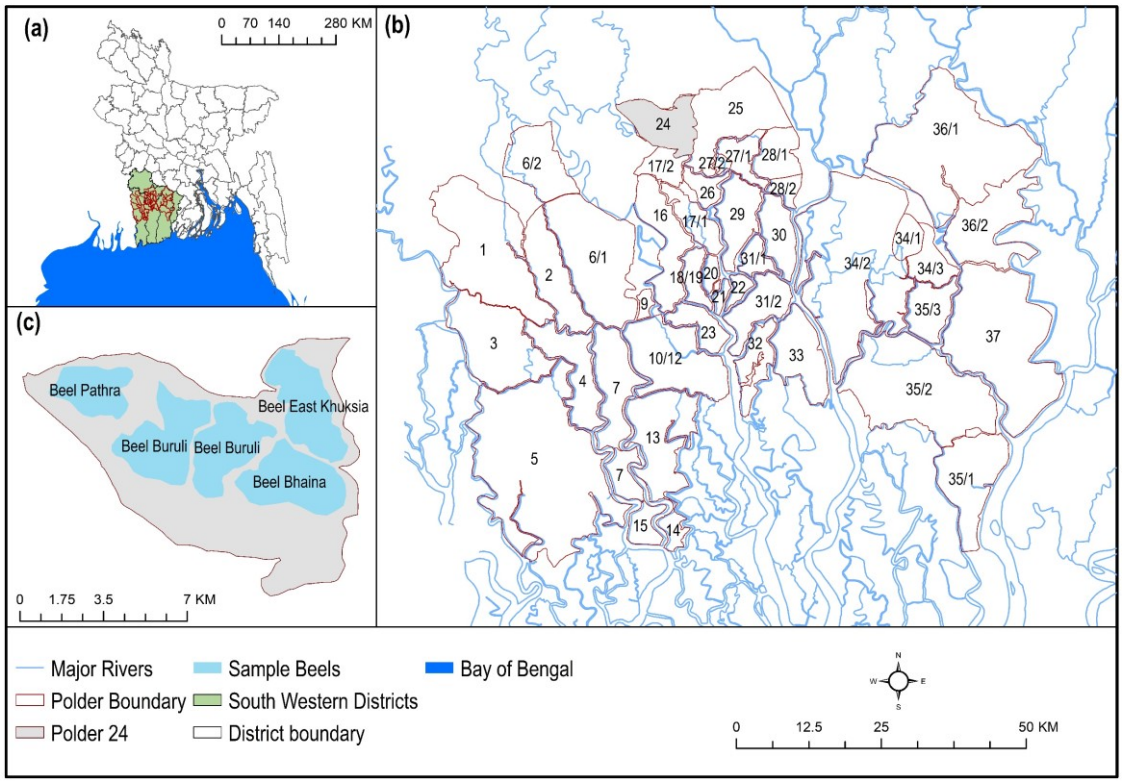

Figure 5.1 Study area map

5.2. Materials and methods

This study was conducted in two stages. First, the influence of various factors on flooding was analysed to derive a flood susceptibility map. Second, potential TRM sites were identified to model sediment deposition in those areas. The potential impact of TRM on flooding was investigated by comparing flood susceptibility 'before and after' the implementation of TRM. To estimate flood susceptibility during the post-TRM scenario,

geomorphological changes due to sedimentation in suitable sites were incorporated in the model.

5.2.1. Study area

The study focused on the south western coastal region of Bangladesh, containing 44 polders located in five coastal districts: Bagerhat, Jessore, Khulna, Pirojpur, and Satkhira (Figure 5.1 (a)). Approximately 5.3 million people live in this region (WorldPop 2018), which includes areas from three physiographic regions of Bangladesh Ganges River floodplains, Ganges tidal floodplain, and old floodplain basins (Brammer 2014). This low-lying deltaic region has a mean elevation of 3.5 m and is heavily intersected by tidal rivers. The Bangladesh Sundarban mangrove forest is located in the south of the study area. Embankments were built in the study area from the 1960s to 1980s to protect about 5187 km^2 of land (WARPO 2018). The region is mainly characterized by aquaculture lands and rural settlements (Abdullah et al. 2019). Although the region is prone to three types of flooding — pluvial, fluvio-tidal, and surge flood — pluvial flooding is the most frequent form of flooding (Adnan et al. 2019b). Frequent pluvial flooding (locally also referred to as 'waterlogging') in the region has decreased agricultural production and may have contributed to out-migration (Wilson et al. 2017). The region receives maximum precipitation during the monsoon months particularly from June to September, generating excess runoff. Inadequate drainage, due to deteriorating drainage channels and unreliable operation of sluice gates, contributes to frequent inundation in the low-lying 'beels' (Adnan et al. 2019b, Talchabhadel et al. 2018a). The current study hypothesized that a loss in land elevation due to land subsidence contributed to a change in different geomorphological conditions determining the probability that an area will be flooded. Restoring sedimentation through TRM will promote a change in those flood conditioning factors, which will reduce the likelihood of flooding in the embanked region.

5.2.2. Flood inventory mapping

A flood inventory map of the study area was derived, analysing flood observation data obtained from remote-sensing imagery. Adnan et al. (2019b) identified the extent of annual flood inundation in the south western embanked region from 1988 to 2012 and attributed each flood to pluvial, fluvio-tidal, and storm surge flood events. The raster maps of binary (flood and non-flood) flood inundation maps of those 25 years were collected and overlaid in GIS to estimate the number of times (frequency) that different cells within the study area were inundated. Cells that remained flood-free were also identified (Supplementary Figure 5.9). The resultant flood inventory map was used to generate random flood and non-flood points for flood susceptibility modelling (Tehrany et al. 2019a). Applying a stratified random sampling method in GIS, we generated a vector layer of 1000 points where flood and non-flood locations were 586 and 414, respectively. The ratio of flood and non-flood locations was determined based on the proportion of the total area either affected or remained flood-free during historical flooding, respectively. About 58.6% of the total area was inundated at least once during the floods from 1988 to 2012. The sample locations were split into two groups; 70% of samples (training data) were used to develop the flood susceptibility model and remaining 30% data (test data) were employed for validating the model (Supplementary Table 5.2).

5.2.3. Deriving flood conditioning factors

The accuracy of hazard susceptibility map depends on the selection of hazard conditioning factors (Sabatakakis et al. 2013). Numerous studies have been conducted on flood hazard susceptibility mapping (Kabenge et al. 2017, Khosravi et al. 2016, Tehrany et al. 2017, Tehrany et al. 2014a, Tehrany et al. 2014b, Mojaddadi et al. 2017, Alam et al. 2017, Arabameri et al. 2019), with various combinations of flood conditioning factors being used. However, the selection of factors should be based on the knowledge of morphological

characteristics of the region under study (Tehrany et al. 2019a). Based on the knowledge obtained from the literature, initially 14 flood conditioning factors were selected under five broad categories: topographic, anthropogenic, geological, hydrological, and locational factors. Raster layers of the 14 flood conditioning factors were generated at 30m spatial resolution. Data used to produce those layers are listed in Supplementary Table 5.1.

Topographic factors included aspect, elevation, slope, curvature, and land subsidence (Supplementary Figure 5.1). Raster layers of the slope, aspect, and curvature were derived from the Advanced Land Observing Satellite (ALOS) Digital Elevation Model (DEM) (JAXA 2015) in ArcGIS. Aspect denotes the direction of slope (Zevenbergen and Thorne 1987), indicating the extent of precipitation and sunshine that an area would receive (Tehrany et al. 2017), which affects the water balance of an area (Singh et al. 2004). Together, elevation and slope influence the occurrence of flooding, as areas with a lower elevation and slope are more susceptible to flooding (Tehrany et al. 2014a, Tehrany et al. 2017, Khosravi et al. 2016, Kabenge et al. 2017). In relation to curvature, surfaces with flat or concave characteristics are more prone to inundation (Tehrany et al. 2017). This study assumes the land subsidence rate as a linear estimate (Brown and Nicholls 2015). A layer of annual land subsidence rate was collected from Adnan et al. (2019b)) where the natural neighbour interpolation method was applied in GIS to convert 205 point measurement of net subsidence (Brown and Nicholls 2015) into a raster. Since the embanked region has been experiencing land subsidence from the beginning of polder construction in the 1960s, the annual land subsidence rate was multiplied by 52 (1960 - 2012) to obtain an estimate of total land subsidence since polder construction.

Four hydrological factors were selected: precipitation, flow accumulation, Stream Power Index (SPI), and Topographic Wetness Index (TWI) (Supplementary Figure 5.2). To prepare the annual mean precipitation layer, 10-day gridded precipitation data from 1948 to

2012 was collected from the Bangladesh Meteorological Department (BMD). Flow accumulation, SPI, and TWI explain the characteristics of natural drainage. The flow accumulation layer was obtained from the DEM in GIS by deriving a continuous drainage network (Planchon and Darboux 2002). Then, a flow direction raster was obtained, applying a single-direction flow algorithm (D8) where one cell routed into the next steepest of the eight neighbouring cells (Seibert and McGlynn 2007). In the next step, a flow accumulation grid was generated, which indicates the accumulated sums of water flowing in the down-slope direction (Kabenge et al. 2017). SPI is a measure of the erosive power of surface runoff (Khosravi et al. 2016). SPI estimates the rate of sediment that would transfer to natural drainage channels. Areas with relatively high SPI values have a greater tendency to accumulate water (Bannari et al. 2017). TWI depicts the likelihood of a surface is wet. A higher TWI value of an area indicates a greater chance that the area will become wetter than the surrounding region (Mojaddadi et al. 2017, Bannari et al. 2017). SPI and TWI were derived using the following equations in GIS.

$$SPI = A_s \times \tan\beta \tag{5.1}$$

$$TWI = \ln\left({A_s}/{\beta}\right) \tag{5.2}$$

where A_s and β indicates the specific catchment area (m^2/m) and slope gradient respectively (Khosravi et al. 2016, Tehrany et al. 2014b, Regmi et al. 2010).

Land-use affects the rate of evapotranspiration and terrain infiltration, which are essential indicators determining the extent and speed of runoff (Thornthwaite and Mather 1957, Kabenge et al. 2017, Tehrany et al. 2019b). Land-use data that was collected for this research included thirteen classes (Supplementary Figure 5.3 (a)). The geological factors included topsoil texture and soil permeability (Supplementary Figure 5.3 (b) and (c)), which also explain the level of infiltration. For instance, clay lowers the infiltration rate amplifying

surface runoff (Bonacci et al. 2006). Generally, the characteristics of soil and land-use determine the water balance of an area (Thornthwaite and Mather 1957). Polders are accompanied by drainage channels and sluice gates to impede saltwater intrusion in the dry season, drain excessive rainwater, and allow fresh river water flow to polders in the wet season for irrigation purposes (Adnan et al. 2019b). However, the construction of polders has reduced the tidal prism, promoting sedimentation in tidal channels and infilled them (Wilson et al. 2017). Inadequate drainage systems in the south western region increased inundation during historical pluvial flood events (Adnan et al. 2019b). In the current study, data on the existing drainage network was collected from Adnan et al. (2019b) who identified drainage channels from a high-resolution satellite image. Finally, two layers were created showing the distance of a given area from adjacent drainage channels and rivers in GIS, applying a Euclidean distance algorithm (Supplementary Figure 5.3 (d) and (e)).

5.2.4. Flood susceptibility modelling

A spatial regression model was developed for flood susceptibility mapping, applying an ensemble of bivariate frequency ratio (FR) and multivariate logistic regression (LR) models. Recent studies have followed different approaches to model flood susceptibility such as weight of evidence (Tehrany et al. 2014b, Khosravi et al. 2016, Tehrany et al. 2017), decision tree (DT) (Tehrany et al. 2019a), support vector machine (SVM) (Tehrany et al. 2019a, Tehrany et al. 2014b, Mojaddadi et al. 2017), FR (Khosravi et al. 2016, Tehrany et al. 2017, Mojaddadi et al. 2017), analytical hierarchy process (AHP) (Khosravi et al. 2016, Kabenge et al. 2017), LR (Tehrany et al. 2014a, Pradhan 2010), and artificial neural networks (ANNs) (Kia et al. 2012). An ensemble of FR and LR models was applied for the following reasons: i) model development is less complex compared to different machine learning techniques, such as ANN, DT, and SVM (Tehrany et al. 2019b); ii) the results of FR model are easy to comprehend (Khosravi et al. 2016); iii) using an ensemble of two

models reduces variance-error and improves prediction accuracy (Althuwaynee et al. 2014); iv) it could potentially eliminate individual bias that the expert opinion-based AHP method is likely to produce, as AHP is based on pair-wise comparisons by experts (Tehrany et al. 2014a, Althuwaynee et al. 2014); v) LR can perform regression with independent variables with continuous and/or discrete type data (Althuwaynee et al. 2014); vi) LR can estimate the probability of occurrence of dependent variables (Bubeck et al. 2013).

5.2.4.1. Multi-collinearity diagnosis and optimizing flood conditioning factors

The selected flood conditioning factors could be subject to multi-collinearity, therefore, variance inflation factors (VIF) (Midi et al. 2010) of 14 selected flood condition factors were estimated using R (Fox et al. 2018), to eliminate the factors susceptible to multi-collinearity. VIF determines the degree of variance, indicating whether coefficients are inflated by multicollinearity. VIF of a variable exceeding 2.5 creates a concern for the model, while a value greater than 10 indicates the presence of multicollinearity (Midi et al. 2010). Twelve flood conditioning factors with a VIF value less than 2.5 (Bai et al. 2011) were selected for modelling flood susceptibility (Supplementary Table 5.3).

5.2.4.2. Frequency ratio (FR) model

The FR model aimed to measure the influence of each class in different flood conditioning factors on flood occurrence. A FR value greater or less than 1 indicates a strong or weak correlation of a factor class with the occurrence of flooding, respectively (Khosravi et al. 2016). For a flood conditioning factor, the FR was estimated using the following equation (Khosravi et al. 2016).

$$FR = \left[N_{pix}(SX_i) \Big/ \sum_{i=1}^{n} N_{pix}(SX_i) \right] \Big/ \left[N_{pix}(X_i) \Big/ \sum_{i=1}^{n} N_{pix}(X_i) \right] \quad (5.3)$$

where $N_{pix}(SX_i)$ denotes the number of training flood pixels within i^{th} class of independent variable X, $N_{pix}(X_i)$ is the total number of pixels within i^{th} class of independent variable X, and n is the total number of classes under variable X.

5.2.4.3. Logistic regression (LR) model

The statistical approach of flood susceptibility modelling assumes that the potential (probability of occurrence) of future flooding areas will be comparable to the frequency and extent of historical floods (Pradhan 2010). The LR model incorporated 700 training flood observation data (flood and non-flood) as a dependent variable and 12 flood conditioning factors as independent variables. A weight to each cell in different flood conditioning factors was provided according to estimated FR, before incorporating them into the LR model (Althuwaynee et al. 2014, Tehrany et al. 2014a). The training flood observation data was used to extract the value of FR of 12 flood conditioning factors in GIS. Then regression coefficients and p-statistics of each variable, as well as the coefficient of determinants (R^2) of the model, were estimated using the 'mlogit' package in R (Croissant and Croissant 2018). The obtained regression coefficients were incorporated in equation 5.4 (Tehrany et al. 2014a) in GIS to derive the probability (p) of flood occurrence in the study area.

$$p = 1/(1 + e^{-z}) \tag{5.4}$$

where p is the probability of an event occurring. In the present situation, p is the estimated annual probability of flooding, indicating the likelihood of a cell being inundated annually, for a similar set of flood conditioning factors explicating inundated areas during the historical events; z is the linear combination of independent variables, which was estimated using the following equation.

$$z = b_0 + b_1x_1 + b_2x_2 + \cdots + b_nx_n \tag{5.5}$$

where b_0 is the model intercept, b_i (i = 1, 2, ..., n) indicates the regression coefficients of independent variables, and x_i (i = 1, 2, ..., n) represents the FR of n number of independent variables (Table 5.2). Obtained flood probability index map was categorized into five equal classes, representing different categories of flood susceptible zones. Besides, a cut-off flood probability value was optimised so that areas with flood probability above the cut-off value were classified as flood susceptible zones, and vice versa. The method used to optimize cut-off flood probability value is explained in Section 5.2.4.4.

5.2.4.4. Sensitivity analysis and model validation

The flood susceptibility model validation was performed using a well-known method called receiver operating characteristic (ROC) curve and subsequent area under the curve (AUC) (Althuwaynee et al. 2014, Khosravi et al. 2016, Tehrany et al. 2014a, Arabameri et al. 2019). ROC values express the ability of the model to correctly separate positive and negative observations in the validation samples (Arabameri et al. 2019). To develop this plot, the estimated annual flood probability values of all cells were sorted in descending order. Then the ordered flood probability index map was classified into 100 categories, with cumulative 1% (0.01) break. The resultant 100 categories of the probability index were plotted on the x-axis, which represents false-positive rates of annual flood probability. Then observed flood points were overlaid on the flood probability index map. The cumulative relative frequency of observed flood points (true positive rate) was plotted against each category of false-positive rate (Tehrany et al. 2019b).

The AUC is a global accuracy statistic, where the thresholds range from 0 (random prediction) to 1 (perfect prediction): Excellent (0.9–1), very good (0.8–0.9), good (0.7–0.8), moderate (0.6–0.7) and weak (<0.6) (Arabameri et al. 2019). AUC values estimated by using training and test data indicate the success and prediction accuracy of the model, respectively (Tehrany et al. 2019b). Moreover, observed relative flood frequency in each test flood

location was plotted against corresponding modelled annual flood probability value and a third-degree polynomial regression model was established.

The values of various statistical indices such as overall accuracy, specificity, sensitivity, positive predictive value, negative predictive value (Tehrany et al. 2019b), and kappa statistic (McHugh 2012) were estimated to measure the comparative performance of each model. Thus, modelled flood probability index values of all observed flood points (training and test) were binarized, optimizing a cut-off flood probability value using the 'OptimalCutpoints' package in R, which is "the optimal point on the ROC curve closest to the point (0, 1)" (López-Ratón et al. 2014).

5.2.5. Analysing the impact of TRM on flooding

5.2.5.1. Simulating sediment deposition in selected TRM sites

To model sediment deposition during the operation of TRM, suitable 'beels' were identified. 'Beels' were delineated using a DEM-based flood routing model (Diaz-Nieto et al. 2011), established for the south western embanked region by Adnan et al. (2019b). A total of 234 'beels' were identified within the embanked region, with sizes ranging from 0.74km^2 to 48.53km^2 (Figure 5.5 (a)). A GIS-based suitability analysis was performed to select TRM sites. First, indicators to perform suitability analysis were selected. Whilst limited information is available on indicators to select TRM sites, Masud et al. (2018) proposed a Sustainability Index of TRM (SITRM), conceptualizing the spatial and temporal impact of TRM based on a characterisation of the tidal river, environment, resilience, floodplain ecosystem, human health, and community. To identify suitable TRM sites, five indicators were selected: i) tidal prism; ii) river salinity; iii) flood-prone areas; iv) crop production; and v) size of the 'beel'. These indicators are associated with the tidal river, environment, resilience, and floodplain ecosystem components of SITRM. The suitability

analysis did not include indicators related to human health and community, due to unavailability of required spatial data for the entire study area.

The inter-tidal volume or tidal prism (P) explains the availability of tidal flow required to implement TRM. A higher P indicates an adequate tidal flow for TRM, given that water carries the required amount of sediment (Talchabhadel et al. 2018a). The study area is comprised of lands from 46 river sub-basins and P was approximated in individual sub-basin using the following equation (Lakhan 2003):

$$P = HA \tag{5.6}$$

where H is the tidal range and A is the surface area of each sub-basin. This is an approximation in basins where the inter-tidal area is significant relative to the overall surface area, but as the bathymetric form through the delta is rather similar, we do not expect this approximation to bias the results. Sub-basins were generated in GIS incorporating river outlet location data collected from BWDB, who also provided daily tidal water level data for each outlet. The difference between the mean water level in each outlet during the high and low tide is the tidal range.

Salinity is an important indicator of floodplain ecosystems. TRM operation allows river water to enter a tidal plain twice a day. A high concentration of salinity in tidal river water will cause an increase in soil salinity, making land unsuitable for crop production (Masud et al. 2018). Therefore, the level of river salinity is inversely correlated with the suitability of a site to operate TRM. Monthly observed river salinity data in each outlet of river sub-basins was collected from the BWDB, which was averaged across the year, where salinity level ranged from 0.23dS/cm to 12.39dS/cm (Supplementary Figure 5.9 (b)). Since TRM primarily intends to minimize flooding problems, ‘beels’ that were frequently affected by flooding are more suitable for TRM. Hence, mean flood frequency in each ‘beel’ was estimated from the developed flood inventory map (Supplementary Figure 5.9 (a)). As, TRM

primarily aims to increase crop production in flood-prone areas (Gain and Schwab 2012), hence 'beels' with land used for agriculture are the most suitable TRM sites. Besides, relatively smaller 'beels' are more suitable for TRM implementation, which makes stakeholders engagement less complex (Masud et al. 2018).

A rank (y) was assigned to each 'beel' according to the level of suitability in a 1 (very low) to 5 (very high) scale, in relation to the value of each suitability parameter (x). Ranks were estimated applying a linear interpolation technique proposed by Davis (2002). If the value of a parameter is positively correlated with the level of suitability for a TRM site, then Equation 5.7 was used, otherwise, Equation 5.8 was applied (Adnan et al. 2019a). For land-use data, a dummy code was provided to each land-use class, based on subjective judgement (Abdullah et al. 2018). Three main categories of land-use such as agriculture, mixed agriculture and aquaculture, and aquaculture were given codes of 3, 2, and 1, respectively.

$$If\ y\ \propto x, \qquad y_n' = \frac{(y_2 - y_1)(x_n' - x_{min})}{(x_{max} - x_{min})} + y_1 \tag{5.7}$$

$$If\ y\ \propto \frac{1}{x}, \qquad y_n' = \frac{(y_2 - y_1)(x_n' - x_{max})}{(x_{min} - x_{max})} + y_1 \tag{5.8}$$

where y_n' is the suitability rank of a parameter for the nth 'beel' (n = 1, 2, 3, …., 234); the maximum rank y_2 = 5; minimum rank y_1 = 1; x_n' is the value of a parameter for the nth 'beel'; x_{max} is the maximum value of a parameter among all 'beels', and x_{min} is the minimum value of a parameter among all 'beels'.

Simulated sediment deposition data were collected from Talchabhadel et al. (2018a) for five 'beels' located in Polder 24 (Figure 5.1 (c)). Talchabhadel et al. (2018a) simulated sediment deposition in TRM sites based on a two-dimensional (2D) numerical model, established through laboratory flume experiments to understand the mechanism of sediment transportation and deposition. During the experiment, a constant discharge of 5.1 l/s as

upstream river flow and 2.8 l/s as downstream tidal flow were provided. To represent high and low tidal flow, the adjustable gate was used. The gate was kept closed for 2 minutes to represent high tide, when the downstream flow from water pump was supplied along with dry sediment, of mean diameter equal to 94 μm and density 2.65 g/cc, from a sediment feeder. Then, the gate was opened for the next 2 minutes, when the downstream supply of water and sediment were stopped, representing a low tide. Thus, a total of 8 minutes of experiments were performed to represent two complete tidal cycles in a day, as is the case in the coastal region of Bangladesh. The study assessed the optimum size of the link canals and the importance of constructing coffer dams in the river upstream of the opening for effective sediment deposition around the attached tidal basin. To make the study less complicated, the experimental setup involved a straight river and tidal basin attached in a perpendicular alignment. Photogrammetric techniques were applied to measure the deposited sediment along with a laser displacement sensor (Supplementary Figure 5.4-Supplementary Figure 5.7).

The 2D numerical model was developed based on the shallow water flow equations and suspended sediment transport. The model was applied to explore the efficacy of the land heightening of the tidal basin with changing discharges and opening sizes. The numerical models were tested in different scenarios and compared with experimental results. The model reproduced the water depth and velocity reasonably well (percentage bias = ± 5 % and coefficient of determination ≥ 0.7). Suspended sediment concentration (SSC) and the deposited sediment were also replicated in good agreement with experimentally measured data. The surface was divided by an unstructured mesh using the GID software developed by the International Center for Numerical Methods in Engineering (CIMNE) (https://www.gidhome.com). A DEM of 5 m resolution was derived from the bathymetric data of March 2007 provided by the Institute of Water Modelling (IWM) Bangladesh. A

Manning roughness coefficient of 0.025 was assigned to meshes covering the river system, channels, and connecting canals, whereas a Manning roughness coefficient of 0.04 was provided in remaining areas. Simulated sediment deposition during six months of TRM implementation in 'beel' Khukshia (*beel*-2, Figure 5.5 (b)) was further validated against observed sediment depth at various locations, collected through field-work in November 2012. Further details on the experimental setup, model development can be found in Talchabhadel et al. (2017a) and Talchabhadel et al. (2018a).

River bathymetry and measured sediment concentration data are not available for the whole area under study. Therefore, based on the simulated sediment deposition in five 'beels', sediment deposition in remaining 'beels' was parameterised, developing an ordinary least square (OLS) regression in GIS. The OLS model included pixelwise height of the deposited sediment as dependent variable and factors explaining the deposition of sediment as independent variables. Five geomorphological variables were identified that explained the height of the deposited sediment in each pixel: i) land elevation (E_l); ii) distance from drainage (link canal) (D_d); iii) TWI; iv) slope (S_l); and v) curvature (C). Supplementary Figure 5.1- Supplementary Figure 5.3 show these variables. The estimated intercept and regression coefficients were used to form Equation 5.9, which was applied to simulate sediment deposition in remaining suitable 'beels'.

$$Sediment\ deposition\ (m) = 1.73 - 0.13E_l - 0.13D_d - 0.04\,TWI - 0.03S_l + 0.04C \quad (5.9)$$

Validation of the developed OLS regression model was performed plotting the parameterized pixelwise sediment height in five 'beels' against the obtained modelled sediment height and estimating the R^2 value of 0.88 (Supplementary Figure 5.8).

5.2.5.2.Estimating the impact of TRM on flooding

The change in land elevation and flood susceptibility for pre- and post-TRM implementation scenarios was compared. TRM has already been implemented in five 'beels'

within Polder 24 (ADB 2007), where simulation of sediment deposition was performed. A 50m resolution DEM was collected from IWM, which was developed from a toposheet map (1:20000) produced by Survey of Bangladesh (SoB) in 1990 - 1991, carrying out an aerial photography survey. The IWM and ALOS DEMs were used to estimate observed land elevation in pre-TRM and post-TRM scenarios in five 'beels', respectively. Because the TRM operations within these areas were interrupted before full sediment accumulation could occur, in practice land accretion was much lower than expected. In these cases, the sediment deposition was modelled for the remainder of the implementation period (1 to 5-year) to estimate the potential sediment accumulation during a 5-year implementation. Finally, the observed and modelled increase in land elevation were compared after the implementation of TRM.

A change in land elevation due to the implementation of TRM promoted changes in four other flood conditioning factors: aspect, slope, curvature, and Stream Power Index (SPI). Since TRM intended to alleviate land subsidence, hence the value of this factor was considered as zero for the post-TRM scenario. Parameterized sediment deposition was added to the existing ALOS DEM to develop DEM for the post-TRM scenario. Following the similar procedure explained in Section 5.2.4, flood susceptibility at post-TRM scenario was estimated.

5.3. Results and discussion

5.3.1. Delineation of flood susceptible zones

5.3.1.1. The outcome of the FR model

Table 5.1 summarizes the outcome of the FR model, showing the relationship between the flood conditioning factors and flooding. Areas with lower elevation and slope as well as curvature with flat and concave characteristics were prone to flooding. Regarding aspect, cells facing east, west, and northwest, as well as flat areas, were highly susceptible

to flooding. A greater percentage of flood locations were found in areas where relatively higher level land subsidence occurred.

Table 5.1 Spatial relationship between flood locations and flood conditioning factors

Variables	Class	Frequency ratio (FR)	Variables	Class	Frequency ratio (FR)
Aspect	Flat (-1)	1.45	**Land uses**	Shrimp culture	0.93
	North (0-22.5)	0.84		Rice field	1.03
	Northeast (22.5-67.5)	0.92		Mixed rice field, shrimp, and other fish culture	3.52
	East (67.5-112.5)	1.00		Mangrove	0
	Southeast (112.5-157.5)	0.80		Shrimp and other fish culture	3.40
	South (157.5-202.5)	0.77		Other crop agriculture land	0.55
	Southwest (202.5-247.5)	0.95		Freshwater fish culture	1.41
	West (247.5-292.5)	1.02		River/Canal	1.26
	Northwest (292.5-337.5)	1.32		Settlement with Homestead Vegetation (Rural)	0.35
	North (337.5-360)	0.91		Settlement with Homestead Vegetation (Urban)	0.46
				Water Body	0
				Others	0
Elevation (m)	≤ 0	1.50	**Soil texture**	Silty clay and silty clay loam	1.78
	0 - 1	1.34		Clay	3.54
	1 - 2	1.29		Silty clay	0.88
	2 - 3	1.30		Silt loam and Silty clay	0.38
	3 - 4	0.98		Unclassified	0.96
	4 - 5	0.68		Silt loam	0.61
	5 - 7	0.25			
	7 - 9	0.15			
	> 9	0		Silty clay and clay	1.34
Slope (degree)	0 – 0.44	1.52		Silt loam and clay	1.02
	0.44 - 0.66	1.23		Silty clay loam and silty clay	0.86
	0.66 – 0.88	1.09		Silty clay loam and silt loam	0.43
	0.88 - 1.09	1.15		Silty clay loam	0
	1.09 - 1.32	0.84			
	1.32 - 1.98	1.09			
	1.98 - 2.64	0.78			
	2.64 - 3.73	0.69			
	3.73 – 56.01	0.38			
Curvature	Convex	0.98	**Soil permeability**	Moderate	0.58
	Flat	1.06		Mostly moderate	1.21
	Concave	1.00		Slow	1.25
Land subsidence (m)	< 0.12	0.32		Unclassified	0.96
	0.12 - 0.16	0.15		Mostly slow with some Moderate	0.39

	0.16 - 0.20	1.47		Mostly moderate with some slow	0.38
	0.20 - 0.23	1.95		Mostly slow	0.64
	0.23 - 0.25	1.17			
	0.25 - 0.26	1.15			
	0.26 - 0.265	0.83			
	0.265 - 0.27	0.69			
	> 0.27	1.31			
Precipitation (mm)	1593 - 1645	1.18	**Distance from drainage channels (m)**	0 - 90	0.93
	1646 - 1706	1.64		90 - 192.09	0.82
	1707 - 1766	1.06		192.09 - 308.87	1.17
	1767 - 1806	1.00		308.87 - 445.98	0.87
	1807 - 1863	1.20		445.98 - 607.45	1.10
	1864 - 1903	0.71		607.45 - 831.93	1.17
	1904 - 1948	1.10		831.93 - 1176.52	0.95
	1949 - 2178	1.04		1176.52 - 2012.01	0.92
	2179 - 2621	0.09		2012.01 - 13232.18	1.30
Stream power index (SPI)	-13.82 to -10.93	0.91	**Distance from rivers (m)**	0 - 180	0.89
	-10.93 to -10.19	1.05		180 - 450	0.95
	-10.19 to -7.02	0.40		450 - 780	0.84
	-7.02 to -3.48	1.30		780 - 1168.46	0.68
	-3.48 to -2.74	1.14		1168.46 - 1636.85	0.68
	-2.74 to -1.99	0.84		1636.85 - 2248.4	0.92
	-1.99 to -1.16	1.06		2248.4 - 3100.61	1.26
	-1.16 to 0.05	1.08		3100.61 - 4477.95	1.49
	0.05 to 10.01	1.32		4477.95 - 12559.4	1.18

Areas characterized by higher values of SPI contained a greater number of floods. Floods occurred primarily in areas that were used mostly for agricultural and aquaculture purposes, compared to settlement areas where a relatively lower number of flood locations were found. In relation to soil texture, four categories of soils contained most of the flood locations: ‘silty clay and silty clay loam’, ‘clay’, ‘silty clay and clay’, and ‘silty clay loam and silty clay’ type soil. Areas with ‘moderate’ or ‘slow’ permeable soils are prone to flooding. Besides, floods are more likely to occur in areas away from adjacent rivers, as water is difficult to drain from those areas.

5.3.1.2. The outcome of the LR model

Table 5.2 summarizes the outcome of the LR model. Among the 12 factors, six were statistically significant (*p*-value less than 0.05). The flood probability index map derived in this study is shown in Figure 5.2 (b). The optimization of flood probability values at

observed flood locations yielded a cut-off (minimum threshold probability) value of 0.6. A major portion of the study area is susceptible to flooding, which was mostly inundated during different historical flood events (Figure 5.2 (a)). The annual probability of flooding in 48% of the studied area is greater than 0.8, where observed mean relative flood frequency is 0.2. This result indicates that inundations occurred during four historical flood events, on average, as the maximum frequency of inundation was 20 in a total of 25 observation years (Supplementary Figure 5.9 (a)).

Table 5.2 Logistic regression model to predict the occurrence or not occurrence of floods

Variables	**Coefficient**	**Standard error**	***p*-value**
Intercept	-36.328	6.957	$1.778\ e^{-07}$ ***
Aspect (A_s)	0.023	0.008	0.003 **
Elevation (E_l)	0.045	0.004	$< 2.2e^{-16}$ ***
Slope (S_l)	-0.008	0.006	0.208
Curvature (C)	0.244	0.067	0.0002 ***
Land subsidence (L_s)	0.004	0.003	0.006 **
Precipitation (P)	0.008	0.005	0.087 ▪
SPI	0.003	0.007	0.614
Land use (L_u)	0.011	0.001	$8.221e^{-10}$ ***
Soil texture (S_t)	0.011	0.004	0.099 ▪
Soil permeability (S_p)	0.008	0.005	0.003 **
Distance from drainage channels (D_d)	0.011	0.010	0.372
Distance from rivers (R_d)	0.008	0.006	0.112

*R^2: 0.77; Significance codes: 0 '***' 0.001 '**' 0.01 '*' 0.05 '▪' 0.1 ' ' 1*

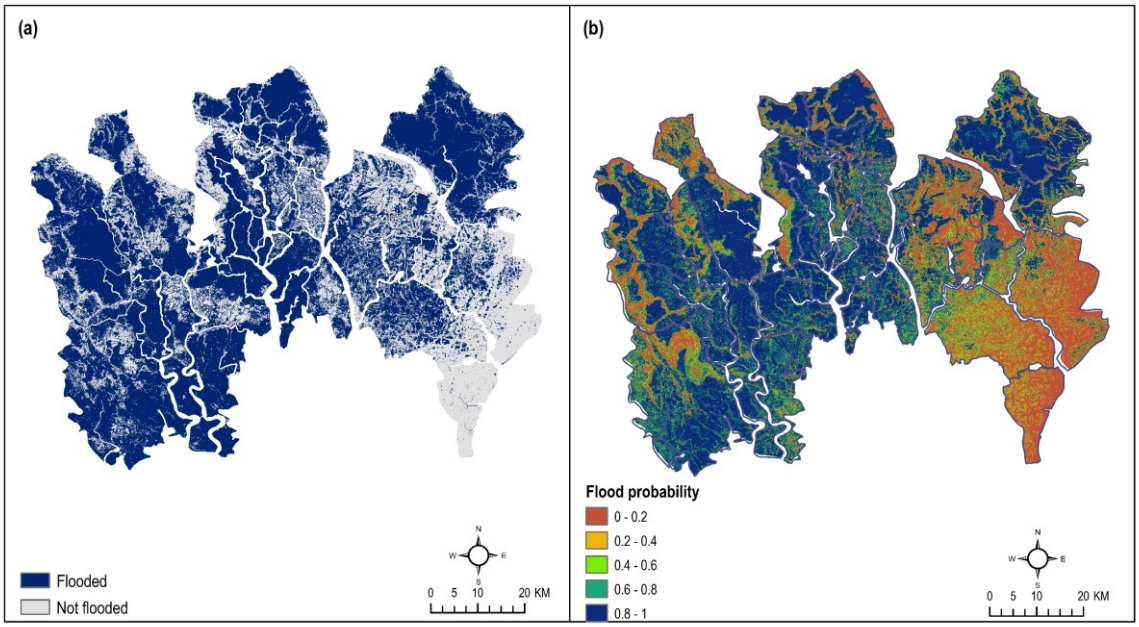

Figure 5.2 (a) Extent of inundation during floods from 1988 to 2012 (b) Annual flood probability index map

5.3.1.3. Model validation

The estimated AUC for test dataset was 0.86, which indicates a 'very good' prediction accuracy. In addition, the AUC of 0.90 for the training dataset implies an 'excellent' success rate of the model (Figure 5.3 (a)). Figure 5.3 (b) shows how the estimated flood probability increased with observed relative flood frequency. A third-degree polynomial equation was generated that explains the type of relationship between observed relative flood frequency and modelled flood probability. The general goodness of fit of this equation is verified by the estimated R^2 value of 0.97.

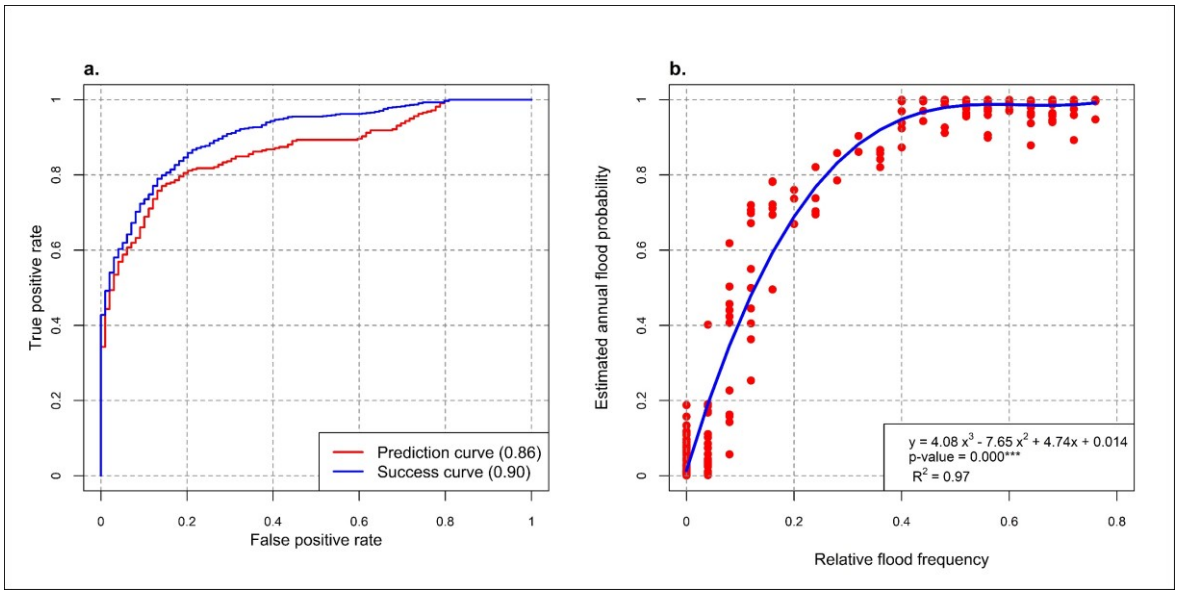

Figure 5.3 (a) ROC curve to validate flood probability map (b) Relative flood frequency and estimated annual flood probability of test flood observation points

Moreover, an overall accuracy of 93% explains the percentage agreement of pixels correctly classified. The Kappa coefficient of 0.85 indicates 'almost perfect' agreements between observed and modelled flood locations (Table 5.3).

Table 5.3 Validation of flood susceptibility model

Statistical index parameters	**Values**
True positive (correctly classified flood locations)	546
True negative (correctly classified non-flood locations)	381
False positive (incorrectly classified flood locations)	33
False negative (incorrectly classified non-flood locations)	40
Positive predictive value (PPV) (%)	95
Negative predictive value (NPV) (%)	90
Sensitivity (%)	93
Specificity (%)	92
Overall accuracy (%)	93
Kappa statistic	0.85

5.3.1.4. Characteristics of flood susceptible region

Since the average flood probability in most of the polders is greater than the minimum threshold flood probability, the major portion of the region is classified as being susceptible to flooding annually. More than 50% of the total area across 30 polders has an annual flood probability value greater than 0.8 (Figure 5.4). The major proportion of agricultural and aquaculture land-use is located within flood susceptible zones (65% and 81%, respectively). More than 90% of the area under mixed agriculture and aquaculture land-use is susceptible to flooding. A substantial proportion of people (44.5%) live in a relatively small proportion (22.8%) of settlement areas, which are susceptible to flooding (Supplementary Table 5.4).

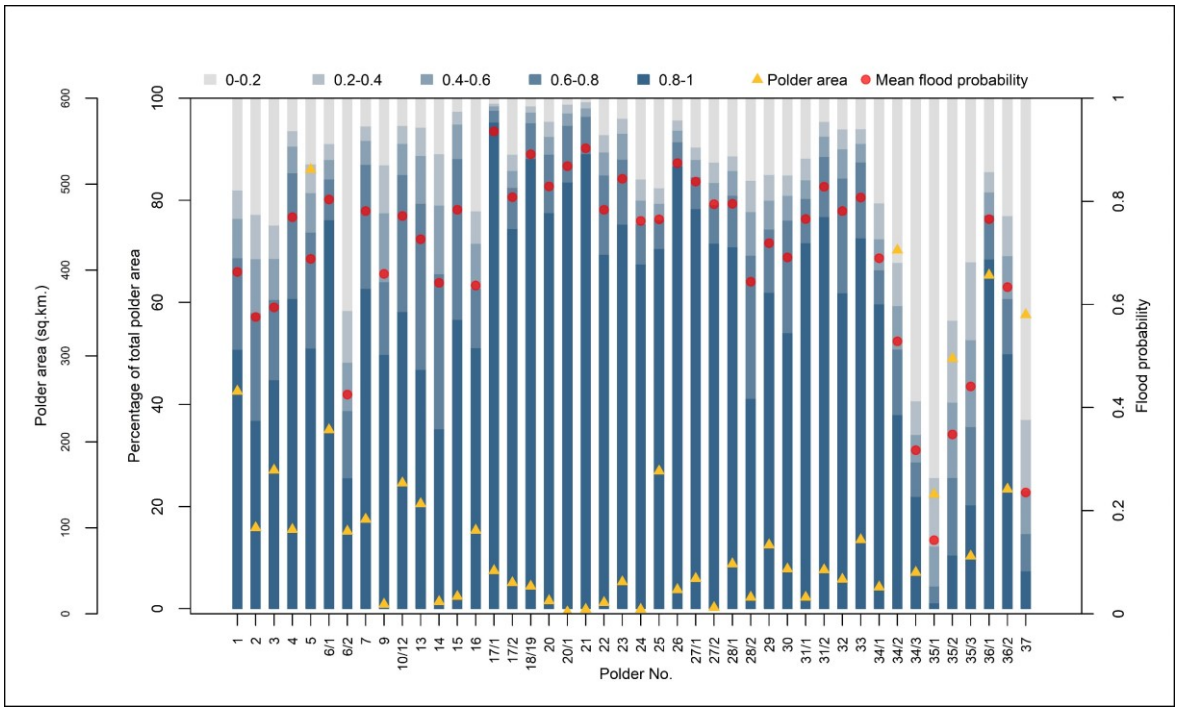

Figure 5.4 Ratio of flood susceptible lands in various polders

5.3.2. Impact of TRM in reducing flood susceptibility

5.3.2.1. Sediment deposition and restoring land elevation

The suitability analysis yielded 106 'beels' that are suitable (estimated suitability rank from 3 (moderate) to 5 (very high)) to operate TRM. Most of the polders in the northern

segment of the study region are suitable, since these areas are highly prone to flooding and where most of the agricultural activities take place, and the salinity level in surrounding rivers is relatively lower (Figure 5.5 (a)). The result of the sediment transportation and deposition model indicated that continuous operation of TRM in sample 'beels' could reclaim a maximum of 1.4m land elevation in 5 years (Figure 5.5 (b)).

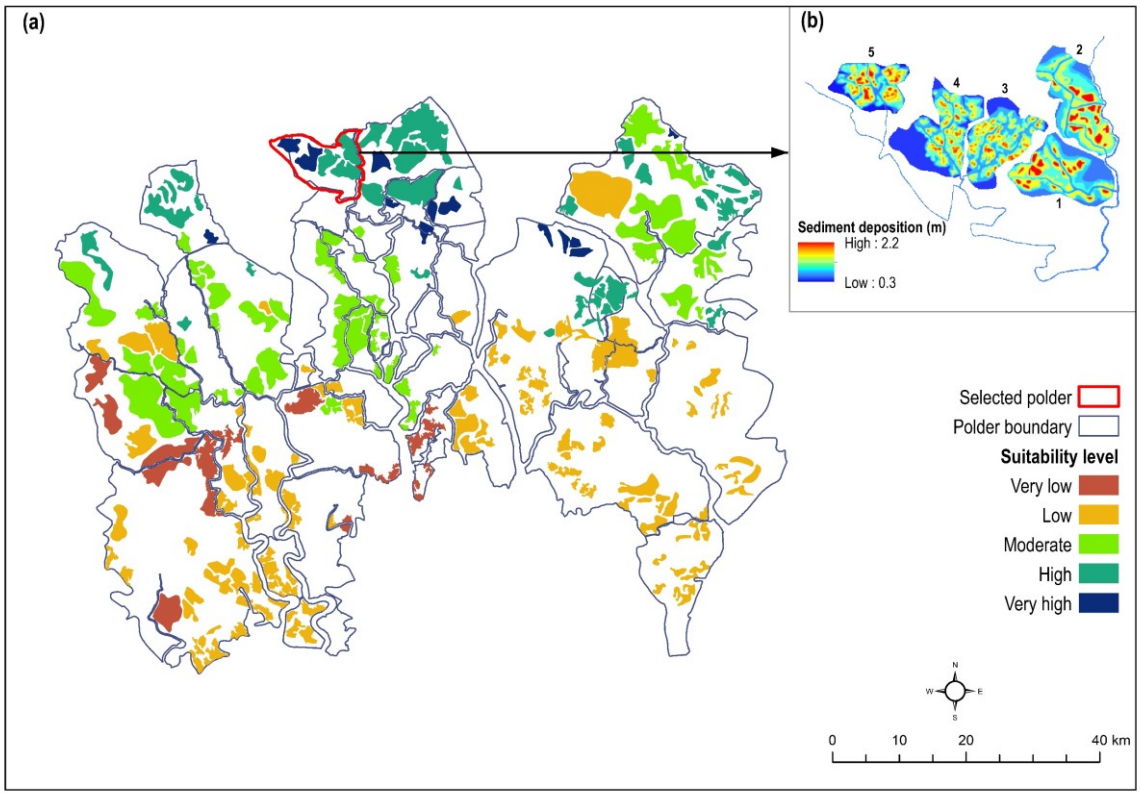

Figure 5.5 (a) Suitable 'beels' for TRM implementation; (b) sediment deposition in selected 'beels'

Figure 5.6 exhibits the extent to which TRM has been able to alter land elevation in five 'beels' in Polder 24. It also shows the land elevation that uninterrupted TRM might have recovered to in the five-year operation time. The mean elevation in all five 'beels' increased as a result of TRM (observed), implemented for various time steps. For instance, the length of TRM operation period in *beel*-1 (Beel Bhaina) was four years (1997 - 2001), whereas disruption in *beel*-2 (Beel Khukshia) caused an extended implementation period of six years (2006 - 2012). Results from the sediment transportation and deposition model

indicated that an uninterrupted and planned implementation (e.g., construction of link canals, rotation of openings) of TRM might have led to a further increase in land elevation than which has been achieved. For instance, the three-year implementation of TRM in *beel*-1 might have recovered a similar depth of sediment that deposited in four years in practice. However, *beel*-2 is an example of an unsuccessful TRM, where interruptions occurred throughout the implementation period. The observed depth of sediment deposition in six years was similar to the estimated depth of sedimentation obtained after two years of TRM implementation. The analysis noted that TRM was the most successful in *beel*-5, as it yielded the highest depth of sediments.

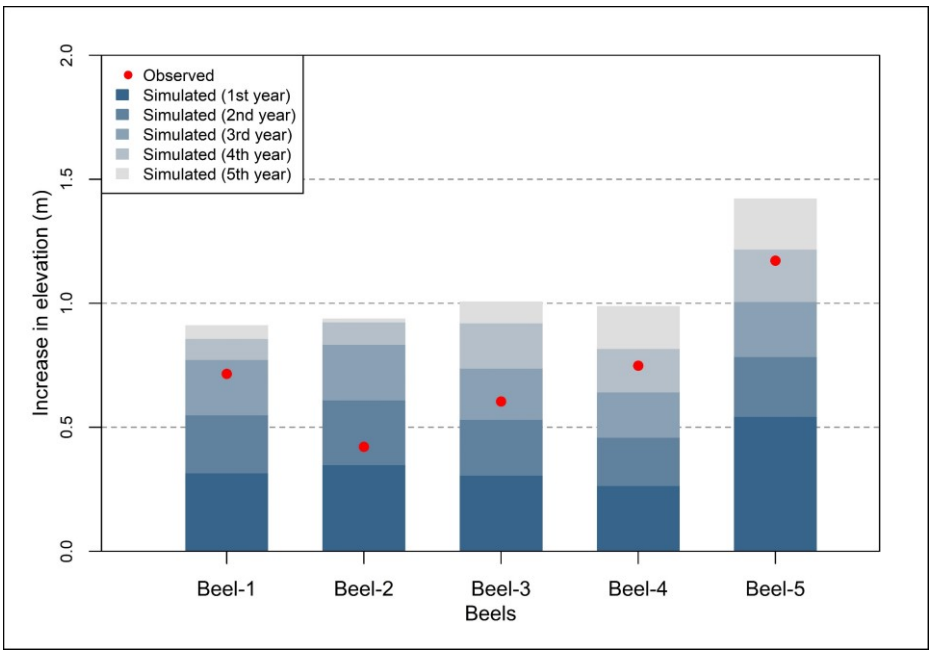

Figure 5.6 Change of land elevation in five selected 'beels' after implementing TRM

5.3.2.2. Flood susceptibility before and after TRM implementation

The application of TRM is predicted to reduce the annual probability of flooding from 0.86 (on average) to 0.57 (on average), in 106 suitable 'beels' located within 25 polders (Figure 5.7). A reduction of annual probability of flooding resulted from a change of various geomorphological flood-inducing factors. Along with increasing the surface elevation, the implementation of TRM could potentially improve the physical condition of natural

drainage basin by reducing the value of SPI which reduces the erosion potential of the surface. Besides, changes in surface curvature would decelerate surface flow. All these changes result in a reduced annual probability of flooding in the TRM sites.

The implementation of TRM reduced flood susceptibility across 'beels' in 13 polders, which were susceptible to flooding before. In general, flood susceptibility in 35% of areas of the selected 'beels' reduced due to TRM. However, the impact of TRM varied across 'beels' in different polders. The maximum reduction in the annual probability of flooding was estimated in 'beels' located within Polder 20 and Polder 29 (Figure 5.7), where the probability of flooding reduced by 0.46, on average.

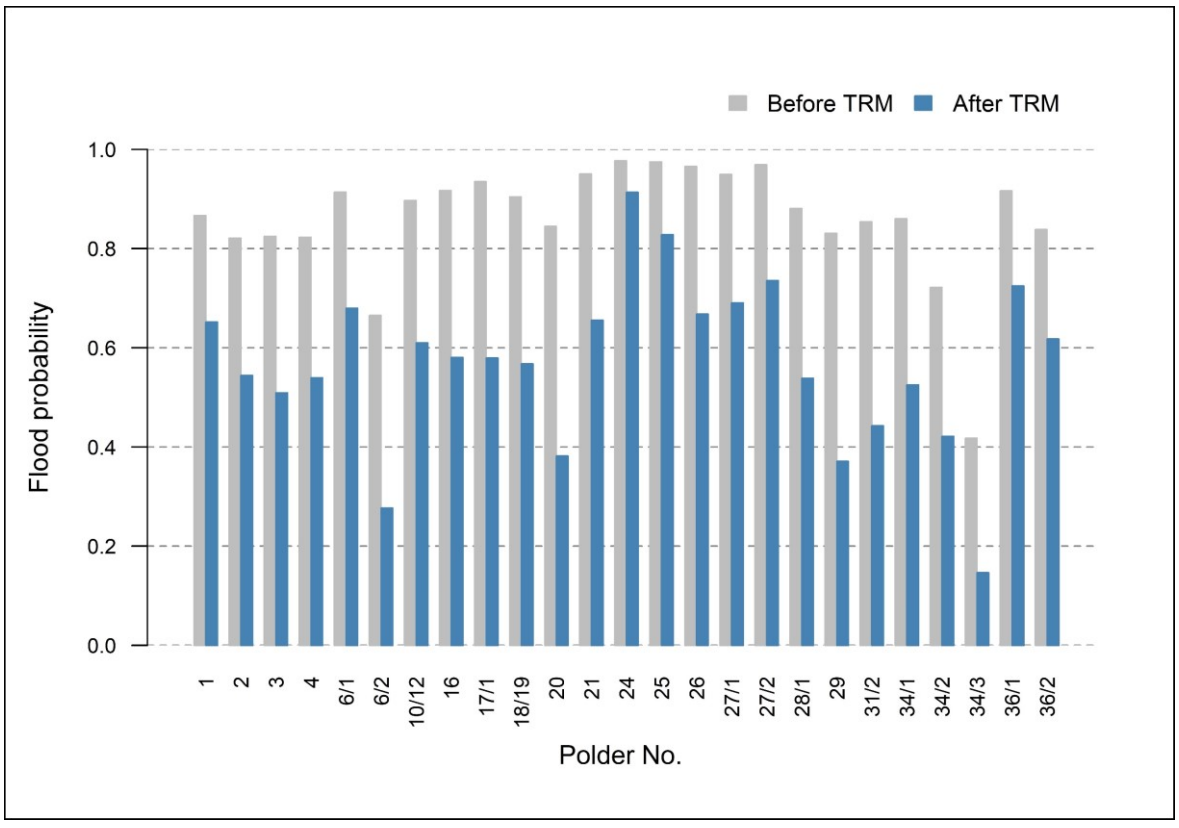

Figure 5.7 Annual probability of flooding in suitable 'beels' in different polders before and after the implementation of TRM

5.4. Conclusion

TRM in the south western coastal region of Bangladesh was implemented to promote sedimentation in low-lying 'beels', creating an opportunity of increased agricultural

production by reducing flooding. In practice, the success of TRM was hampered by interruptions during its operation, primarily caused by various implementation hurdles such as social unrest, conflict, and issues related to compensation. This study modelled the potential effectiveness of TRM in restoring land elevation and reducing flood susceptibility in the study area. A flood susceptibility model has been developed that successfully predicts flooding locations based on coordination of conditioning factors, the most influential being land elevation, aspect, curvature, land-use, land subsidence, and soil permeability. The study identified 106 suitable 'beels' where flooding could potentially be alleviated by a change in land elevation that could, in turn, be achieved by sediment deposition during TRM implementation. Sediment deposition in identified 'beels' was parameterised based on simulated sediment data on five sample 'beels'. Flood susceptibility in those 'beels' was compared between pre- and post-TRM implementation scenarios.

The results indicated that floods in the south western embanked region primarily occurred in areas with common characteristics such as low elevation and slope, flat landscape-scale curvature, high land subsidence rates and SPI, and moderate to low soil permeability. The study also estimated that a major portion of the total region is susceptible to flooding, being inundated during various historical flood events. Agricultural and aquaculture activities mostly take place in these flood susceptible zones. Wider implementation of TRM would result in increased land elevation, which could alleviate land subsidence and modify several geomorphological factors such as aspect, slope, curvature, and SPI. Such changes in the surface could help to reduce the probability of flooding in a range of polders. The results described here further indicate that an uninterrupted 5-year implementation of TRM might have resulted in a greater increase in land elevation (in 'beels') than has actually been achieved in practice, due to interruptions in implementation of several TRM projects.

Modelling sediment transportation in low-lying areas is a complex and data-intensive process. Scarcity of data, including observed sedimentation, makes it difficult to model sediment deposition hydrodynamically for the entire region. Accuracy of the flood susceptibility modelling results depends on input parameters used, particular the DEM. The ALOS DEM is considered to be the most accurate freely available DEM, which has a low root mean square error (1.78 m) in vertical accuracy (Hasan et al. 2020). To address the uncertainty related to DEM accuracy, topographical and hydrological parameters were discretised into various quantile classes and incorporated to the flood susceptibility model. Relevant discretised variables were also used to parameterise sediment deposition in suitable 'beels'.

This study attempted to assess the suitability of a site for TRM implementation mainly from the perspective of the physical environment. Socio-economic and governance considerations have proved to be critical to the successful implementation of TRM, but these have not been addressed in this study. This study shows the extent to which an uninterrupted implementation of TRM could help to alleviate flood susceptibility in the region. It further characterises polders according to the level of flood susceptibility as well as suitability to implement TRM, which could be a useful guide for national organizations like BWDB, who are responsible for managing water resources in polders.

Appendix C: Supplementary Materials to Chapter 5

Supplementary tables

Supplementary Table 5.1 Major dataset used in this research

Data	Description	Sources
Digital elevation model (DEM)	The Advanced Land Observing Satellite (ALOS) DEM of 30m spatial resolution	(JAXA 2015)
Land-use	Land use and land cover data for 2013	(http://www.espadelta.net/) (Mukhopadhyay et al. 2018)
Population	Gridded population data of 90m spatial resolution	(WorldPop 2018)
Precipitation data	Gridded (5km grid points) precipitation data of 10-day temporal resolution from 1965-2012	Bangladesh Meteorological Department (www.bmd.gov.bd/)
Soil texture data	Topsoil texture data with attributes of texture types, such as 'silt loam', 'clay', 'silty clay', etc.	Bangladesh Agricultural Research Council (http://www.barc.gov.bd/)
Soil permeability	Soil permeability level ('very low' to 'very high')	Bangladesh Agricultural Research Council (http://www.barc.gov.bd/)
Spatial data	Geographic Information System (GIS) data on polder boundary, polder number, river lines etc.	The Water Resources Planning Organization (WARPO) (www.warpo.gov.bd/)

Supplementary Table 5.2 Flood observation data used to develop and validate the flood susceptibility model

Dataset	Flood points	Non-flood points	Total
Training dataset	426	274	**700**
Test dataset	160	140	**300**
Total	**586**	**414**	**1000**

Supplementary Table 5.3 Multicollinearity diagnosis of selected flood conditioning factors

Selected variables	Variance inflation factor (VIF)	Mean VIF
Aspect	1.049	1.397
Elevation	2.445	
Slope	1.274	
Curvature	1.469	
Land subsidence	1.179	
Precipitation	1.544	
SPI	1.734	
Land-use	1.392	
Soil texture	1.204	
Soil permeability	1.315	
Distance from drainage channels	1.058	
Distance from rivers	1.098	

Supplementary Table 5.4 Population and land uses in flood susceptible areas of varying degrees

Exposure	Categories of flood probability				
	0 – 0.2	**0.2 – 0.4**	**0.4 – 0.6**	**0.6 – 0.8**	**0.8 – 1**
Population (%)	38	9	8.5	13.5	31
Land-use (% of area)					
Shrimp culture	9.4	5.0	6.5	16.8	62.2
Rice field	21.5	6.5	7.0	13.8	51.2
Mixed rice field, shrimp, and other fish culture	0.7	1.8	2.9	4.4	90.2
Mangrove	34.7	9.7	18.7	21.5	15.3
Shrimp and other fish culture	2.0	3.7	3.9	4.1	86.2
Other crop agriculture land	25.6	8.0	8.0	18.1	40.3
Freshwater fish culture	13.5	5.7	6.2	10.8	63.9
Settlement with Homestead Vegetation (Rural)	48.0	10.4	9.8	14.6	17.3
Settlement with Homestead Vegetation (Urban)	71.4	8.1	6.8	6.7	7.0
Others	0.2	0.2	0.5	11.7	87.4

Supplementary figures

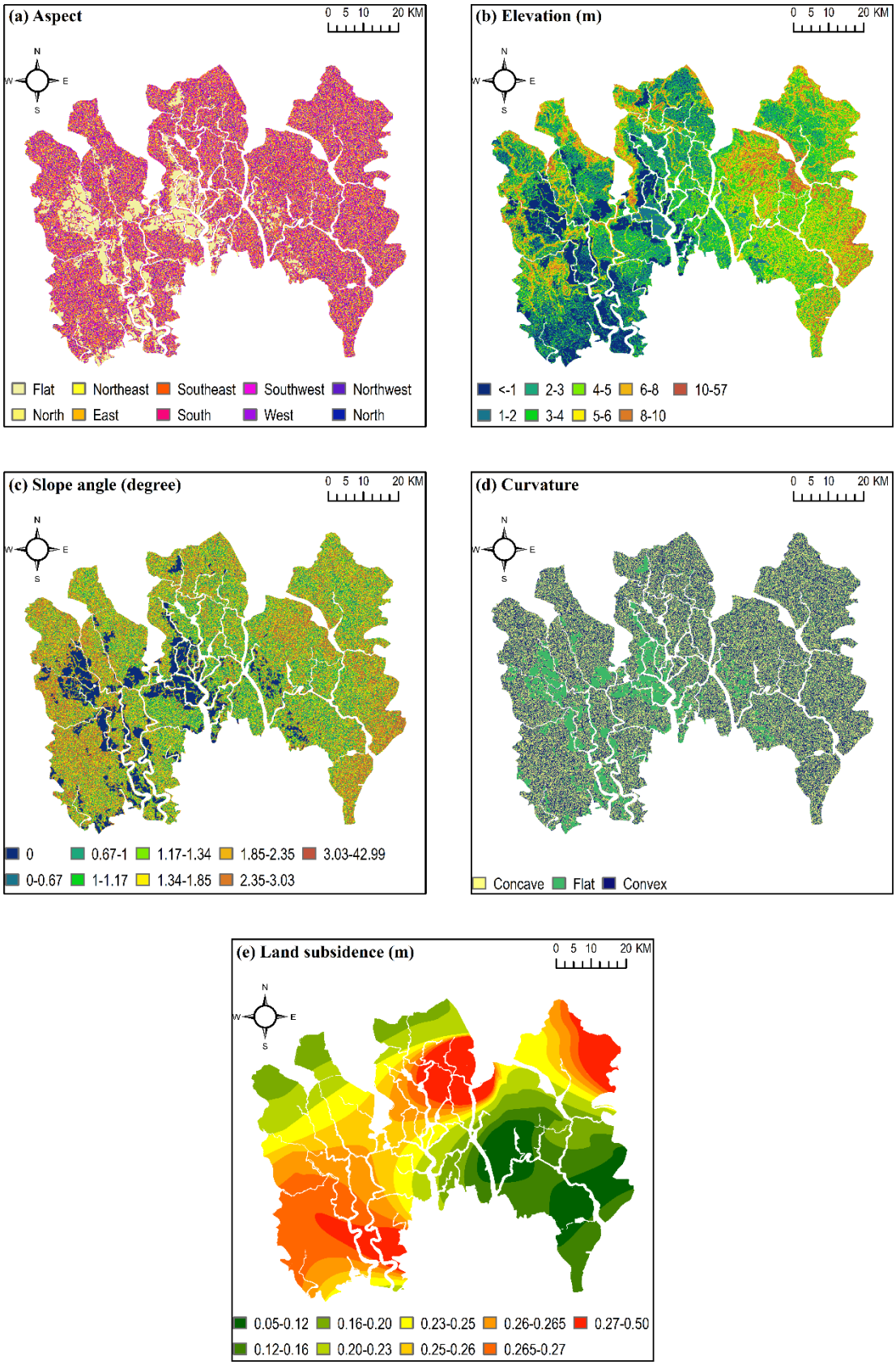

Supplementary Figure 5.1 Topographic factors contribute to flood

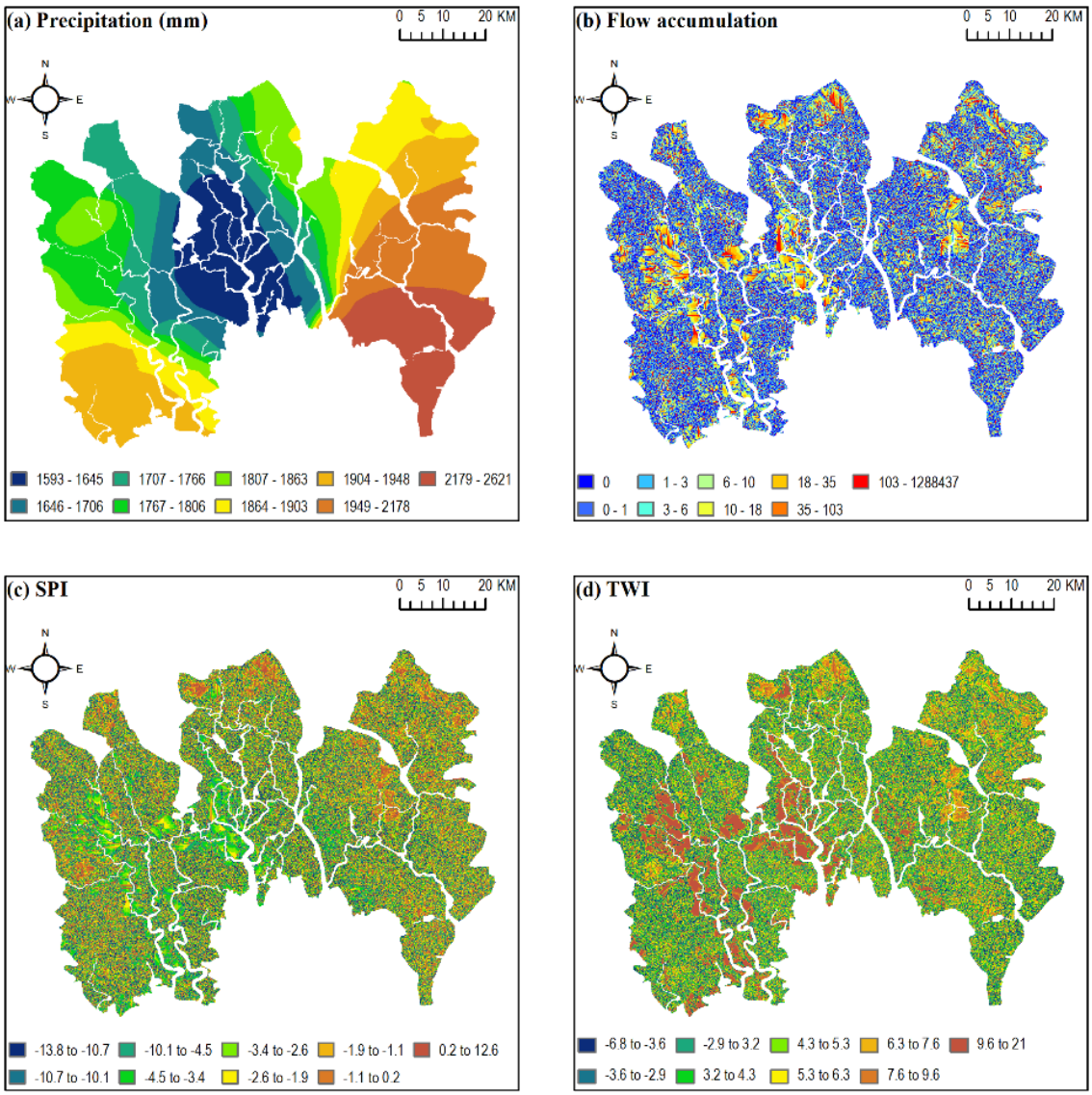

Supplementary Figure 5.2 Hydrological factors influence flood

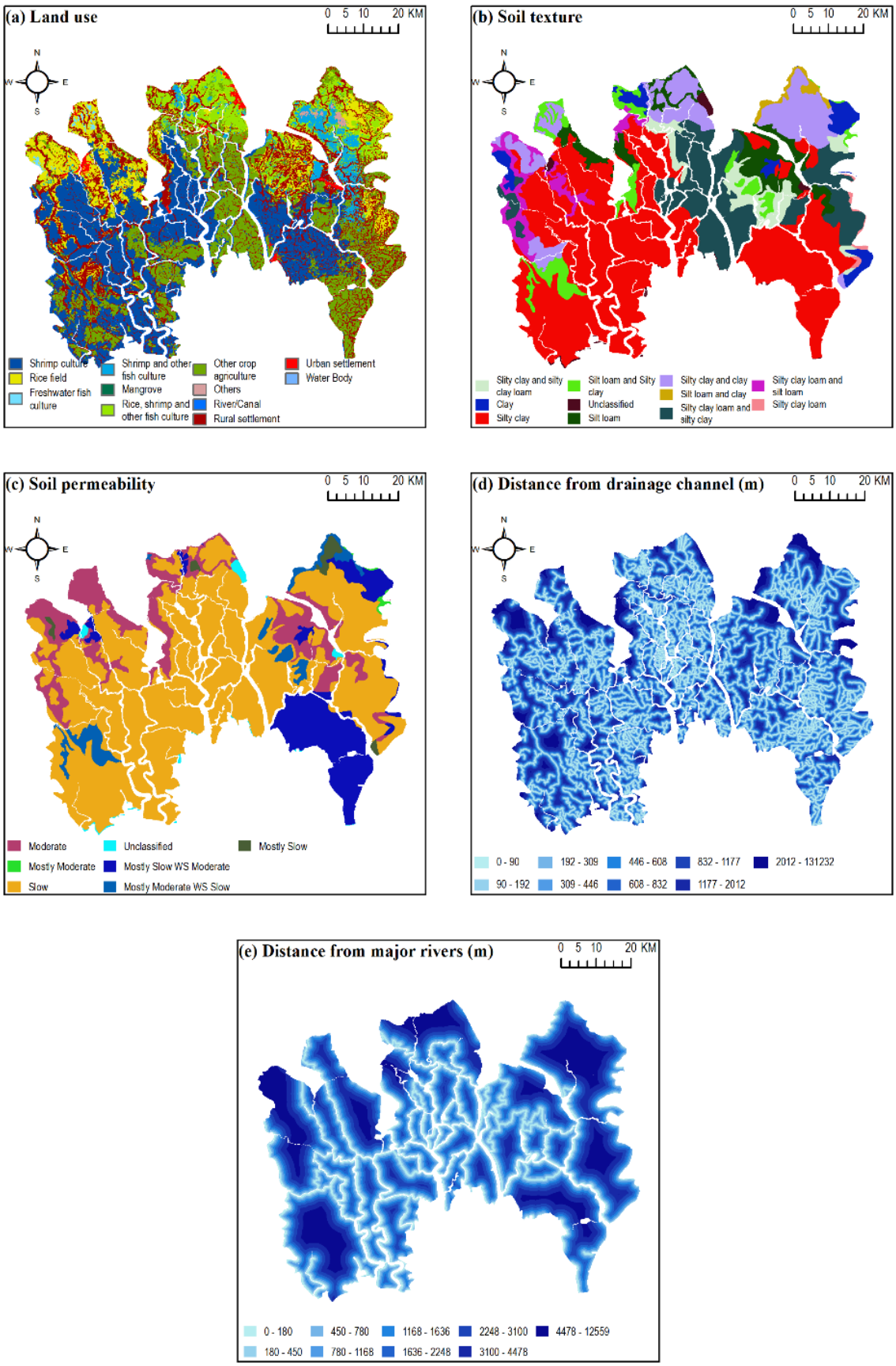

Supplementary Figure 5.3 Anthropogenic, geological, and locational factors influencing flood

Experimental study for sediment transport modelling

Supplementary Figure 5.4 Experimental facility: photos of bed level (left) and bed level measurement using laser displacement sensor (right) case II

Source:(Talchabhadel et al. 2017a)

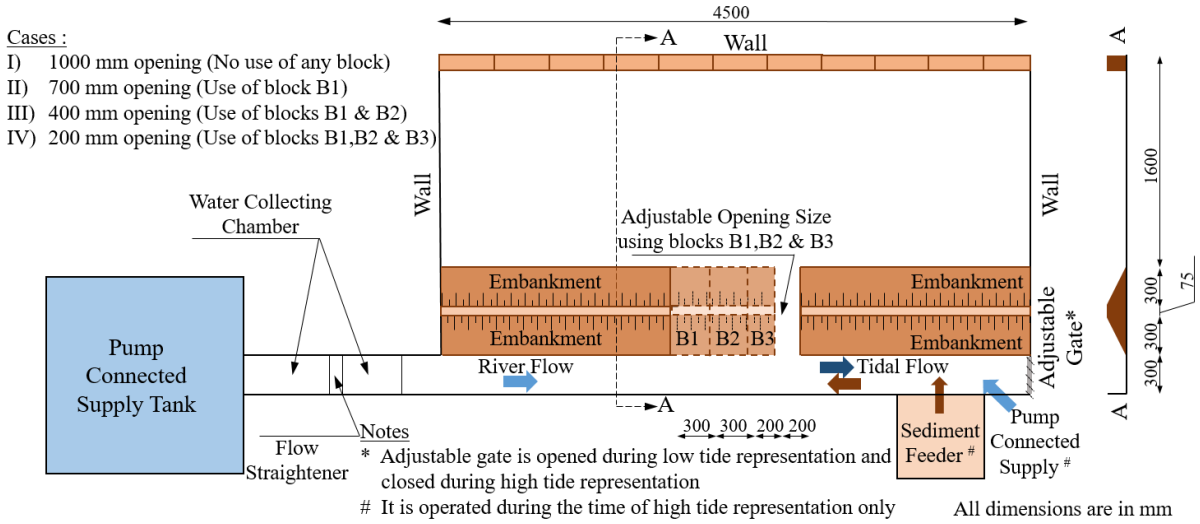

Supplementary Figure 5.5 Schematic view of the experimental setup

Source: (Talchabhadel et al. 2018b, Talchabhadel et al. 2016a)

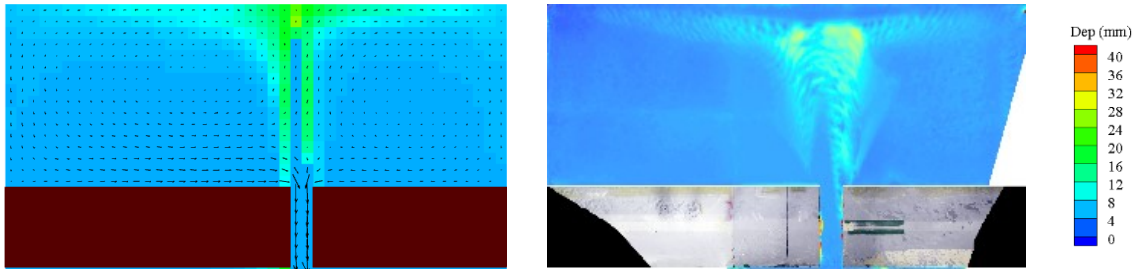

Simulation Experiment

Supplementary Figure 5.6 Sample comparison of simulated and experimental results of deposited sediment after repetitive tidal movement

Source:(Talchabhadel et al. 2017b, Talchabhadel et al. 2017a)

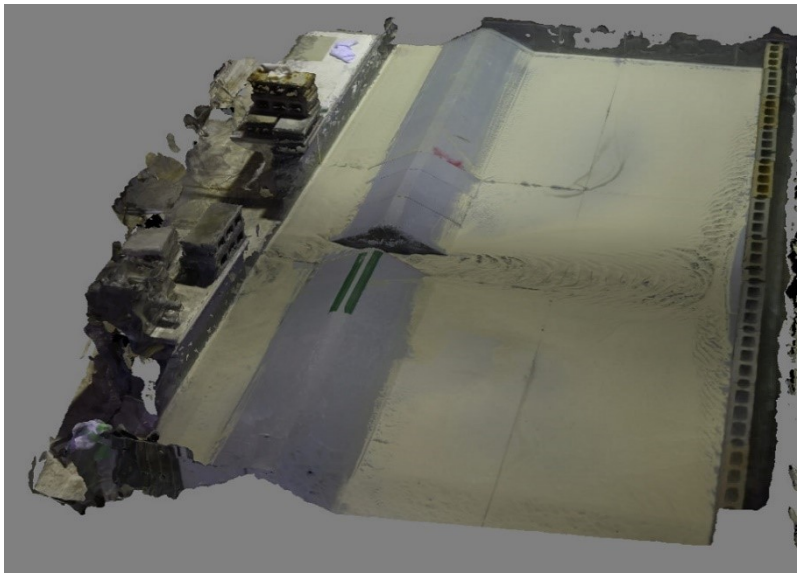

Supplementary Figure 5.7 Perspective view (3D spatial data from digital images)

Source: (Talchabhadel et al. 2017b)

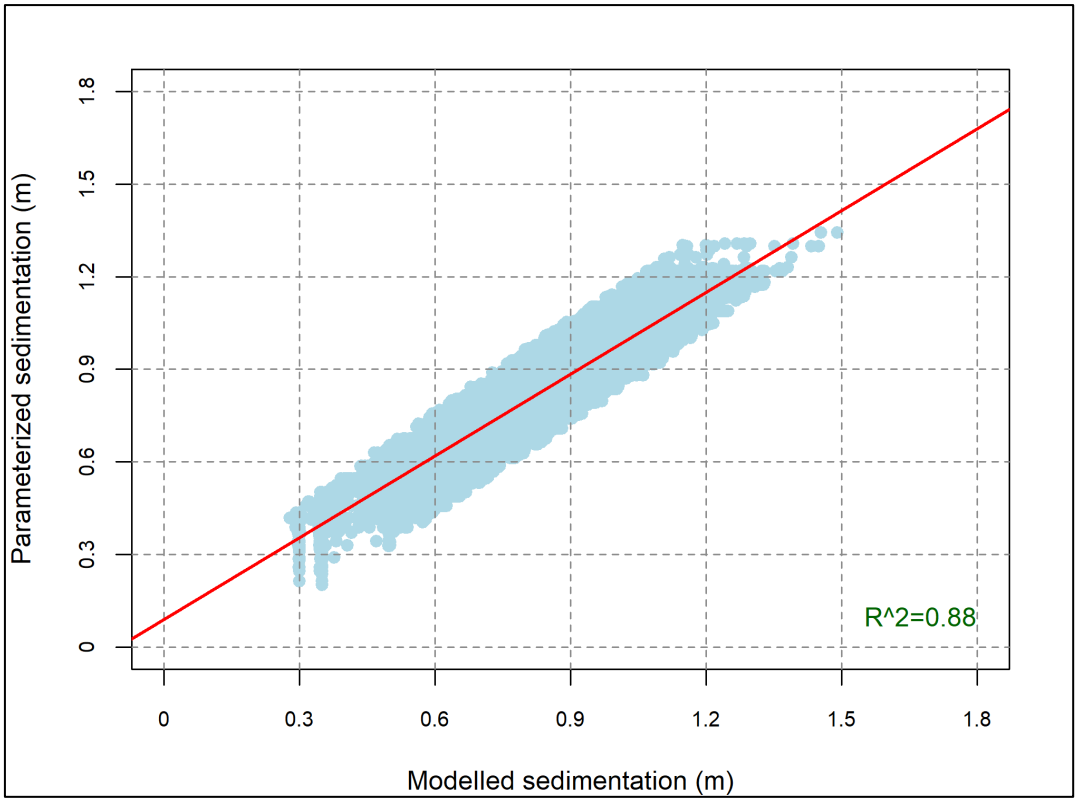

Supplementary Figure 5.8 Validation of suitability model to select candidate TRM sites

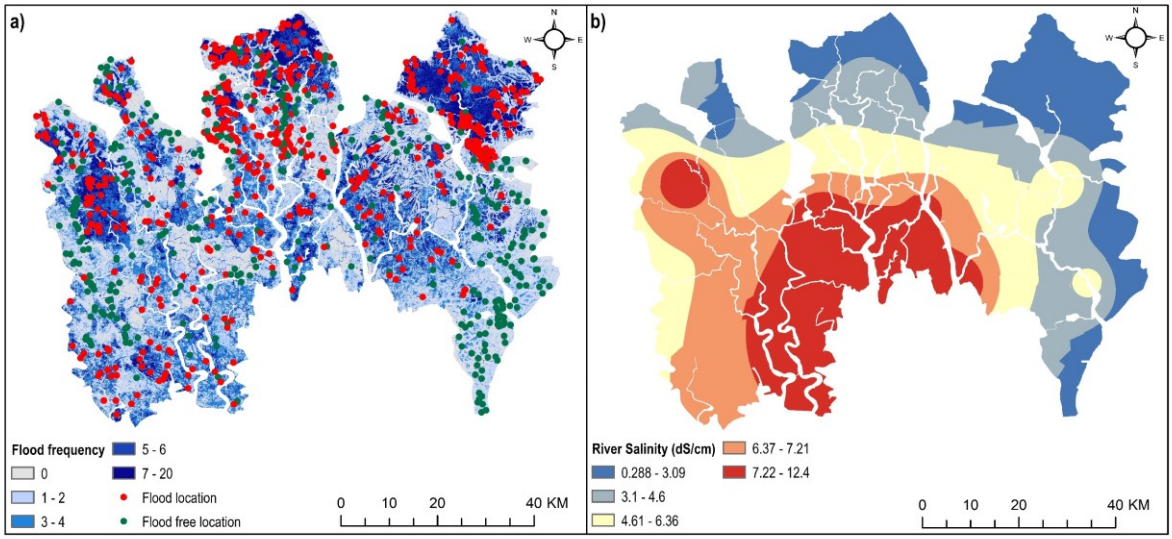

Supplementary Figure 5.9 a) Flood inventory map; b) River salinity map

Chapter 6 Conclusions

6.1. Summary of the Thesis

This thesis aims to diagnose complex flooding processes and adaptation options, to assess the effectiveness of different flood interventions in the coastal region of Bangladesh. Three peer-reviewed journal articles have been presented that provide evidence on how the broad goal of this thesis has been achieved.

Chapter 2 presents a critical discussion on the challenges in understanding the impacts of different flood adaptation options in complex coastal systems. The chapter also contains discourses on possible ways forward to address those challenges. Challenges have been discussed concerning the complexities in (i) coastal flood processes, (ii) flood risk assessment, and (iii) estimating the impacts of potential future flood adaptation options. A comprehensive understanding of coastal flooding processes is a challenging task as flood could occur from multiple sources. The presence of structural flood control measure could alter the hydrological regime of a protected area. Accurate assessments of risk to complex coastal flooding depend on the selection of methods for flood hazard and vulnerability assessments, that should consider the dynamics of land use changes and societal impacts. The choice of potential future flood adaptation options should be driven by a scientific evaluation of their potential impacts on the environment. Therefore, new research is required that would be able to conduct an ex-post evaluation of flood interventions, quantify the societal impacts of flood risk in a dynamic coastal system, and predict potential future impacts of flood adaptation options.

To address the first challenge identified in chapter 2, chapter 3 evaluates the impacts of coastal embankments, creating polders, in Bangladesh on the frequency and extent of inundations caused by different types of flooding. The chapter analyses historical floods in the coastal zone in Bangladesh in every year within 1988-2012, diagnosing whether the

floods were attributable to monsoonal precipitation (pluvial flooding), high upstream river discharge into the tidal delta (fluvio-tidal flooding), or cyclone-induced storm surges. Pluvial flooding resulted in 11.4% of the domain being flooded, on average. Fluvio-tidal and surge floods were less frequent but caused more inundation (21.8% and 30.2% area on average). Construction of the polders has increased the extent of the pluvial flooded area by 6.5%. Polders have provided some protection against storm surges and fluvio-tidal events. The chapter presents a spatial evaluation of polders' effectiveness which should help to inform plans for an adaptation of Bangladesh's coastal zone to flood hazards.

Chapter 4 addresses the second challenge identified in chapter 2, analysing land use change dynamics and societal impacts of flooding in a flood risk study. The construction of polders significantly modified the pattern of flooding, leading to substantial land use changes in the coastal region of Bangladesh. The chapter presents a framework to model dynamics of the land use changes and flood risk to estimate their impacts on poverty. Analysing historical land use changes, a combined Logistic Regression, Markov Chain, and Cellular Automata model is established to predict future land use. A spatial statistics model is developed to estimate poverty, in terms of the Wealth Index (WI), incorporating land use change, flood risk, and other socio-economic as well as spatial indicators. Flood risk is found to be positively correlated with land use change. Despite consistent national GDP growth in Bangladesh in recent years, the rate of increase of WI is likely to be low in the future because flood risk and patterns of LULC change have a negative effect on WI.

To address challenges in understanding the impacts of future flood interventions, chapter 5 provides an ex-ante analysis of Tidal River Management (TRM). TRM has been adopted in an attempt to address the worsening impacts of pluvial flooding, salinity, and siltation in riverbeds, by restoring sedimentation in low-lying. But this measure yielded both positive and negative impacts on local communities and the environment. The chapter

develops a flood susceptibility model to estimate the annual probability of flooding. A GIS-based suitability analysis has been performed to identify places suitable for implementing TRM, where sediment deposition is simulated if TRM were to be implemented. Flood susceptibility in suitable areas was compared between pre- and post-TRM implementation scenarios. The chapter estimates the extent to which TRM could restore land elevation in identified locations. It also shows the extent to which an uninterrupted implementation of TRM could help to alleviate flood susceptibility in the region.

6.2. Research contributions

This thesis provides a framework to evaluate the impacts of structural (polders) and nature-based (Tidal River Management (TRM)) flood interventions. In doing so, quantified evidence is presented. The main research contributions achieved within this thesis are summarised in the following paragraphs:

A new methodology for classifying historical flood events is presented, which combined both the remote sensing data-based flood observation and hydrometeorological gauge records. Remote sensing technology provides a powerful and inexpensive tool to detect the spatial extent of flooding events (Malinowski et al. 2015). Many recent studies have focused on monitoring flooding events using remote sensing techniques (Memon et al. 2015, Malinowski et al. 2015, Jain et al. 2005). However, in the case of coastal flooding, particularly in a complex delta system where floods occur from multiple sources, identification of the extent of inundation does not provide a comprehensive understanding of flood processes. This research integrates remote sensing-based flood observations with hydrological gauge records to classify flood events into various types (i.e. pluvial, fluvio-tidal, and surge).

To assess the impacts of polders on the frequency and extent of flooding, a 'no-embankment' counterfactual scenario is developed. Studies that concentrated on the ex-post

evaluation of structural flood interventions have conducted empirical assessments, primarily by comparing hydrological records between the pre- and post-implementation scenarios (Choudhury et al. 2004, Heine and Pinter 2012). Other studies conducted a benefit-cost analysis to evaluate flood investments (Ramirez et al. 1988, Palanisami and Easter 1984). The availability of a long-time series records hydrological observations is the prerequisite to conduct such studies. Regions where such empirical data are unavailable, as is the case of the coastal region of Bangladesh, carrying out an ex-post evaluation of flood defences is a challenging task. By modelling different forms of inundation to estimate what flooding might have been had the polders not been constructed, this research has provided insights into the polders' effectiveness.

In this research, flood risks have been estimated for dynamic changes of land use. It has been widely recognised that the pattern of land use influences flood risk by impacting local hydrology (Wheater and Evans 2009, Szwagrzyk et al. 2018, McColl and Aggett 2007) as well as influencing exposure of the property to flood risk (Lee and Brody 2018). Whilst many studies have considered the general impact of land use on flooding, there are fewer studies attempted to capture the dynamics of land use change in flood risk estimation (Szwagrzyk et al. 2018, Mitsova 2014). This research quantifies the influence of current and potential future land use on flood risk.

This research also estimates the societal impacts of flood hazards. Floods impact on society could range from direct to indirect as well as from tangible to intangible impacts (Bubeck et al. 2017, Penning-Rowsell et al. 2005). In section 2.3.4 and section 4.1, it has been discussed that the coexistence of flooding and poverty could create a poverty trap (Borgomeo et al. 2017, Islam et al. 2015). The damages caused by recurring flood events can lower quality of life in the communities. On the other hand, poverty increases flood vulnerability (Dube et al. 2018). The influence of flooding on poverty in a complex delta

system is poorly understood. Existing studies related to flooding and poverty are mostly qualitative, with a few studies have applied quantitative approaches to estimate the negative influence of flooding on poverty (Borgomeo et al. 2017, Akter and Mallick 2013, Brouwer et al. 2007). However, there is a lack of quantified evidence on the spatial relationship of flood risk and poverty. This research presents a novel approach to quantify the spatio-temporal change of poverty in relation to land use change and flood risk.

Chapter 2 discusses the implications of the ex-ante evaluation of flood intervention in understanding the potential impacts of future flood interventions. The chapter also highlights various challenges in carrying out such an analysis. The multifaceted impacts of flood interventions on floodplain geomorphology, hydrology, and anthropogenic environments (Hupp et al. 2009, Gergel et al. 2002, Morrison et al. 2018, Steinfeld and Kingsford 2013) create challenges in conducting the ex-ante evaluation. In the case of coastal Bangladesh, although evidence indicates that TRM brings positive impacts in alleviating pluvial flooding problem in the embanked regions, poor selection of sites and unplanned operation hindered its success (Talchabhadel et al. 2018a, Gain et al. 2017). Although a few studies focused on assessing the impact on TRM on agricultural production (Masud et al. 2020), the impacts of TRM on the floodplain geomorphology and hydrology are largely unknown. The current research presents a novel approach to optimise TRM sites. A modelling approach is proposed which integrates simulated sediment deposition in a flood susceptibility model to quantify the impacts of TRM for flood alleviation.

6.3. Policy implications

The main goal of this thesis is to quantify the effectiveness of different coastal flood interventions, enabling policymakers to make scientifically informed decisions, particularly in prioritising coastal flood risk management options. The outcomes of three articles,

presented in this thesis, yield different policy recommendations which could be useful for governments, engineers, and planners.

6.3.1. Prioritising polders for implementing alternative adaptation strategies

The Government of Bangladesh has adopted the Bangladesh Delta Plan (BDP) 2100 where 'coastal zone and polder management' is one of the 19 thematic studies conducted while formulating the plan. The BDP identifies complex flooding processes as one of the major factors responsible for various coastal issues such as environmental degradation and loss of livelihoods of coastal inhabitants. One of the objectives of this thematic study is to scientifically evaluate existing problems related to polders (Khan 2018).

Chapter 3 of this thesis provides empirical evidence for both the beneficial and harmful impacts of polder construction. In this chapter, the effectiveness of polders is evaluated for three different types of flooding. It characterises polders according to their effectiveness in withstanding against different types of flooding. The findings of this chapter emphasise the need for developing adaptation plans in relation to the nature of flooding. For instance, a few polders were unable to withstand against major historical fluvio-tidal and surge induced flooding. Recognising the need for strengthening the coastal embankments, existing initiatives such as the Coastal Embankment Improvement Project (CEIP), funded by the World Bank, aims to rehabilitate and/or reconstructing polders that are prone to damages during flood events. This type of approach is, however, subject to a large investment. The spatial information of polders' effectiveness provided in the chapter would be useful in prioritising areas for such large infrastructure investment under the CEIP. Chapter 3 also identifies polders prone to pluvial flood hazard, which is one of the major issues inhibiting long-term development prospects in the south western coastal region. The identified pluvial flood-prone polders could be selected for implementing complementary

adaptation measures, such as TRM (see section 6.3.3) and land use planning (see section 6.3.2), to the structural flood control system.

6.3.2. Developing land use plans and poverty alleviation policies

For the last two decades, the Government of Bangladesh has been aiming to formulate an efficient coastal management plan, focusing on land use planning. To ensure comprehensive coastal management, the Integrated Coastal Zone Management Plan (ICZMP) was formulated in 1999 (MoWR 1999). The ICZMP then led to the formulation of the Coastal Zone Policy (CZP) in 2005 and the Coastal Development Strategy (CDS) in 2006. The CZP primarily aimed at reducing poverty and developing sustainable livelihoods, addressing complex issues in the coastal region, whereas the CDS focused on developing a coastal land use plan (MoWR 2005). Implementation of these policies was however static, which is reportedly associated with a lack of scientific knowledge on the vulnerability and hazard (Parvin et al. 2008), as well as, a lack of political stability and funds (Paul and Rashid 2017). Together, a lack of coordination among different sectors/agencies, several of the initiatives failed to address complex coastal systems and issues comprehensively (Iftekhar 2006). More recently, The Ministry of Land of Bangladesh has undertaken the Coastal Land Zoning projects at a few pilot sub-districts (*Upazila*). Unplanned conversion of coastal lands and damage of land uses due to natural hazards, particularly coastal flooding, have been identified as major issues contributing to the degradation of land resources (Mia et al. 2011).

Chapter 4 of this thesis highlights that a lack of risk-oriented residential development, in addition to a significant transformation of agricultural lands to aquaculture use, is potentially increasing flood risk, restricting the growth of the Wealth Index (WI) in the coastal region. Evidence from the recent studies indicates that shrimp farming has no significant association with poverty, as farms are mostly owned by external investors (Johnson et al. 2016). The relevant public organization should consider the dynamics of land

use change, flood risk, and poverty while developing potential future land use plans. This thesis provides spatial information on flood risk and land use changes, as well as, their association with poverty, which could inform stakeholders such as the Ministry of Land in identifying areas required land use policy intervention. Chapter 4 proposes a methodology to assess poverty in relation to flood risk as well as land use change. The results help identify areas with higher-level poverty at present-day and future scenarios. The method of spatiotemporal assessment of poverty presented in the chapter would act as a decision support system for national bodies in developing local level poverty alleviation plans, which is simultaneously transferable to other areas along with coastal Bangladesh.

6.3.3. Implementing Tidal River Management (TRM)

TRM has been a widely discussed topic in recent years in both research and practice, perceived as an alternative to structural flood control systems (Gain et al. 2017, Seijger et al. 2019). However, outcomes of this research suggest that TRM, which has potentials to alleviate pluvial flooding problems by restoring sedimentation in low-lying 'beels', can complement the hard engineering. TRM has been prioritised in the BDP as a measure for alleviating various issues resulting from increased pluvial flooding (Khan 2018). The results of Chapter 5 in this thesis indicate that TRM can bring long-term benefits alleviating pluvial flood susceptibility in the embanked area. However, this measure is not applicable everywhere, as the suitability of TRM sites depends on the tidal prism, type of land use, amount of sediment supply, salinity level in the river water, and size of the 'beel'. Therefore, the identification of suitable sites should be the prerequisite of TRM projects. This thesis develops an approach to selecting suitable TRM sites. Such an approach could be a useful guide for national organizations such as the Bangladesh Water Development Board (BWDB), who are responsible for selecting TRM sites and implementing this measure.

6.4. Limitations and future research

Despite the contribution made in this thesis, a comprehensive scientific understanding of complex coastal systems and their effects on flood interventions is still a challenging task. When interpreting the findings obtained in this thesis, various sources of uncertainty related to the modelling of flood inundations, flood risks, land use change, poverty, and TRM have been discussed. The works presented in this thesis could be expanded in different directions so that those uncertainties could be minimised. Some specific examples of future research direction and activities are given in the following paragraphs:

In chapter 3, the identification of historically flooded areas from the Landsat satellite imagery is subject to uncertainty. The presence of cloud cover during the monsoon period impelled this research to compare water surfaces between pre and post-monsoon periods, to detect flood inundations. This uncertainty could be addressed by using satellite-borne Synthetic Aperture Radar (SAR) images, as they have cloud-penetrating capability (Hoque et al. 2011). Sentinel 10–20 m spatial resolution images are a type of open access SAR data, and observation scenario maps are available since September 2014 (Rahman and Di 2017). For flood observation after 2014, Sentinel data could be used for mapping the areal extent of flooding.

The simulation of flood inundation for counterfactual scenario is also subject to uncertainty. Several assumptions and simplifications have been made to develop this scenario. For instance, 'without' polders, only geomorphological changes have been incorporated in the model. While establishing the pluvial flood model, the unavailability of drainage network impelled this research to identify the channels from satellite images. Pluvial flooding is modelled for scenarios where water leaves polders by evapotranspiration and drainage channels, as well as only by evapotranspiration. The research found that the

later scenario explains closely the observed inundation obtained from remote sensing data. For fluvio-tidal and storm surge modelling, various sources of uncertainties are discussed in Haque et al. (2018). The uncertainties related to the modelling of flood inundation could be minimised with properly validated hydraulic drainage network model for pluvial flooding (Jamali et al. 2018), and hydrodynamic model for fluvio-tidal and surge induced flooding (Wing et al. 2017, Wing et al. 2019).

In chapter 4, the results of land use change model indicate that the study area is likely to experience a transformation of lands from agriculture to aquaculture use in the near future, following a trend of the historical land use change. Although this research shows that such a change influences negatively the Wealth Index, its impact on human lives has not been quantified comprehensively. The existing studies have demonstrated that intensive aquaculture and subsequent salinity intrusion results in poverty, promoting food insecurity, rural unemployment, social unrest, conflicts and forced migration (Johnson et al. 2016). In this research, land use change model does not include exogenous covariates such as individuals' behaviour and government actions. Future research could consider the agent-based modelling (ABM) approach, which can incorporate individual-related factors in land use change modelling (Arsanjani et al. 2013). In this chapter, flood risk assessment is carried out to estimate direct economic damage due to floods of various return periods. Results from the existing studies show that the failures of critical infrastructure systems, such as transportation, production, and energy during a flood event could cause indirect damage (Koks et al. 2019). In future research, the indirect impacts of flooding could be considered in estimating flood risk.

The scope of chapter 5 is limited in assessing the potential impact of TRM for flood alleviation, considering an uninterrupted implementation of this approach. However, implementation hurdles such as social unrest, conflict, and issues related to compensation

are some of the major issues restricting success of TRM (Gain et al. 2017). Besides, the present research optimises TRM sites using biophysical parameters; various socioeconomic parameters could also influence the success of TRM (Masud et al. 2018). In this thesis, the cost-benefit analysis of TRM has not been conducted. This approach is likely to create short term unemployment in the agricultural sector, as it makes areas unsuitable for crop production. Therefore, institutional strengthening is the key to the uninterrupted implementation of TRM, as well as, in ensuring necessary compensation for the poor and marginalised farmers. The implementation agency will need to ensure a clear agreement with the stakeholders, especially the landowners, through a participatory approach (Gain et al. 2017). Nonetheless, this approach would be beneficial in the long run in suitable areas. For instance, Masud et al. (2020) estimated financial benefits of TRM (after 5-15 years of implementing this approach) in term of increased agricultural productivity in two 'beels' where this approach has been implemented and compared the results with nine non-TRM 'beels'. They found that TRM sites yield a greater agricultural production per unit area than non-TRM sites, due to a reduction in waterlogging.

TRM involves active sediment management, implying that an adequate supply of sediment is prerequisite to implement this measure. However, the western part of the GBM delta is likely to be a sediment starved region by the end of the twenty-first century, primarily because of the projected socioeconomic changes in the catchment, together with the plan of constructing new water infrastructure (e.g. reservoir) in the upstream river (Darby et al. 2020). Further investigation on sediment supply at the river basin scale in south western coast is necessary to analyse the feasibility of future TRM projects. Nonetheless, TRM shows potential in alleviating pluvial flooding problems within the embanked areas, which would help to increase agricultural production and improving socioeconomic conditions of the inhabitants.

Finally, future research should focus on developing systems that promote and enhance adaptation and resilience in the Bangladesh coastal zone. Increased collection of coastal observation data using the latest technologies available (e.g. remote sensing, artificial intelligence) as well as ground observation is quintessential. Development of validated models through collaborative environments would minimise uncertainties that existing modelling frameworks contain. To manage challenges associated with the dynamics of climate change, the development of a diagnostic and analytical tool is essential to assist in adaptive planning and decision-making.

6.5. Transferrable lessons and concluding remarks

Coastal flood management in active delta systems such as Bangladesh coastal zone is a challenging task. In Bangladesh, the coastal embankments had a profound influence on the geomorphological, hydrological, and anthropogenic environments, creating challenges in understanding the effectiveness of different flood interventions, types of knowledge which are essential to managing future flood risk. Findings of this research underline the importance of implementing multiple types of flood adaption options, ranging from structural interventions to nature-based solutions.

Whilst this current research focuses on the south western embanked area, knowledge obtained from this would be transferrable to other areas along Bangladesh's coast, as well as, in deltaic coasts with similar geomorphological and hydrological settings. Deltas where a substantial proportion of areas are below the sea level, as well as, areas prone to cyclone induced storm surges, would receive a certain degree of benefits from coastal embankments in terms of protecting areas from inundation. Syvitski et al. (2009) classified many of those regions as 'Deltas in peril' and 'Deltas in greater peril'. However, it should be noted that whilst floodplain engineering involves major investments, it could result in land subsidence, which has already been an issue in those deltas. Therefore, carrying out an ex-ante evaluation

of potential future flood management options is quintessential. Sustainable management of water and sediment in deltas must be considered in future delta management plans. Policies related to the transboundary river should be reviewed to ensure adequate flow and sediment supply in deltas located in the downstream. Therefore, geopolitical measures should be combined with the management of biophysical and socioeconomic environments to achieve long-term success in comprehensive flood management in deltas.

Appendix D: Co-author Paper Contribution Statements

The following statements provide details of the contributions made by co-authors to papers included within this thesis:

Certificate of Authorship of Dissertation Work for Mohammed Sarfaraz Gani Adnan

To the Director of Graduate Studies,
School of Geography and the Environment,
University of Oxford.

I hereby certify that Mohammed Sarfaraz Gani Adnan carried out the majority of the work contained in the articles described below, which form part of his DPhil thesis:

- Have coastal embankments reduced flooding in Bangladesh?
- The effects of changing land use and flood hazard on poverty in coastal Bangladesh
- The potential of Tidal River Management for flood alleviation in South Western Bangladesh

Signature:

Date: 23 March 2020

Professor Jim Hall
Professor of Climate and Environmental Risk
Environmental Change Institute, School of Geography and the Environment
University of Oxford
South Parks Road
Oxford OX1 3QY
United Kingdom
Email: jim.hall@ouce.ox.ac.uk

Certificate of Authorship of Dissertation Work for Mohammed Sarfaraz Gani Adnan

To the Director of Graduate Studies,
School of Geography and the Environment,
University of Oxford.

I hereby certify that Mohammed Sarfaraz Gani Adnan carried out the majority of the work contained in the article described below, which form part of his DPhil thesis:

- Have coastal embankments reduced flooding in Bangladesh?

Signature:

Date: Feb 8, 2020

Professor Anisul Haque
Institute of Water and Flood Management
Bangladesh University of Engineering and Technology
Dhaka 1000, Bangladesh
Email: anisul@iwfm.buet.ac.bd

Certificate of Authorship of Dissertation Work for Mohammed Sarfaraz Gani Adnan

To the Director of Graduate Studies,
School of Geography and the Environment,
University of Oxford.

I hereby certify that Mohammed Sarfaraz Gani Adnan carried out the majority of the work contained in the article described below, which form part of his DPhil thesis:

- The effects of changing land use and flood hazard on poverty in coastal Bangladesh

Signature:

Date: 21st February 2020

Abu Yousuf Md Abdullah
School of Public Health and Health Systems
Faculty of Applied Health Sciences
University of Waterloo,
200 University Avenue West, Waterloo
ON N2L 3G1, Canada
Email: aymabdullah@uwaterloo.ca

Certificate of Authorship of Dissertation Work for Mohammed Sarfaraz Gani Adnan

To the Director of Graduate Studies,
School of Geography and the Environment,
University of Oxford.

I hereby certify that Mohammed Sarfaraz Gani Adnan carried out the majority of the work contained the article described below, which is part of his DPhil thesis. The title of the article is as follows:

- The effects of changing land use and flood hazard on poverty in coastal Bangladesh

Signature:

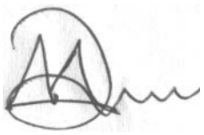

Date: 21 February 2020

Dr Ashraf Dewan
Kent Street, Bentley 6102
School of Earth and Planetary Sciences (EPS), Curtin University
Perth, Western Australia
Phone: 08 9266 4930
Email: A.Dewan@curtin.edu.au

Certificate of Authorship of Dissertation Work for Mohammed Sarfaraz Gani Adnan

To the Director of Graduate Studies,
School of Geography and the Environment,
University of Oxford.

I hereby certify that Mohammed Sarfaraz Gani Adnan carried out the majority of the work contained in the article described below, which form part of his DPhil thesis:

- The potential of Tidal River Management for flood alleviation in South Western Bangladesh

Signature:

Date: March 17, 2020

Dr. Rocky Talchabhadel
Disaster Prevention Research Institute
Kyoto University, Japan
Email: rocky@uh31.dpri.kyoto-u.ac.jp

Certificate of Authorship of Dissertation Work for Mohammed Sarfaraz Gani Adnan

To the Director of Graduate Studies,
School of Geography and the Environment,
University of Oxford.

I hereby certify that Mohammed Sarfaraz Gani Adnan carried out the majority of the work contained in the article described below, which form part of his DPhil thesis:

- The potential of Tidal River Management for flood alleviation in South Western Bangladesh

Signature:

Date: March 18, 2020

Professor Hajime Nakagawa
Disaster Prevention Research Institute
Kyoto University, Japan
Email: nakagawa@uh31.dpri.kyoto-u.ac.jp

Bibliography

Abdullah, A. Y. M., *et al.* 2018. Modeling soil salinity using direct and indirect measurement techniques: A comparative analysis. *Environmental Development,* 29, 67-80.

Abdullah, A. Y. M., *et al.* 2019. Spatio-Temporal Patterns of Land Use/Land Cover Change in the Heterogeneous Coastal Region of Bangladesh between 1990 and 2017. *Remote Sensing,* 11(7), 790.

Abedin, M. A. and Shaw, R. 2015. The role of university networks in disaster risk reduction: Perspective from coastal Bangladesh. *International Journal of Disaster Risk Reduction,* 13, 381-389.

ADB, 2007. *Bangladesh: Khulna-Jessore Drainage Rehabilitation Project - Project Performance Evaluation Report.* Bangladesh: Asian Development Bank

Adnan, M. S. G., *et al.* 2019a. The use of watershed geomorphic data in flash flood susceptibility zoning: a case study of the Karnaphuli and Sangu river basins of Bangladesh. *Natural Hazards,* 99(1), 425–448.

Adnan, M. S. G., Haque, A. and Hall, J. W. 2019b. Have coastal embankments reduced flooding in Bangladesh? *Science of the Total Environment,* 682, 405-416.

Adnan, M. S. G., *et al.* 2020. The potential of Tidal River Management for flood alleviation in South Western Bangladesh. *Science of the Total Environment,* 731.

Adnan, S. G. and Kreibich, H. 2016. An evaluation of disaster risk reduction (DRR) approaches for coastal delta cities: a comparative analysis. *Natural Hazards,* 83(2), 1257-1278.

Ahmed, B., *et al.* 2013. Simulating land cover changes and their impacts on land surface temperature in Dhaka, Bangladesh. *Remote Sensing,* 5(11), 5969-5998.

Ahmed, K. R. and Akter, S. 2017. Analysis of landcover change in southwest Bengal delta due to floods by NDVI, NDWI and K-means cluster with landsat multi-spectral

surface reflectance satellite data. *Remote Sensing Applications: Society and Environment,* 8, 168-181.

Ahmed, S. 2018. Shrimp farming at the interface of land use change and marginalization of local farmers: critical insights from southwest coastal Bangladesh. *Journal of Land Use Science,* 13(3), 251-258.

Akber, M. A.*, et al.* 2017. Changes of shrimp farming in southwest coastal Bangladesh. *Aquaculture International,* 25(5), 1883-1899.

Akber, M. A.*, et al.* 2018. Impact of land use change on ecosystem services of southwest coastal Bangladesh. *Journal of Land Use Science,* 13(3), 238-250.

Akter, S. and Mallick, B. 2013. The poverty–vulnerability–resilience nexus: Evidence from Bangladesh. *Ecological Economics,* 96, 114-124.

Alam, M. S., Sasaki, N. and Datta, A. 2017. Waterlogging, crop damage and adaptation interventions in the coastal region of Bangladesh: A perception analysis of local people. *Environmental Development,* 23, 22-32.

Ali, L., 2002. *An integrated approach for the improvement of flood control and drainage schemes in the coastal belt of Bangladesh.* CRC Press.

Althuwaynee, O. F.*, et al.* 2014. A novel ensemble bivariate statistical evidential belief function with knowledge-based analytical hierarchy process and multivariate statistical logistic regression for landslide susceptibility mapping. *Catena,* 114, 21-36.

Amir, M. S. I. I. and Khan, M. S. A., 2019. An Innovative Technique of Tidal River Sediment Management to Solve the Waterlogging Problem in Southwestern Bangladesh. *Coastal Management.* Elsevier, 165-199.

Apel, H.*, et al.* 2009. Flood risk analyses - How detailed do we need to be? *Natural Hazards,* 49(1), 79-98.

Apel, H.*, et al.* 2006. A Probabilistic Modelling System for Assessing Flood Risks. *Natural Hazards,* 38(1), 79-100.

Arabameri, A.*, et al.* 2019. A comparison of statistical methods and multi-criteria decision making to map flood hazard susceptibility in Northern Iran. *Science of the Total Environment,* 660, 443-458.

Arsanjani, J. J.*, et al.* 2013. Integration of logistic regression, Markov chain and cellular automata models to simulate urban expansion. *International Journal of Applied Earth Observation and Geoinformation,* 21(1), 265-275.

Arto, I.*, et al.*, 2020. Delta Economics and Sustainability. *Deltas in the Anthropocene.* Springer, 179-200.

Arto, I.*, et al.* 2019. The socioeconomic future of deltas in a changing environment. *Science of the Total Environment,* 648, 1284-1296.

Auerbach, L. W.*, et al.* 2015. Flood risk of natural and embanked landscapes on the Ganges-Brahmaputra tidal delta plain. *Nature Climate Change,* 5(2), 153-157.

Awal, M. 2014. Water logging in south-western coastal region of Bangladesh: local adaptation and policy options. *Science Postprint,* 1(1), e00038.

Bai, S.*, et al.* 2011. GIS-based rare events logistic regression for landslide-susceptibility mapping of Lianyungang, China. *Environmental Earth Sciences,* 62(1), 139-149.

Bamberg, S.*, et al.* 2017. Threat, coping and flood prevention – A meta-analysis. *Journal of Environmental Psychology,* 54, 116-126.

Bangalore, M., Smith, A. and Veldkamp, T. 2019. Exposure to Floods, Climate Change, and Poverty in Vietnam. *Economics of Disasters and Climate Change,* 3(1), 79-99.

Bannari, A.*, et al.*, Detection of Areas Associated with Flash Floods and Erosion Caused by Rainfall Storm Using Topographic Attributes, Hydrologic Indices, and GIS. In:

Pirasteh, S. and Li, J., ed., 2017 Cham: Global Changes and Natural Disaster Management: Geo-information Technologies, 155-174.

Bates, P. D.*, et al.* 2005. Simplified two-dimensional numerical modelling of coastal flooding and example applications. *Coastal Engineering,* 52(9), 793-810.

Bates, P. D., Pappenberger, F. and Romanowicz, R. J., 2014. Uncertainty in flood inundation modelling. *Applied Uncertainty Analysis for Flood Risk Management.* 232-269.

BBS, 2015. *Bangladesh Disaster-related Statistics 2015. Climate Change and Natural Disaster Perspectives* Dhaka, Bangladesh: Bangladesh Bureau of Statistics (BBS), Ministry of Planning.

Beckers, A.*, et al.* 2013. Contribution of land use changes to future flood damage along the river Meuse in the Walloon region. *Natural Hazards and Earth System Sciences,* 13, 2301-2318.

Beven, K. and Hall, J., 2014. *Applied uncertainty analysis for flood risk management.* Imperial College Press.

Bhuiyan, M. J. A. N. and Dutta, D. 2012. Analysis of flood vulnerability and assessment of the impacts in coastal zones of Bangladesh due to potential sea-level rise. *Natural Hazards,* 61(2), 729-743.

Bilskie, M.*, et al.* 2014. Dynamics of sea level rise and coastal flooding on a changing landscape. *Geophysical Research Letters,* 41(3), 927-934.

Bonacci, O., Ljubenkov, I. and Roje-Bonacci, T. 2006. Karst flash floods: an example from the Dinaric karst (Croatia). *Nat. Hazards Earth Syst. Sci.,* 6(2), 195-203.

Borgomeo, E., Hall, J. W. and Salehin, M. 2017. Avoiding the water-poverty trap: insights from a conceptual human-water dynamical model for coastal Bangladesh. *International Journal of Water Resources Development*, 1-23.

Bouwer, L.*, et al.* 2009. Inundation scenarios for flood damage evaluation in polder areas.

Brammer, H. 1990. Floods in Bangladesh: I. Geographical background to the 1987 and 1988 floods. *Geographical Journal,* 156(1), 12-22.

Brammer, H. 2014. Bangladesh's dynamic coastal regions and sea-level rise. *Climate Risk Management,* 1, 51-62.

Brouwer, R.*, et al.* 2007. Socioeconomic Vulnerability and Adaptation to Environmental Risk: A Case Study of Climate Change and Flooding in Bangladesh. *Risk Analysis,* 27(2), 313-326.

Brown, S. and Nicholls, R. J. 2015. Subsidence and human influences in mega deltas: The case of the Ganges–Brahmaputra–Meghna. *Science of the Total Environment,* 527-528, 362-374.

Bubeck, P.*, et al.* 2013. Detailed insights into the influence of flood-coping appraisals on mitigation behaviour. *Global Environmental Change,* 23(5), 1327-1338.

Bubeck, P., Otto, A. and Weichselgartner, J., 2017. Societal impacts of flood hazards. *Oxford Research Encyclopedia of Natural Hazard Science.*

Cazcarro, I.*, et al.* 2018. Biophysical and socioeconomic state and links of deltaic areas vulnerable to climate change: Volta (Ghana), Mahanadi (India) and Ganges-Brahmaputra-Meghna (India and Bangladesh). *Sustainability,* 10(3), 893.

CEIP, 2013. *Technical feasibility studies and detailed design for Coastal Embankment Improvement Programme (CEIP).* Dhaka: Ministry of Water Resources, Government of the People's Republic of Bangladesh.

Chandler, R.*, et al.* 2014. Uncertainty in rainfall inputs. *Applied Uncertainty Analysis for Flood Risk Management, edited by: Beven, KJ and Hall, JW, Imperial College Press: London*, 101-152.

Chatterton, J., Penning-Rowsell, E. and Priest, S., 2014. The many uncertainties in flood loss assessments. *Applied Uncertainty Analysis for Flood Risk Management.* World Scientific, 335-356.

Chen, J., Hill, A. A. and Urbano, L. D. 2009. A GIS-based model for urban flood inundation. *Journal of Hydrology,* 373(1), 184-192.

Chen, W. B. and Liu, W. C. 2014. Modeling flood inundation induced by river flow and storm surges over a river basin. *Water (Switzerland),* 6(10), 3182-3199.

Childs, C. 2004. Interpolating surfaces in ArcGIS spatial analyst. *ArcUser, July-September,* 3235, 569.

Choi, W., Pan, F. and Wu, C. 2017. Impacts of climate change and urban growth on the streamflow of the Milwaukee River (Wisconsin, USA). *Regional Environmental Change,* 17(3), 889-899.

Choudhury, N. Y., Paul, A. and Paul, B. K. 2004. Impact of costal embankment on the flash flood in Bangladesh: A case study. *Applied Geography,* 24(3), 241-258.

Church, J. A.*, et al.*, 2013. *Sea level change.* PM Cambridge University Press.

Coles, S.*, et al.*, 2001. *An introduction to statistical modeling of extreme values.* Springer.

Corner, R. J., Dewan, A. M. and Chakma, S., 2014. Monitoring and prediction of land-use and land-cover (LULC) change. *Dhaka megacity.* Springer, 75-97.

Croissant, Y. and Croissant, M. Y. 2018. Package 'mlogit'.

Darby, S. E.*, et al.*, 2020. Fluvial sediment supply and relative sea-level rise. *Deltas in the Anthropocene.* Springer, 103-126.

Dasgupta, A. 2007. Floods and poverty traps: Evidence from Bangladesh. *Economic and Political Weekly*, 3166-3171.

Dasgupta, S.*, et al.* 2015. Climate change and soil salinity: The case of coastal Bangladesh. *Ambio,* 44(8), 815-826.

Davis, J., 2002. *Statistics and Data Analysis in Geology - 3rd Edition.* USA: John Wiley and Sons.

Dawson, R. J.*, et al.* 2011. Assessing the effectiveness of non-structural flood management measures in the Thames Estuary under conditions of socio-economic and environmental change. *Global Environmental Change,* 21(2), 628-646.

Day, J. W.*, et al.* 2016. Approaches to defining deltaic sustainability in the 21st century. *Estuarine, coastal and shelf science,* 183, 275-291.

De Bono, A. and Chatenoux, B., 2014. *A global exposure model for GAR 2015.* Geneva: United Nations Office for Disaster Risk Reduction (UNISDR).

Deb, M. and Ferreira, C. M. 2017. Potential impacts of the Sunderban mangrove degradation on future coastal flooding in Bangladesh. *Journal of Hydro-Environment Research,* 17, 30-46.

Demirkesen, A.*, et al.* 2007. Coastal flood risk analysis using Landsat-7 ETM+ imagery and SRTM DEM: A case study of Izmir, Turkey. *Environmental Monitoring and Assessment,* 131(1-3), 293-300.

Dewan, A., 2013. *Floods in a megacity: geospatial techniques in assessing hazards, risk and vulnerability.* Springer.

Dewan, A. M. and Yamaguchi, Y. 2009. Land use and land cover change in Greater Dhaka, Bangladesh: Using remote sensing to promote sustainable urbanization. *Applied Geography,* 29(3), 390-401.

Di Baldassarre, G.*, et al.* 2017. Drought and flood in the Anthropocene: feedback mechanisms in reservoir operation. *Earth System Dynamics,* 8(1), 1-9.

Di Baldassarre, G.*, et al.* 2010. Flood-plain mapping: a critical discussion of deterministic and probabilistic approaches. *Hydrological Sciences Journal–Journal des Sciences Hydrologiques,* 55(3), 364-376.

Di Baldassarre, G., *et al.* 2013. Socio-hydrology: conceptualising human-flood interactions. *Hydrol. Earth Syst. Sci.,* 17(8), 3295-3303.

Diaz-Nieto, J., *et al.* 2011. GIS Water-Balance Approach to Support Surface Water Flood-Risk Management. *Journal of Hydrologic Engineering,* 17(1), 55-67.

Dingman, S. L., 2002. *Physical hydrology.* 2nd Edition ed.: Waveland Press.

Dube, E., Mtapuri, O. and Matunhu, J. 2018. Flooding and poverty: Two interrelated social problems impacting rural development in Tsholotsho district of Matabeleland North province in Zimbabwe. *Jàmbá: Journal of Disaster Risk Studies,* 10(1), 1-7.

Dutta, D., *et al.* 2015. Assessment of ecological disturbance in the mangrove forest of Sundarbans caused by cyclones using MODIS time-series data (2001–2011). *Natural Hazards,* 79(2), 775-790.

Ebert, A., *et al.* 2010. Socio-environmental change and flood risks: The case of Santiago de Chile. *Erdkunde*, 303-313.

Falconer, R., *et al.* 2009. Pluvial flooding: new approaches in flood warning, mapping and risk management. *Journal of Flood Risk Management,* 2(3), 198-208.

Feng, G., *et al.* 2016. Trend analysis and forecast of precipitation, reference evapotranspiration, and rainfall deficit in the Blackland Prairie of Eastern Mississippi. *Journal of Applied Meteorology and Climatology,* 55(7), 1425-1439.

Fox, J., *et al.* 2018. Package 'car'.

Gain, A. K., *et al.* 2017. Tidal river management in the south west Ganges-Brahmaputra delta in Bangladesh: Moving towards a transdisciplinary approach? *Environmental Science and Policy,* 75, 111-120.

Gain, A. K. and Schwab, M. 2012. An assessment of water governance trends: the case of Bangladesh. *Water Policy,* 14(5), 821-840.

Gao, Y., *et al.* 2014. Risk assessment of tropical storm surges for coastal regions of China. *Journal of Geophysical Research: Atmospheres,* 119(9), 5364-5374.

Gergel, S. E., Dixon, M. D. and Turner, M. G. 2002. Consequences of human-altered floods: levees, floods, and floodplain forests along the Wisconsin River. *Ecological applications,* 12(6), 1755-1770.

Gilleland, E. and Katz, R. W. 2016. Extremes 2.0: an extreme value analysis package in r. *Journal of Statistical Software,* 72(8), 1-39.

Hall, J. W., 2014. Flood Risk Management: Decision Making Under Uncertainty. *In:* Beven, K. and Hall, J. eds. *Applied Uncertainty Analysis for Flood Risk Management.* London: Imperial College Press, 3-24.

Hall, J. W., Berkhout, F. and Douglas, R. 2015. Responding to adaptation emergencies. *Nature Climate Change,* 5(1), 6-7.

Hall, J. W., *et al.* 2003a. A methodology for national-scale flood risk assessment. *Proceedings of the Institution of Civil Engineers: Water and Maritime Engineering,* 156(3), 235-247.

Hall, J. W., *et al.* 2003b. Quantified scenarios analysis of drivers and impacts of changing flood risk in England and Wales: 2030–2100. *Global Environmental Change Part B: Environmental Hazards,* 5(2), 51-65.

Hall, J. W., Harvey, H. and Manning, L. J. 2019. Adaptation thresholds and pathways for tidal flood risk management in London. *Climate Risk Management,* 24, 42-58.

Hall, J. W., *et al.* 2003c. Integrated Flood Risk Management in England and Wales. *Natural Hazards Review,* 4(3), 126-135.

Hall, J. W., *et al.* 2006. Impacts of climate change on coastal flood risk in England and Wales: 2030–2100. *Philosophical Transactions of the Royal Society A: Mathematical, Physical and Engineering Sciences,* 364(1841), 1027-1049.

Hallegatte, S., *et al.* 2013. Future flood losses in major coastal cities. *Nature Climate Change,* 3(9), 802.

Hallegatte, S., *et al.* 2011. Assessing climate change impacts, sea level rise and storm surge risk in port cities: a case study on Copenhagen. *Climatic change,* 104(1), 113-137.

Hanson, S., *et al.* 2011. A global ranking of port cities with high exposure to climate extremes. *Climatic change,* 104(1), 89-111.

Haque, A., Kay, S. and Nicholls, R. J., 2018. Present and Future Fluvial, Tidal and Storm Surge Flooding in Coastal Bangladesh. *Ecosystem Services for Well-Being in Deltas.* Springer, 293-314.

Haque, A. and Nicholls, R. J., 2018. Floods and the Ganges-Brahmaputra-Meghna Delta. *Ecosystem Services for Well-Being in Deltas.* Springer, 147-159.

Haque, A. and Rahman, M. 2016. Flow Distribution and Sediment Transport Mechanism in the Estuarine Systems of Ganges-Brahmaputra-Meghna Delta. *International Journal of Environmental Science and Development,* 7(1), 22.

Hasan, M. K., Kumar, L. and Gopalakrishnan, T. 2020. Inundation modelling for Bangladeshi coasts using downscaled and bias-corrected temperature. *Climate Risk Management,* 27, 100207.

Hazra, S., *et al.*, 2020. The Mahanadi Delta: A Rapidly Developing Delta in India. *In:* Nicholls, R. J., *et al.* eds. *Deltas in the Anthropocene.* Cham: Springer International Publishing, 53-77.

Heine, R. A. and Pinter, N. 2012. Levee effects upon flood levels: an empirical assessment. *Hydrological Processes,* 26(21), 3225-3240.

Hino, M. and Hall, J. W. 2017. Real options analysis of adaptation to changing flood risk: Structural and nonstructural measures. *ASCE-ASME Journal of Risk and Uncertainty in Engineering Systems, Part A: Civil Engineering,* 3(3), 04017005.

Hoa, L. T. V.*, et al.* 2008. Infrastructure effects on floods in the Mekong River Delta in Vietnam. *Hydrological Processes: An International Journal,* 22(9), 1359-1372.

Hoque, R.*, et al.* 2011. Flood monitoring, mapping and assessing capabilities using RADARSAT remote sensing, GIS and ground data for Bangladesh. *Natural Hazards,* 57(2), 525-548.

Hosmer Jr, D. W., Lemeshow, S. and Sturdivant, R. X., 2013. *Applied logistic regression.* John Wiley & Sons.

Hossain, M. A.*, et al.*, 2012. Climate Change and its Impacts on the Livelihoods of the Vulnerable People in the Southwestern Coastal Zone in Bangladesh. *In:* Leal Filho, W. ed. *Climate Change and the Sustainable Use of Water Resources.* Berlin, Heidelberg: Springer Berlin Heidelberg, 237-259.

Houston, D.*, et al.* 2011. Pluvial (rain-related) flooding in urban areas: the invisible hazard. *York: Joseph Rowntree Foundation*.

Huang, S.*, et al.* 2007. The effectiveness of polder systems on peak discharge capping of floods along the middle reaches of the Elbe River in Germany. *Hydrology and Earth System Sciences Discussions,* 11(4), 1391-1401.

Hui, R., Jachens, E. and Lund, J. 2016. Risk-based planning analysis for a single levee. *Water Resources Research,* 52(4), 2513-2528.

Huizinga, J., de Moel, H. and Szewczyk, W., 2017. *Global flood depth-damage functions: Methodology and the database with guidelines.* Joint Research Centre (Seville site).

Hupp, C. R., Pierce, A. R. and Noe, G. B. 2009. Floodplain geomorphic processes and environmental impacts of human alteration along coastal plain rivers, USA. *Wetlands,* 29(2), 413-429.

Huq, M.*, et al.*, 2010. *Vulnerability of Bangladesh to cyclones in a changing climate: potential damages and adaptation cost.* The World Bank.

Huq, N., *et al.* 2015. Climate change impacts in agricultural communities in rural areas of coastal Bangladesh: a tale of many stories. *Sustainability,* 7(7), 8437-8460.

Iftekhar, M., Conservation and management of the Bangladesh coastal ecosystem: overview of an integrated approach. ed. *Natural Resources Forum*, 2006, 230-237.

Ikeuchi, H., *et al.* 2017. Compound simulation of fluvial floods and storm surges in a global coupled river-coast flood model: Model development and its application to 2007 Cyclone Sidr in Bangladesh. *Journal of Advances in Modeling Earth Systems,* 9(4), 1847-1862.

Islam, G. M. T., *et al.* 2015. Implications of agricultural land use change to ecosystem services in the Ganges delta. *Journal of Environmental Management,* 161, 443-452.

Islam, M., Kotani, K. and Managi, S. 2016a. Climate perception and flood mitigation cooperation: A Bangladesh case study. *Economic Analysis and Policy,* 49, 117–133.

Islam, M. A., *et al.* 2016b. Coastal multi-hazard vulnerability assessment along the Ganges deltaic coast of Bangladesh–A geospatial approach. *Ocean & Coastal Management,* 127, 1-15.

Islam, M. A., *et al.* 2016c. Coastal multi-hazard vulnerability assessment along the Ganges deltaic coast of BangladesheA geospatial approach. *Ocean & Coastal Management,* 127, 1-15.

Islam, M. F., Bhattacharya, B. and Popescu, I. 2019. Flood risk assessment due to cyclone-induced dike breaching in coastal areas of Bangladesh. *Natural Hazards and Earth System Sciences,* 19(2), 353-368.

Jain, S. K., *et al.* 2005. Delineation of flood-prone areas using remote sensing techniques. *Water Resources Management,* 19(4), 333-347.

Jamali, B., *et al.* 2018. A rapid urban flood inundation and damage assessment model. *Journal of Hydrology,* 564, 1085-1098.

ALOS global digital surface model "ALOS world 3D-30m (AW3D30)" (2015). City: Japan Aerospace Exploration Agency (JAXA).

Johnson, F. A.*, et al.* 2016. Is shrimp farming a successful adaptation to salinity intrusion? A geospatial associative analysis of poverty in the populous Ganges–Brahmaputra–Meghna Delta of Bangladesh. *Sustainability Science,* 11(3), 423-439.

Jones, K. L.*, et al.* 2008. Surface hydrology of low-relief landscapes: Assessing surface water flow impedance using LIDAR-derived digital elevation models. *Remote Sensing of Environment,* 112(11), 4148-4158.

Jonkman, S. and Vrijling, J. 2008. Loss of life due to floods. *Journal of Flood Risk Management,* 1(1), 43-56.

Kabenge, M.*, et al.* 2017. Characterizing flood hazard risk in data-scarce areas, using a remote sensing and GIS-based flood hazard index. *Natural Hazards,* 89(3), 1369-1387.

Karamouz, M.*, et al.* 2019. Building infrastructure resilience in coastal flood risk management. *Journal of Water Resources Planning and Management,* 145(4).

Karim, M. F. and Mimura, N. 2008. Impacts of climate change and sea-level rise on cyclonic storm surge floods in Bangladesh. *Global Environmental Change,* 18(3), 490-500.

Kawasaki, A., Kawamura, G. and Zin, W. W. 2020. A local level relationship between floods and poverty: A case in Myanmar. *International Journal of Disaster Risk Reduction,* 42, 101348.

Kay, S., Caesar, J. and Janes, T., 2018. Marine Dynamics and Productivity in the Bay of Bengal. *Ecosystem Services for Well-Being in Deltas.* Springer, 263-275.

Kay, S.*, et al.* 2015. Modelling the increased frequency of extreme sea levels in the Ganges-Brahmaputra-Meghna delta due to sea level rise and other effects of climate change. *Environmental Sciences: Processes and Impacts,* 17(7), 1311-1322.

Khan, M. M. H., *et al.* 2015. Natural disasters and land-use/land-cover change in the southwest coastal areas of Bangladesh. *Regional Environmental Change,* 15(2), 241-250.

Khan, Z. H., 2018. *Bangladesh Delta Plan 2100 - Baseline Studies on Water Resources Management (Coast and Polder Issues).* Dhaka, Bangladesh: General Economics Division (GED), Bangladesh Planning Commission.

Khosravi, K., *et al.* 2016. A GIS-based flood susceptibility assessment and its mapping in Iran: a comparison between frequency ratio and weights-of-evidence bivariate statistical models with multi-criteria decision-making technique. *Natural Hazards,* 83(2), 947-987.

Kia, M. B., *et al.* 2012. An artificial neural network model for flood simulation using GIS: Johor River Basin, Malaysia. *Environmental Earth Sciences,* 67(1), 251-264.

Kityuttachai, K., *et al.* 2013. CA-Markov analysis of constrained coastal urban growth modeling: Hua Hin seaside city, Thailand. *Sustainability,* 5(4), 1480-1500.

Kjeldsen, T. R., Lamb, R. and Blazkova, S. D. 2014. Uncertainty in flood frequency analysis. *Applied Uncertainty Analysis for Flood Risk Management*, 153-197.

Klijn, F., Asselman, N. and Van der Most, H. 2010. Compartmentalisation: flood consequence reduction by splitting up large polder areas. *Journal of Flood Risk Management,* 3(1), 3-17.

Koks, E. 2018. Moving flood risk modelling forwards. *Nature Climate Change,* 8(7), 561-562.

Koks, E., *et al.* 2019. Understanding Business Disruption and Economic Losses Due to Electricity Failures and Flooding. *International Journal of Disaster Risk Science*.

Kummu, M., Taka, M. and Guillaume, J. H. 2018. Gridded global datasets for gross domestic product and Human Development Index over 1990–2015. *Scientific Data,* 5, 180004.

Lakhan, V. C., 2003. *Advances in coastal modeling.* Elsevier.

Lázár, A. N.*, et al.*, 2020. Choices: Future Trade-Offs and Plausible Pathways. *Deltas in the Anthropocene.* Springer, 223-245.

Lee, Y. and Brody, S. D. 2018. Examining the impact of land use on flood losses in Seoul, Korea. *Land use policy,* 70, 500-509.

Lian, J. J., Xu, K. and Ma, C. 2013. Joint impact of rainfall and tidal level on flood risk in a coastal city with a complex river network: A case study of Fuzhou City, China. *Hydrology and Earth System Sciences,* 17(2), 679-689.

Lillesand, T., Kiefer, R. W. and Chipman, J., 2014. *Remote sensing and image interpretation.* John Wiley & Sons.

Lin, N.*, et al.* 2010. Risk assessment of hurricane storm surge for New York City. *Journal of Geophysical Research: Atmospheres,* 115(D18).

Liu, H. and Wang, L. 2008. Mapping detention basins and deriving their spatial attributes from airborne LiDAR data for hydrological applications. *Hydrological Processes: An International Journal,* 22(13), 2358-2369.

Liu, Y.*, et al.* 2003. A diffusive transport approach for flow routing in GIS-based flood modeling. *Journal of Hydrology,* 283(1-4), 91-106.

Logan, T., Guikema, S. and Bricker, J. 2018. Hard-adaptive measures can increase vulnerability to storm surge and tsunami hazards over time. *Nature Sustainability,* 1, 526-530.

López-Ratón, M.*, et al.* 2014. OptimalCutpoints: an R package for selecting optimal cutpoints in diagnostic tests. *Journal of Statistical Software,* 61(8), 1-36.

Malinowski, R., *et al.* 2015. Detection and delineation of localized flooding from WorldView-2 multispectral data. *Remote Sensing,* 7(11), 14853-14875.

Masud, M. M. A., Gain, A. K. and Azad, A. K. 2020. Tidal river management for sustainable agriculture in the Ganges-Brahmaputra delta: Implication for land use policy. *Land use policy,* 92, 104443.

Masud, M. M. A., *et al.* 2018. Sustainability impacts of tidal river management: Towards a conceptual framework. *Ecological Indicators,* 85, 451-467.

McColl, C. and Aggett, G. 2007. Land-use forecasting and hydrologic model integration for improved land-use decision support. *Journal of Environmental Management,* 84(4), 494-512.

McHugh, M. L. 2012. Interrater reliability: the kappa statistic. *Biochemia Medica,* 22(3), 276-282.

Memon, A. A., *et al.* 2015. Flood monitoring and damage assessment using water indices: A case study of Pakistan flood-2012. *The Egyptian Journal of Remote Sensing and Space Science,* 18(1), 99-106.

Merz, B., *et al.* 2010a. Fluvial flood risk management in a changing world. *Natural Hazards and Earth System Science,* 10(3), 509-527.

Merz, B., *et al.* 2010b. Review article" Assessment of economic flood damage". *Natural Hazards and Earth System Sciences,* 10(8), 1697-1724.

Messner, F. and Meyer, V., 2006. Flood damage, vulnerability and risk perception–challenges for flood damage research. *Flood risk management: hazards, vulnerability and mitigation measures.* Springer, 149-167.

Meyer, V., Haase, D. and Scheuer, S. 2009. Flood risk assessment in European river basins—concept, methods, and challenges exemplified at the Mulde river. *Integrated Environmental Assessment and Management,* 5(1), 17-26.

Mia, A. H.*, et al.*, 2011. *Study of detailed coastal land zoning with two pilot districts of plain land project.* Dhaka: Ministry of Land.

Midi, H., Sarkar, S. K. and Rana, S. 2010. Collinearity diagnostics of binary logistic regression model. *Journal of Interdisciplinary Mathematics,* 13(3), 253-267.

Mirza, M. Q. and Ericksen, N. J. 1996. Impact of water control projects on fisheries resources in Bangladesh. *Environmental Management,* 20(4), 523-539.

Mitsova, D. 2014. Coupling land use change modeling with climate projections to estimate seasonal variability in runoff from an urbanizing catchment near Cincinnati, Ohio. *ISPRS International Journal of Geo-Information,* 3(4), 1256-1277.

Mitsova, D., Shuster, W. and Wang, X. 2011. A cellular automata model of land cover change to integrate urban growth with open space conservation. *Landscape and Urban Planning,* 99(2), 141-153.

Mojaddadi, H.*, et al.* 2017. Ensemble machine-learning-based geospatial approach for flood risk assessment using multi-sensor remote-sensing data and GIS. *Geomatics, Natural Hazards and Risk,* 8(2), 1080-1102.

Moniruzzaman, M., 2012. Impact of Climate Change in Bangladesh: Water Logging at South-West Coast. *In:* Leal Filho, W. ed. *Climate Change and the Sustainable Use of Water Resources.* Berlin, Heidelberg: Springer Berlin Heidelberg, 317-336.

Montz, B. E. and Tobin, G. A. 2008. Livin'large with levees: Lessons learned and lost. *Natural Hazards Review,* 9(3), 150-157.

Morrison, R. R.*, et al.* 2018. Spatial relationships of levees and wetland systems within floodplains of the Wabash Basin, USA. *JAWRA Journal of the American Water Resources Association,* 54(4), 934-948.

MoWR, 1999. *Integrated Coastal Zone Management Concepts and Issues: A Government of Bangladesh Policy Note.* Dhaka: Ministry of Water Resources.

MoWR, 2005. *Coastal Zone Policy.* Dhaka: Ministry of Water Resources.

Mukhopadhyay, A.*, et al.*, 2018. Land Cover and Land Use Analysis in Coastal Bangladesh. *In:* Nicholls, R. J.*, et al.* eds. *Ecosystem Services for Well-Being in Deltas: Integrated Assessment for Policy Analysis.* Cham: Springer International Publishing, 367-381.

Mutahara, M.*, et al.* 2018. Social learning for adaptive delta management: Tidal River Management in the Bangladesh Delta. *International Journal of Water Resources Development,* 34(6), 923-943.

Narayan, S.*, et al.* 2012. A holistic model for coastal flooding using system diagrams and the Source–Pathway–Receptor (SPR) concept. *Natural Hazards and Earth System Science,* 12(5), 1431-1439.

Neumann, B.*, et al.* 2015. Future coastal population growth and exposure to sea-level rise and coastal flooding-a global assessment. *PloS one,* 10(3), e0118571.

Nicholls, R. J.*, et al.* 2008. Ranking port cities with high exposure and vulnerability to climate extremes.

Nied, M.*, et al.* 2014. On the relationship between hydro-meteorological patterns and flood types. *Journal of Hydrology,* 519(PD), 3249-3262.

Nishat, A., Nishat, B. and Abdullah Khan, M. F., 2010. A Strategic View of Land Management Planning in Bangladesh. *Flood Risk Science and Management.* 484-498.

Nowreen, S., Jalal, M. R. and Khan, M. S. A. 2014. Historical analysis of rationalizing South West coastal polders of Bangladesh. *Water Policy,* 16(2), 264-279.

Olsen, A.*, et al.* 2015. Comparing methods of calculating expected annual damage in urban pluvial flood risk assessments. *Water,* 7(1), 255-270.

Palanisami, K. and Easter, K. W. 1984. Ex post evaluation of flood control investments: A case study in North Dakota. *Water Resources Research,* 20(12), 1785-1790.

Panda, A. and Sahu, N. 2019. Trend analysis of seasonal rainfall and temperature pattern in Kalahandi, Bolangir and Koraput districts of Odisha, India. *Atmospheric Science Letters,* 20(10), e932.

Parvin, G. A.*, et al.*, 2017. Land use change in southwestern coastal Bangladesh: Consequence to food and water supply. *Land use management in disaster risk reduction.* Springer, 381-401.

Parvin, G. A., Takahashi, F. and Shaw, R. 2008. Coastal hazards and community-coping methods in Bangladesh. *Journal of Coastal Conservation,* 12(4), 181-193.

Paul, B. K. and Rashid, H., 2017. *Climatic Hazards In Coastal Bangladesh - Non-Structural and Structural Solutions.* I ed. Cambridge, United States: Elsevier.

Payo, A.*, et al.* 2017. Modeling daily soil salinity dynamics in response to agricultural and environmental changes in coastal Bangladesh. *Earth's Future,* 5(5), 495-514.

Penning-Rowsell, E.*, et al.* 2005. The benefits of flood and coastal risk management: a handbook of assessment techniques. *ISBN 1904750516*.

Penning-Rowsell, E. and Korndewal, M. 2019. The realities of managing uncertainties surrounding pluvial urban flood risk: An ex post analysis in three European cities. *Journal of Flood Risk Management,* 12(3), e12467.

Penning-Rowsell, E. C.*, et al.* 2019. Policy Processes in Flood Risk Management. *Water Science, Policy, and Management: A Global Challenge*, 197-214.

Planchon, O. and Darboux, F. 2002. A fast, simple and versatile algorithm to fill the depressions of digital elevation models. *Catena,* 46(2-3), 159-176.

Poussin, J. K., Botzen, W. W. and Aerts, J. C. 2015. Effectiveness of flood damage mitigation measures: Empirical evidence from French flood disasters. *Global Environmental Change,* 31, 74-84.

Pradhan, B. 2010. Flood susceptible mapping and risk area delineation using logistic regression, GIS and remote sensing. *Journal of Spatial Hydrology,* 9(2).

Pradhan, B., Oh, H. J. and Buchroithner, M. 2010. Weights-of-evidence model applied to landslide susceptibility mapping in a tropical hilly area. *Geomatics, Natural Hazards and Risk,* 1(3), 199-223.

Qiang, Y.*, et al.* 2017. Changes in Exposure to Flood Hazards in the United States. *Annals of the American Association of Geographers,* 107(6), 1332-1350.

Raber, G. T.*, et al.* 2007. Impact of LiDAR nominal post-spacing on DEM accuracy and flood zone delineation. *Photogrammetric engineering & remote sensing,* 73(7), 793-804.

Rahman, M. M.*, et al.*, 2020. Ganges-Brahmaputra-Meghna Delta, Bangladesh and India: A Transnational Mega-Delta. *Deltas in the Anthropocene.* Springer, 23-51.

Rahman, M. S. and Di, L. 2017. The state of the art of spaceborne remote sensing in flood management. *Natural Hazards,* 85(2), 1223-1248.

Rahman, M. T. U.*, et al.* 2017. Temporal dynamics of land use/land cover change and its prediction using CA-ANN model for southwestern coastal Bangladesh. *Environmental Monitoring and Assessment,* 189(11), 565.

Rahman, R. and Salehin, M., 2013. Flood Risks and Reduction Approaches in Bangladesh. *In:* Shaw, R., Mallick, F. and Islam, A. eds. *Disaster Risk Reduction Approaches in Bangladesh.* Tokyo: Springer, 65-90.

Ramirez, J.*, et al.* 1988. Ex post analysis of flood control: Benefit-cost analysis and the value of information. *Water Resources Research,* 24(8), 1397-1405.

Rao, A. R. and Hamed, K., 2000. *Flood frequency analysis.* USA: CRC press.

Regmi, N. R., Giardino, J. R. and Vitek, J. D. 2010. Modeling susceptibility to landslides using the weight of evidence approach: Western Colorado, USA. *Geomorphology,* 115(1-2), 172-187.

Rogger, M.*, et al.* 2017. Land use change impacts on floods at the catchment scale: Challenges and opportunities for future research. *Water Resources Research,* 53(7), 5209-5219.

Rojas, R., Feyen, L. and Watkiss, P. 2013. Climate change and river floods in the European Union: Socio-economic consequences and the costs and benefits of adaptation. *Global Environmental Change,* 23(6), 1737-1751.

Roy, K.*, et al.* 2017. Social, hydro-ecological and climatic change in the southwest coastal region of Bangladesh. *Regional Environmental Change,* 17(7), 1895-1906.

Sabatakakis, N.*, et al.* 2013. Landslide susceptibility zonation in Greece. *Natural Hazards,* 65(1), 523-543.

Salman, A. M. and Li, Y. 2018. Flood risk assessment, future trend modeling, and risk communication: a review of ongoing research. *Natural Hazards Review,* 19(3), 04018011.

Sang, L.*, et al.* 2011. Simulation of land use spatial pattern of towns and villages based on CA–Markov model. *Mathematical and Computer Modelling,* 54(3-4), 938-943.

Santos, M. and Fragoso, M. 2016. Precipitation thresholds for triggering floods in the Corgo Basin, Portugal. *Water,* 8(9), 376.

Sanyal, J. and Lu, X. X. 2004. Application of remote sensing in flood management with special reference to monsoon Asia: A review. *Natural Hazards,* 33(2), 283-301.

Sarp, G. and Ozcelik, M. 2017. Water body extraction and change detection using time series: A case study of Lake Burdur, Turkey. *Journal of Taibah University for Science,* 11(3), 381-391.

Sayers, P. B., Hall, J. W. and Meadowcroft, I. C. 2002. Towards risk-based flood hazard management in the UK. *Proceedings of the Institution of Civil Engineers: Civil Engineering,* 150(1 SPECIAL ISSUE), 36-42.

Schanze, J., 2006. Flood risk management–a basic framework. *Flood risk management: hazards, vulnerability and mitigation measures.* Springer, 1-20.

Schmitt, T. G., Thomas, M. and Ettrich, N. 2004. Analysis and modeling of flooding in urban drainage systems. *Journal of Hydrology,* 299(3-4), 300-311.

Segeren, W. 1983. Introduction to Polders of the World. *Water International,* 8(2), 51-54.

Seibert, J. and McGlynn, B. L. 2007. A new triangular multiple flow direction algorithm for computing upslope areas from gridded digital elevation models. *Water Resources Research,* 43(4).

Seijger, C.*, et al.* 2019. Rethinking sediments, tidal rivers and delta livelihoods: Tidal river management as a strategic innovation in Bangladesh. *Water Policy,* 21(1), 108-126.

Shah, M. A. R., Rahman, A. and Chowdhury, S. H. 2018. Challenges for achieving sustainable flood risk management. *Journal of Flood Risk Management,* 11, S352-S358.

Shahbazian, Z.*, et al.* 2019. Integrating logistic regression and cellular automata–Markov models with the experts' perceptions for detecting and simulating land use changes and their driving forces. *Environmental Monitoring and Assessment,* 191(7), 422.

Singh, R. K., Hari Prasad, V. and Bhatt, C. M. 2004. Remote sensing and GIS approach for assessment of the water balance of a watershed. *Hydrological Sciences Journal,* 49(1), 131-142.

Singh, S. K. 2017. Unified extreme-value distribution. *Journal of Irrigation and Drainage Engineering,* 143(12).

Steele, J. E.*, et al.* 2017. Mapping poverty using mobile phone and satellite data. *Journal of The Royal Society Interface,* 14(127), 20160690.

Steinfeld, C. and Kingsford, R. T. 2013. Disconnecting the floodplain: earthworks and their ecological effect on a dryland floodplain in the Murray–Darling Basin, Australia. *River Research and Applications,* 29(2), 206-218.

Stone, M. C., Byrne, C. F. and Morrison, R. R. 2017. Evaluating the impacts of hydrologic and geomorphic alterations on floodplain connectivity. *Ecohydrology,* 10(5), e1833.

Syvitski, J. P. 2008. Deltas at risk. *Sustainability Science,* 3(1), 23-32.

Syvitski, J. P.*, et al.* 2009. Sinking deltas due to human activities. *Nature Geoscience,* 2(10), 681-686.

Szabo, S., Ahmad, S. and Adger, W. N., 2018. Population Dynamics in the South-West of Bangladesh. *Ecosystem Services for Well-Being in Deltas.* Palgrave Macmillan, Cham, 349-365.

Szabo, S.*, et al.* 2016. Soil salinity, household wealth and food insecurity in tropical deltas: evidence from south-west coast of Bangladesh. *Sustainability Science,* 11(3), 411-421.

Szwagrzyk, M.*, et al.* 2018. Impact of forecasted land use changes on flood risk in the Polish Carpathians. *Natural Hazards,* 94(1), 227-240.

Talchabhadel, R., Nakagawa, H. and Kawaike, K. 2016a. Experimental study on suspended sediment transport to represent Tidal Basin Management. *Journal of Japanese Society of Civil Engineers, Ser B1 (Hydraulic Engineering),* 72(4), I_847-I_852.

Talchabhadel, R., Nakagawa, H. and Kawaike, K., Tidal River Management (TRM) and Tidal Basin Management (TBM): A case study on Bangladesh. ed. *E3S Web of Conferences*, 2016b.

Talchabhadel, R., Nakagawa, H. and Kawaike, K., Sediment management in tidal river: A case study of East Beel Khuksia, Bangladesh. ed. *E3S Web of Conferences*, 2018a.

Talchabhadel, R.*, et al.* 2017a. Experimental investigation on opening size of tidal basin management: a case study in southwestern Bangladesh. *Journal of Japanese Society of Civil Engineers, Ser B1 (Hydraulic Engineering),* 73(4), I_781-I_786.

Talchabhadel, R.*, et al.* 2017b. Experimental and Numerical Study of Tidal Basin Management around Link Canal: A Case Study of Bangladesh. *DPRI Annuals*.

Talchabhadel, R.*, et al.* 2018b. Three-Dimensional Simulation of Flow and Sediment Transport Processes in Tidal Basin. *Journal of Japan Society of Civil Engineers,* 74(4), I_955-I_960.

Tareq, S. M.*, et al.* 2018. Evaluation of climate-induced waterlogging hazards in the south-west coast of Bangladesh using Geoinformatics. *Environmental Monitoring and Assessment,* 190(4), 230.

Tehrany, M. S., Jones, S. and Shabani, F. 2019a. Identifying the essential flood conditioning factors for flood prone area mapping using machine learning techniques. *Catena,* 175, 174-192.

Tehrany, M. S.*, et al.* 2019b. Evaluating the application of the statistical index method in flood susceptibility mapping and its comparison with frequency ratio and logistic regression methods. *Geomatics, Natural Hazards and Risk,* 10(1), 79-101.

Tehrany, M. S.*, et al.* 2014a. Flood susceptibility mapping using integrated bivariate and multivariate statistical models. *Environmental Earth Sciences,* 72(10), 4001-4015.

Tehrany, M. S., Pradhan, B. and Jebur, M. N. 2014b. Flood susceptibility mapping using a novel ensemble weights-of-evidence and support vector machine models in GIS. *Journal of Hydrology,* 512, 332-343.

Tehrany, M. S.*, et al.* 2017. GIS-based spatial prediction of flood prone areas using standalone frequency ratio, logistic regression, weight of evidence and their ensemble techniques. *Geomatics, Natural Hazards and Risk,* 8(2), 1538-1561.

Thompson, C. M. and Frazier, T. G. 2014. Deterministic and probabilistic flood modeling for contemporary and future coastal and inland precipitation inundation. *Applied Geography,* 50, 1-14.

Thornthwaite, C. W. and Mather, J. R., 1957. *Instructions and tables for computing potential evapotranspiration and the water balance.* Drexel Institute of Technology, Centerton, NJ (EUA). Laboratory of Climatology.

Tockner, K. and Stanford, J. A. 2002. Riverine flood plains: present state and future trends. *Environmental conservation,* 29(3), 308-330.

Tuong, T. P.*, et al.*, 2014. *Messages from the Ganges Basin development challenge: unlocking the production potential of the polders of the coastal zone of Bangladesh through water management investment and reform.* CGIAR Challenge Program on Water and Food.

Valbuena, D.*, et al.* 2010. An agent-based approach to model land-use change at a regional scale. *Landscape ecology,* 25(2), 185-199.

van den Hurk, B.*, et al.* 2015. Analysis of a compounding surge and precipitation event in the Netherlands. *Environmental Research Letters,* 10(3), 035001.

Van Staveren, M. F., Warner, J. F. and Khan, M. S. A. 2017. Bringing in the tides. From closing down to opening up delta polders via Tidal River Management in the southwest delta of Bangladesh. *Water Policy,* 19(1), 147-164.

Verburg, P. H.*, et al.* 2004. Land use change modelling: current practice and research priorities. *GeoJournal,* 61(4), 309-324.

Vousdoukas, M. I.*, et al.* 2018. Climatic and socioeconomic controls of future coastal flood risk in Europe. *Nature Climate Change,* 8(9), 776.

Wahl, T.*, et al.* 2015. Increasing risk of compound flooding from storm surge and rainfall for major US cities. *Nature Climate Change,* 5(12), 1093.

Wang, M.*, et al.* 2019. Predicting land use changes in northern China using logistic regression, cellular automata, and a Markov model. *Arabian Journal of Geosciences,* 12(24), 790.

Wang, Y., Colby, J. D. and Mulcahy, K. A. 2002. An efficient method for mapping flood extent in a coastal floodplain using Landsat TM and DEM data. *International Journal of Remote Sensing,* 23(18), 3681-3696.

Ward, P. J.*, et al.* 2011. How are flood risk estimates affected by the choice of return-periods? *Natural Hazards & Earth System Sciences,* 11(12).

Ward, P. J.*, et al.* 2017. A global framework for future costs and benefits of river-flood protection in urban areas. *Nature Climate Change,* 7(9), 642-646.

Ward, P. J.*, et al.* 2015. Usefulness and limitations of global flood risk models. *Nature Climate Change,* 5(8), 712-715.

Warner, J. F., van Staveren, M. F. and van Tatenhove, J. 2018. Cutting dikes, cutting ties? Reintroducing flood dynamics in coastal polders in Bangladesh and the netherlands. *International Journal of Disaster Risk Reduction,* 32, 106-112.

WARPO, 2018. National Water Resources Database(NWRD). Bangladesh: Water Resources Planning Organization (WARPO).

Wheater, H. and Evans, E. 2009. Land use, water management and future flood risk. *Land use policy,* 26, S251-S264.

White, G. F., 1945. *Human adjustment to floods.* (Doctor of Philosophy). The University of Chicago.

Wilson, C., *et al.* 2017. Widespread infilling of tidal channels and navigable waterways in the human-modified tidal deltaplain of southwest Bangladesh. *Elementa-Science of the Anthropocene,* 5(78).

Wing, O. E., *et al.* 2017. Validation of a 30 m resolution flood hazard model of the conterminous U nited S tates. *Water Resources Research,* 53(9), 7968-7986.

Wing, O. E., *et al.* 2019. A flood inundation forecast of Hurricane Harvey using a continental-scale 2D hydrodynamic model. *Journal of Hydrology X,* 4, 100039.

Winsemius, H. C., *et al.* 2018. Disaster risk, climate change, and poverty: assessing the global exposure of poor people to floods and droughts. *Environment and Development Economics,* 23(3), 328-348.

WorldPop, 2018. Bangladesh 100m Population, Version 2. *In:* Southampton, U. o. ed. UK.

Wright, L. D., Resio, D. T. and Nichols, C. R., 2019a. Causes and Impacts of Coastal Inundation. *Tomorrow's Coasts: Complex and Impermanent.* Springer, 103-118.

Wright, L. D., Syvitski, J. and Nichols, C. R., 2019b. Coastal Complexity and Predictions of Change. *Tomorrow's Coasts: Complex and Impermanent.* Springer, 3-23.

Xu, H. 2006. Modification of normalised difference water index (NDWI) to enhance open water features in remotely sensed imagery. *International Journal of Remote Sensing,* 27(14), 3025-3033.

Youssef, A. M., Pradhan, B. and Hassan, A. M. 2011. Flash flood risk estimation along the St. Katherine road, southern Sinai, Egypt using GIS based morphometry and satellite imagery. *Environmental Earth Sciences,* 62(3), 611-623.

Zegwaard, A., *et al.* 2019. Sameness and difference in delta planning. *Environmental science & policy,* 94, 237-244.

Zevenbergen, L. W. and Thorne, C. R. 1987. Quantitative analysis of land surface topography. *Earth surface processes and landforms,* 12(1), 47-56.